2013

Electrical, Optical And Chemical Properties Of Organic Photo Sensitve Materials

Zheng Shi
University of Central Florida

ELECTRICAL, OPTICAL AND CHEMICAL PROPERTIES OF ORGANIC PHOTO SENSITIVE MATERIALS

by

ZHENG SHI
B.S. China Pharmaceutical University, China, 2007
M.S. University of Central Florida, 2012

A dissertation submitted in partial fulfillment of the requirements
for the degree of Doctor of Philosophy
in the Department of Chemistry
in the College of Sciences
at the University of Central Florida
Orlando, Florida

Spring Term
2013

Major Professor: Yi Liao

ABSTRACT

Light as a "green" source of energy has become increasingly attractive throughout the past century and has shown versatility for the application of activating chemical reactions. Compared with traditional energy sources, it provides a more direct, selective and controllable method. My PhD study was focused on the study of photochemistry of organic materials in two different systems. The first system is regarding reversible photoacids which generate protons on irradiation. With the aim of systematically studying these novel types of long lived photoacids, a series of photoacids was designed, synthesized and whose chemical mechanism was thoroughly investigated. This type of photoacid changes from a weak acid to a strong acid with a pH change of several units, which achieves nearly complete proton dissociation upon visible light irradiation. The whole process is reversible and the half-life of the proton-dissociation state is long enough to be used in many applications. Besides fundamental studies, different applications based on this type of photoacids were also completed. An esterification reaction was catalyzed and the volume of a pH-sensitive polymer was altered due to the large amount of photo generated protons from this photoacid. A reversible electrical conductivity change of polyaniline (PANI) was also achieved by doping with this reversible photoacid. In order to induce a large conductivity increase, an irreversible photoacid generator (PAG) was embedded in a novel PANI/PAG/PVA novel composition. In this system, Poly (vinyl alcohol) (PVA) forms a hydrogen-bonding network to facilitate proton transfer between the PAG and PANI. A final electrical conductivity of 10^{-1} S cm^{-1} was successfully achieved after irradiation.

The second system in which I explored photochemistry of organic molecules concerns Photo-retro-Diels-Alder (PrDA) reactions and a variety of Diels-Alder (DA) adducts were designed for these studies. UV light was used to trigger the retro-Diels-Alder reactions. Quantum yield of

each DA adducts was investigated. This revealed that the photo-reactivity of this process depends on the electron-donating ability of the diene and the electron-withdrawing ability of the dienophile component. Mechanistic studies of this PrDA reaction reveal that a charge-separated intermediate is generated from a singlet excited state. This was applied to an unsaturated cyclic α-diketones (DKs), which underwent PrDA reactions and generated anthracene derivatives and carbon monoxide (CO), which itself plays profound and important roles in biological systems. These unsaturated cyclic α-diketones (DKs) encapsulated in micelles are effective CO-releasing molecules (CORMs) and are capable of carrying and releasing CO in cellular systems. This novel type of organic CORMs has potentially low toxicity and generates fluorescence, which provides a useful tool for the study of the biological functions of CO.

ACKNOWLEDGMENTS

First of all, I would like to express my deeply-felt thanks to my PhD advisor, Dr. Yi Liao, for providing me such a great opportunity to purse my PhD degree. With his warm encouragement and thoughtful guidance in past five and half years, I change from an undergraduate student without any research idea to a PhD student with my own opinion. It's my great honor to work with him.

I also want to thank the other committee members: Dr. Dmitry Kolpashchikov, Dr. Shengli Zou, Dr. Ming Su, and Dr. Ye Jingdong, who provided encouraging and constructive feedback. It is no easy task, reviewing a thesis, and I am grateful for their thoughtful and detailed comments. In particular, I would like express my gratitude to Dr. Ming Su who gave me a chance to work in his lab on various topics. He has also provided insightful discussions about the research. I hope that I could be as lively and energetic as him.

I am also very grateful to Dr. Ping Peng for his friendly advice and knowledge and many insightful discussions and suggestions while he was a postdoc in Dr. Liao's group. He is one of my primary resources for getting hand-on experience on organic synthesis.

I would like to thank Dr. Matthew Rex for his help and teaching on HPLC and GC-MS. He is a great analytical chemist and enthusiastic friend. I also thank my colleagues, Ms. Sarah Lefave and Mr. Dan Strohecker who worked with me in the same lab for years. We shared emotion and success, worked together to make our workplace even better. Dan also helped me a lot while I started my projects about photoacids and the candidacy exam. I would also thank graduate student Ms. Jennifer Reed for her helpful discussions and supportive suggestions. Special thanks also to Mr. Bingling Sui for providing me many help with different kinds of instruments.

I also thank my friends for providing support and friendship that I needed. I would like Dr. Yan Tang for being supportive throughout my time here and teaching me with a good attitude to face problems. I think of her as my sister. Special thanks to Guangming Tao for his help with my dissertation research and the happiness he brought.

I especially thank my family. My dear parents provided unconditional love and care to me. I love them so much, and I would not make it this far without them. I know I always have my family to count on when times are rough. Also I want to thank my other family members for their encouragement and support over the years.

This thesis was funded by Air Force Office of Scientific Research and National Science Foundation, and I would like to thank both organizations for their generous support.

Thank you!

TABLE OF CONTENTS

LIST OF FIGURES

LIST OF SCHEMES

LIST OF TABLES

CHAPTER 1. INTRODUCTION

1.1 Significance of Dissertation Research

Light is one form of "green" energy which has steadily become more and more attractive since last century. In 1912, the father of photochemistry and nine-time Nobel Prize nominee Giacomo Ciamician published "The photochemistry of the future" in Science[1]. He wrote, "*On the arid lands there will spring up industrial colonies without smoke and without smokestacks; forests of glass tubes will extend over the plains and glass buildings will rise everywhere; inside of these will take the photochemical processes that hitherto have been the guarded secret of the plants, but that will have been mastered by human industry…*" Today, photovoltaic solar panels allow for the conversion of solar energy to electricity for powering so many homes and buildings that Ciamician's dream may very well come true. Aside from this attractive ideal, the discovery of photochemistry has also fostered an explosion of interesting chemical research.

1.1.1 Mechanistic Background

The study of chemical reaction, isomerizations and physical behavior that may be triggered by the visible and/or ultraviolet light is called photochemistry[2]. A molecule absorbs a proton of light and changes its electronic structure, inducing novel reactivity with other molecules. Each type of molecule has a different photochemical mechanism; however they all obey the same basic laws of photochemistry.

The first law of photochemistry, the Grotthuss-Draper law, states that light must be absorbed by a compound for photochemistry to occur. According to this law, all of the light used in the experiments should match with the absorption wavelength of the compounds, otherwise no photochemistry will occur.

The second law of photochemistry, the Stark-Einstein law, states that for each photon of light absorbed by a chemical system, only one molecule is activated for a photochemical reaction. This law was derived by Albert Einstein during his development of the quantum (photon) theory of light. Photochemistry under ordinary light intensities obeys this law very well. With the new technique of laser, two-photon reactions could active one molecule to a higher energy level than one photon absorption.

In photochemistry, short-wavelength visible and/or ultraviolet light are often used to trigger the most photochemical reactions. The equation $E= hc/\lambda$ explains the reason for this: longer wavelengths of visible light has less energy than those short wavelengths light. One major consequence of this is that short wavelengths of light impart enough energy to break or reorganize most covalent bonds in the molecule to effect a photochemical reaction. Other wavelengths of lights may incur other effects. For example, far-infrared light will cause the vibrational excitation of molecules and increase the temperature.

When a molecule absorbs a photon from the light, it will cause an electron to be promoted to a higher energy level. The Jablonski Diagram (Figure 1) illustrates the principal photo physical radiative and nor-radiative processes displayed by organic molecules in solution. S0, S1, T2 represent the ground electronic state (S0), first excited singlet state (S1), second excited triplet state (T2) and so on. The horizontal lines represent the vibrational levels of each electronic sate. Straight arrows indicate radiative transitions, and “wiggle” arrows indicate non-radiative transitions. The boxes detail the electronic spins in each orbital, with electrons shown as up and down arrows, to distinguish their spin[2]. Excited states may occur as singlet states and triplet states, based on their electron spin angular momentum. The distinction between singlet and triplet states is important because photon induced excitation leads to a state of the same

multiplicity. Because most of the ground states are singlet, absorption of a photon will usually result in singlet excited state. An excited state will return to the ground state by emitting a photon; this phenomenon is called fluorescence. Intersystem crossing may convert a singlet state to a lower energy triplet state, or vice versa. Phosphorescence is the radiative decay of an electron from a triplet state back to the ground state. Non-radiative decays may take place by intermolecular energy transfer to a different molecule.

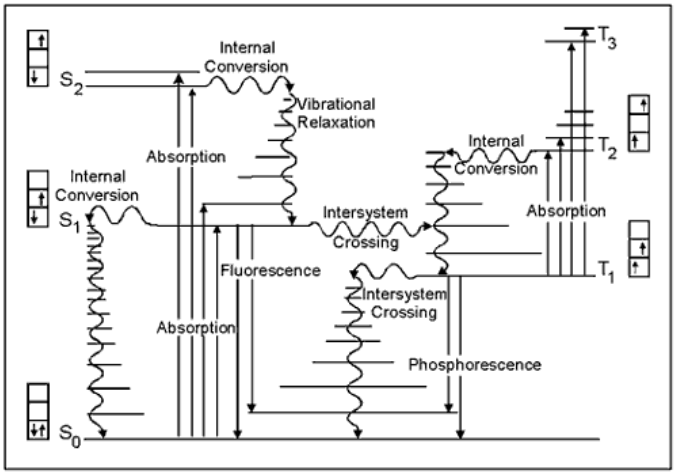

Figure 1. The basic concepts of Jablonski diagram

Although electronically excited state can be produced by thermal activation, this method is very inefficient in the formation of excited states of organic molecules compared to photochemical activation[3]. Also, photochemistry can provide more spatial and temporal control than thermal method.

In the presented dissertation research, the focus is on photochemistry in two major areas: the first one is on the fundamental study of photoacids and their applications in material chemistry. The second area concerns the systematic study of the Photo-retro-Diels-Alder reaction and its applications.

1.1.2 Photoacids

The process of proton transfer is prevalent in a broad array of chemical processes that encompass numerous systems[4]. Photoacids are a kind of molecules that reversibly undergo proton photo dissociation and thermal reassociation. Irradiation of photoacids by various wavelengths of light to liberate protons could spatially and temporally control these systems in a noncontact way, and convert optical radiation to other types of energy. The proton transfer from an aromatic molecule to the surrounding solvent is closely related to the electronic structure of not only the protonated form, but also the deprotonated form. Proton transfer in the solution is determined by the electronic rearrangement of the excited acid, the microenvironment around it, and solvent properties[5]. The geminate recombination of the two separated ions affects the overall proton-dissociation process. Since the 1970s, many reviews have been published based on photoacids[6, 7]. Photoacids have received a great deal of attention because of their fundamental importance and various possibilities for applications, such as the control of molecular and supramolecular events [8-10], switching conductive polymer electrical properties [11, 12], serving as effective photo protecting agents[13-15] and use in photodynamic therapy[16, 17].

In this dissertation research, part of the research effort has been devoted to discover a novel long lifetime photoacid which generates large concentration of protons in solution whose acidity may be directly tested using a commercial pH meter. Earlier research could only study photoacids' the excited-state proton transfer (ESPT) and calculate the excited state pK_as by picoseconds laser spectroscopy. Most steady-state techniques cannot be used to study these photoprototropic equlilibra because of the extremely short lifetime of the conjugated base of the photoacid in the ground state [18]. Another important feature about this photoacid is its reversibility. It is also desirable to develop a photoacid whose acidity can be controlled using irradiation with different

wavelengths of light. To realize this research goal, protonated merocyanine was developed as a model system for the pH change test and application experiments. The pK_a of photoacid can be changed by modifying the electron-donating group or electron-withdrawing group in the protonated merocyanine. In order to demonstrate the application of this type of photoacid, I used it to precisely control a model acid-catalyzed process, change a pH-sensitive material's physical property, and modulate electrical materials' conductivity.

Another part of the research effort was devoted to increasing the photo-induced conductivity of polyaniline (PANI-EB) by adding photo-acid generators (PAGs). The Nobel Prize in Chemistry for the year 2000 was awarded jointly to Alan J. Heeger, Alan G. MacDiarmid and Hideki Shirakawa "for the discovery and development of conductive polymers". Discovery of conductive polymers such as PANI opened a new area of research for polymers, in which they could be used as electronic materials. PANI was one of the most widely investigated conductive polymers in last century and tremendous advances have been made based on these research. A new research area has been open owing to a deeper understanding of the chemistry, electrochemistry, structure, electrical, and optical phenomena of conductive polymers. Their relative ease of synthesis by chemical or electrochemical oxidative polymerization of monomers and stability in many different environments make them of great interest to the field of materials chemistry. Polyaniline was first reported in 1862 by Letheby[19]. In 1910-1912, polyaniline was found to exist as four different oxidation states, each of which was an "octamer"[20, 21]. On every important discovery was that emeraldine oxidation state of polyaniline could change its conductivity upon being doped with acid[22]. Compared with a normal acid, doping with a photoacid could change the conductivity of PANI with more precise spatial control and less damage to the electrical device as a whole. In this dissertation research, several photoacid

generators were doped with PANI; however the conductivity increase of composites comprised of only PANI and PAG composition is not large enough for real application. In order to significantly increase the conductivity of PANI from an insulator to a semiconductor without using strong acid vapors, additional polyvinyl alcohol was added and the mechanism was studied in this dissertation.

1.1.3 Photo-retro-Diels-Alder Reaction

From 1935, the mechanism of the Diels-Alder cycloaddition has been the subject of many investigations and controversial interpretations[23]. Between 1965 and 1969, Woodward and Hoffmann defined the term pericyclic reaction and stated the rules for conservation of the symmetric orbital in this process[24]. This theory could successfully explain most Diels-Alder cycloaddition reactions; however there are some nonconcerted mechanisms could not be applied. Bartlett *et al.*[25-28] proposed a radical mechanism to produce cyclobutane derivatives. Since a conjugated diene and a dienophile could form a substituted cyclohexene system, Diels-Alder reaction has been proven to be one of the most versatile strategies for six-membered carbocycle synthesis[29].Some of the Diels-Alder reactions are reversible and those decomposition reaction of the cyclic system is called the retro-Diels-Alder (rDA) reaction, which has evolved into a powerful synthetic tool and has been used for preparing many reactive, strained chemicals. It usually forms or regenerates an unsaturated bond, but often requires high temperature which is a major drawback. In order to help this cycloreversion reaction more applicable, several techniques have been developed, such as acid catalysis[30], antibody catalysis[31], silica gel[32] or alumina catalysis[33]. Photo-rDA (PrDA) reactions, which allow spatical and temporal control, have been reported by some individual cases and may find application in photoresponsive materials, photolithography, drug delivery, and mechanistic research. For example, Nozaki and Kato found

that the DA adduct of anthracene and styrene yielded anthracene under photo irradiation, while the adduct of anthracene and 2-butene is photostable[34]. Although many individual cases have been studied, no systematic research of PrDA reactions has been done.

In this part of dissertation research, I studied the mechanism of PrDA reaction and generated a guide which could predict whether a compound will undergo PrDA reaction or not. To experimentally and theoretically study this reaction, a variety of normal-electron-demand DA adducts were prepared. The quantum yield of these adducts was very carefully measured for the first time. All the results support a mechanism that involves a charge-separated intermediate generated from a singlet excited state.

Based on this Photo-retro-Diels-Alder reaction mechanism, those cyclic Diels-Alder adducts were studied as one of the application. The unsaturated cyclic α-diketones (DKs) generates carbon monoxide (CO) and anthracene derivatives. Since the beginning of last century John Haldane first described the physiological effects of CO on the human body[35], CO has been discovered not only as a "silent killer" but also a signaling mediator in many biological processes[36]. Trying to find a safety and controllable method to administer CO to a specific part of the body become a very attractive area. These unsaturated cyclic α-diketones (DKs) could only be activated by visible light which provide a new type of CO therapeutic agent candidate.

CHAPTER 2. LONG LIVD REVERSIBLE PHOTOACID

2.1 Introduction

Ground-state proton transfer reactions are one of the most fundamental and important process in chemistry. The excited-state proton transfers (ESPT) reactions are not so famous in general chemistry. However, in the realm of photochemistry, ESPT reactions are the indispensible building block in fundamental and applied area. Both the intermolecular and intramolecular ESPT reactions have been applied in many areas: As mechanistic tools, intermolecular ESPT reactions have been used in pH[37] and pOH jump[38] experiments to study the proton hydration dynamics[39, 40], photolithography[41]. In biology environment, intermolecular ESPT reactions have also been developed as probes around proteins[42], micelles[43, 44] and films[45]. Analogous intramolecular reactions also have many applications, such as chemical lasers[46], energy storage systems and information storage devices at a molecular level[47]and polymer stabilizers[48, 49].

As early as 1930s, Weber was the first to discover 1-naphthylamine-4-sulfonate showed strong pH dependence of the emission spectrum[50]. The correct explanation about this observation was not given until 1949 by Förster[51]who first mentioned the field of excited state intermolecular proton transfers ($ESI_{er}PT$). One year later[52], he proposed famous Förster cycle which is a valuable method to predict the excited-state pKa based on the ground-state pKa and the excited-state energy difference between the unprotonated and protonated forms of the photoacid:

$$\boldsymbol{pK_a^* = pK_a + (E_{RO-} - E_{ROH})/2.3\,RT} \quad (1)$$

Weller[53] continued the previous work and reviewed[54] the early study on excited-state intramolecular proton transfers ($ESI_{er}PT$) which laid the fundamentals for this area. After that

this area attracted a lot attention and brought a quick development. Vander Donckt[55]reviewed $ESI_{er}PT$ about rationalized excited-state acid-base equilibria based on charge transfer and resonance theories. In 1976, Ireland and Wyatt [56]published an extensive review on thermodynamic acidities of $ESI_{er}PT$ which gives a whole picture about the development in this area at that point. Until 1980^{th}, the steady-state method was still the main tool to study the kinetics of the proton transfers step in singlet states and measure the protonation and deprotonation rates. Not until the development of experiment techniques with fast time resolution, the real-time determination of many singlet states could not be solved since its relatively short lifetime. The short lifetime of the proton-dissociation state is limited by the lifetime of the conjugated base of the photoacid in the ground sate, which could be useful for some fast processes. However, photo induced proton concentration of these previously reported photoacid usually is too small to control other chemical processes. Arnaut, L[37]reported a extremely long-lived photoacid with nearly one second of the proton releasing time, which was estimated by pump-probe absorption spectroscopy. Increase the lifetime of the proton dissociation state could increase the potential usage of the photoacid in many other areas, such as controlling molecular and supramolecular events[57], so here we introducing an intramolecular photoreaction, photochromic reaction, to stabilize the proton dissociation state.

The history of photochromism will go back to the end of nineteenth century when people discovered the first example of the phenomenon of photochromism in both organic substances and inorganic complexes[58]. Photochromism is a reversible transformation of chemical species in one or both directions by different region light irradiation. The study of organic materials' photochromism began to receive increased interest around 1940[59]. The systematic studies of a photochromism consist of three parts: First one is acquiring an insight into the mechanism of the

photo processes. Second one is determining the structure of the colored and uncolored compounds. The last one is developing synthetic methods.

$$A(\lambda 1) \xrightarrow{hv1} B(\lambda 2) \xrightarrow{hv2,\Delta} A(\lambda 1) \quad (2)$$

Predominantly in the photochromism reaction, compound B has at least one longer wavelength than compound A's. Most of the activating radiation is in the UV region (300 nm to 400 nm) and some of them are in the visible region (400 nm to 700 nm). Reversibility is the most important feature of the photochromism. Usually, the reverse reaction (B→A) occurs under extra heat stimulus, such as spiropyrans spirooxazines. However, in some other systems, such as arylethenes, compound B is thermally stable and the reverse reaction occurs by a photochemical mechanism.

Photochromic transformation and the changes in the chemical and physical properties are related to the system geometry modification and electronic difference. These kinds of material have two major applications: One is directly related with the spectral changes between two compounds (A and B), such as photochromic ophthalmic lenses. The other application depends on the change of physical and chemical properties, such as optoelectronic systems.

Although photochromic compounds have been proved to induce proton transfer and consequent molecular events before, the lifetime of their proton-dissociation state was not reported. This chapter reports a long-lived photoacid based on a photochromic reaction and demonstrates its applications in catalyzing an esterfication reaction and altering the volume of a pH-sensitive polymer.

2.2 Photoacid Based on Merocyanine

2.2.1 Study of Photoacid 1

In this chapter, we focus on UV and pH change of several long-lived photoacid based on merocyanine structure. These novel photoacids were synthesized by our lab members following a literature method[60]. The process of photoreaction was monitored by UV-Vis spectroscopy. According to the UV-Vis spectra, the mechanism of the photoreaction is proposed as in the scheme 1. In an aqueous solution, the protonated merocyanine (MEH) form of 1 was irradiated by 419 nm light and induces a trans- to cis- isomerization of MEH. The cis-MEH will release a proton and change to the deprotonated cis-merocyanine (ME) form, and then undergoes a nucleophilic ring closing reaction to yield spiropyran (SP) form. In the dark, this whole reaction is reversible and SP form will change back to the MEH form at room temperature. Extra using 570 nm light, which is only absorbed by ME structure, also helps the transformation from MEH to SP. During this whole process, photoirradiation induces trans-cis isomerization rather than proton dissociation.

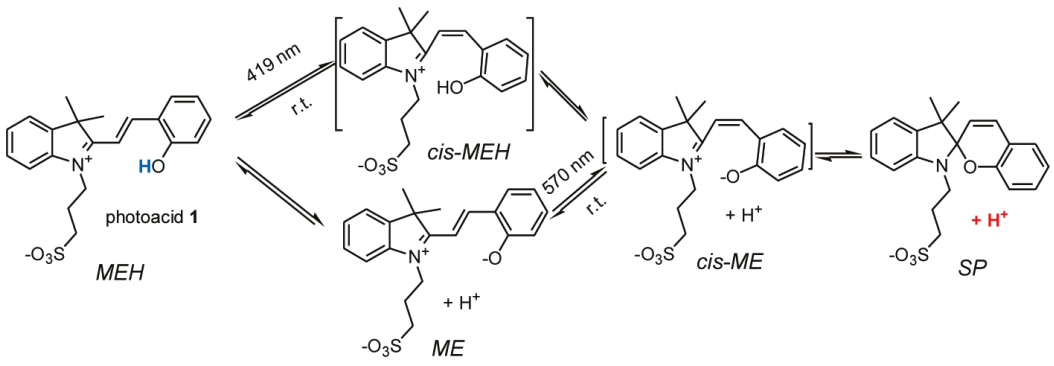

Scheme 1. The proposed mechanism

Figure 2 is the pH change of a 5.88×10^{-4} M photoacid 1in aqueous solution. This solution started with pH value of 5.5, so the pK_a of photoacid 1 was calculated to be 7.8 based on this pH number.

Then the pH of the solution dropped to 3.2, which is more than 2 units' difference after 3minutes 419 nm light irradiation. Compare with the theoretical value for complete proton dissociation (3.2), the value of photoacid 1 is very close, so it's a strong acid under irradiation. The reverse reaction is very fast when the light turned off. It only took 1minute to increase to pH 4.5 and then gradually returned to its original value in 5 minutes. This compound still has very good reversibility and stability even after 15 cycles. Therefore by control the light on and off, the proton concentration could be easily modified.

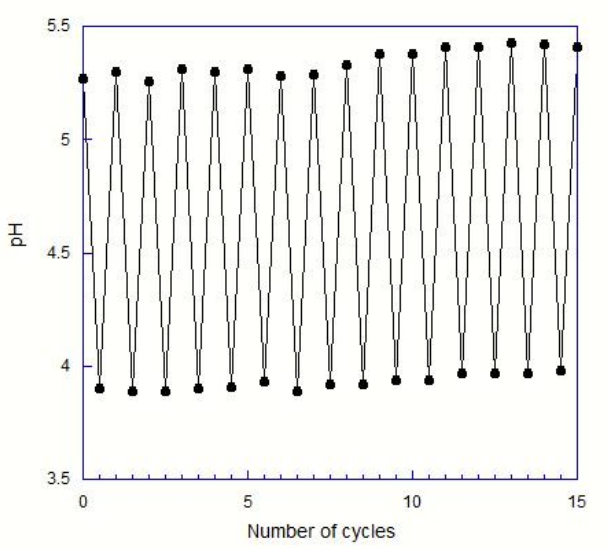

Figure 2. Cycles of pH change of photoacid 1

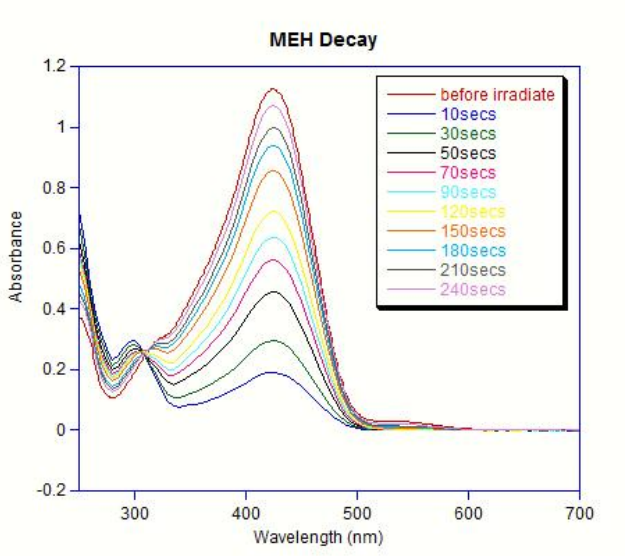

Figure 3. The UV-Vis spectra of photoacid 1 solution after 419 nm 10minutes irradiation

Figure 3 shows the UV-Vis spectra of photoacid 1 in aqueous solution. As shown in the spectra, this photoacid kept the MEH form (λ_{max}=470 nm) after dissolved in water in the dark. After 10 minutes 419 nm visible light irradiation, most of the MEH form changed to the SP form, which absorbs at 300 nm[61]. From 10 seconds to 240 seconds in dark after irradiation, SP form converted back to the MEH form without any extra stimuli and MEH concentration almost recovered to the initial value. In the spectra, there was a small peak around 570 nm after dissolved in the water which represents the ME form and this explains why the initial solution is weakly acidic. After irradiation, this peak quickly disappeared, and only leaving the SP and MEH form in the solution. In the dark, ME structure recovered at the same time as MEH peak increased without isosbestic point. Both of these indicates ME structure could not be the intermediate between SP and MEH. The disappearance of ME could be due to the equilibrium between MEH and ME: with more and more MEH form converted to the SP form and lower the pH of solution, ME form will change to MEH to increase the concentration of MEH. The 419 nm light irradiation induces a trans-cis isomerization of MEH. Cis-MEH loose a proton to generate cis-ME, and then this cis-ME undergoes a nucleophilic ring closing reaction to form SP. In the

dark, this process will go back and convert MEH again. The 570 nm irradiation is only absorbed by ME structure and helped MEH to SP transformation.

The UV-Vis spectroscopy is also used to monitor the lifetime of the proton-dissociation state. As showed in the spectroscopy graph, the UV-Vis spectra were tested every 20 second after irradiation. The overall concentration subtracts the MEH concentration will be the proton concentration. Through these data Figure 4 was obtained by the first 100s' data which was fit to a first order kinetic equation. Since the rate constant k=0.009138 s^{-1}, the half-life time of the proton dissociation state was 76s ($t_{1/2}$ =0.693/k) according to this graph. However the real case is much more complicated since it's a reversible reaction. Although this half-life time is only an estimation, it is consisted with the pH change. This first order decay is a reasonable approximation for the early stage of the proton concentration decay.

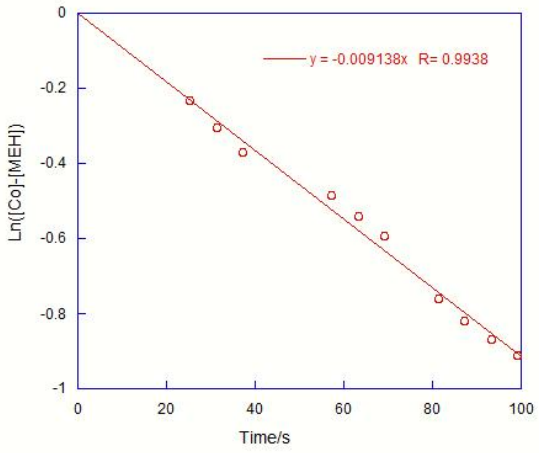

Figure 4. Fitted first order reaction equation

There are two major advantages compare with other photochromism photoacid: First, this process is only need one light source instead of two light sources with different wavelengths. Second, this light source is in the visible region instead of using UV light.

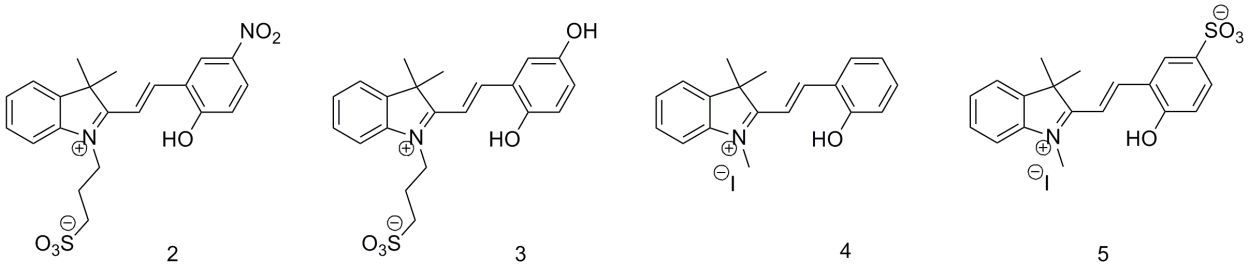

Figure 5. Derivatives of MEH synthesized

To further understand the factors that affect the photoacidity, several similar compounds were synthesized followed the same method of compound 1 (Figure 5). Each of these compounds was studied by the UV-Vis spectrum and pH meter.

2.2.2 Study of Photoacid 2

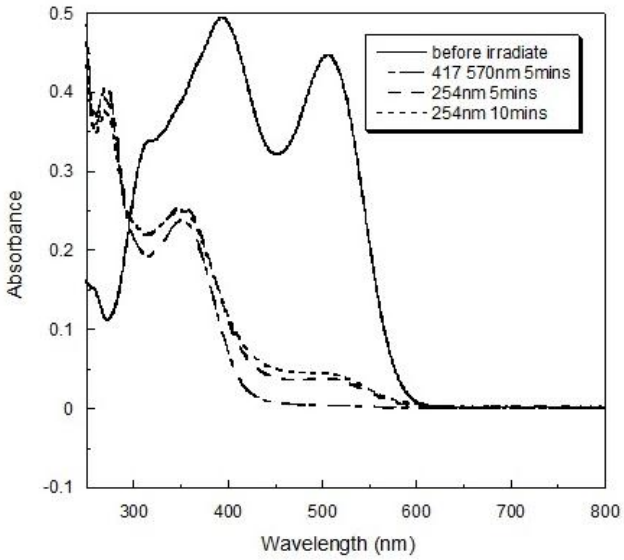

Figure 6. The UV-Vis spectra of photoacid 2 in water with different light stimuli

In Figure 6, the solid line shows the UV-Vis spectra of photoacid 2 dissolved in water in the dark. The two major peaks represent the MEH form (λ_{max} = 400 nm) and the ME form (λ_{max} =560 nm). Unlike photoacid 1, a large amount of MEH form of this compound converts to ME form in the initial solution. Then both of the absorption of MEH and ME form decreased by irradiated at 419

and 570 nm for 5mins, at the same time the peak at 270 nm increased which is assigned to the SP form[62]. From the UV-Vis spectra, the ME form totally disappear after 419 and 570 nm irradiation, leaving the SP to be observed. But the reverse process of this compound is not as good as the photoacid 1, which SP form will revert to the MEH in the dark. With 254 nm UV light irradiation, partial of the SP structure revert to the ME structure but remain most of the SP structure unchanged.

The pH study also confirmed the UV-Vis data. A 3.20×10^{-4}mol/L compound 2 aqueous solution initially has a pH value 4.86, which is lower than the photoacid 1 and also confirmed by UV-Vis spectra. When the solution was irradiated with 419 and 570 nm light, which is closed to the MEH form (λ_{max} = 400 nm) and the ME form (λ_{max} =560 nm), pH drops to 3.87. Then the pH slightly changes after 254 nm irradiation. However heat is an efficient method to convert the SP form of this compound back to MEH form, which is confirmed by pH change (Figure 7) and UV-Vis data (Figure 8). The pH of this SP solution after heating immediately increases to 4.59. SP peak decreased and the MEH peak and ME peak significantly increased. Photoacid 2 also shows reversible changes, however the stability of this reversible change is not as good as photoacid 1.Compare with photoacid 1, and photoacid2 has an electron-withdrawing group NO_2 on the phenol moiety, which increased its initial acidity in the dark. The pK_a of photoacid 2 in the dark is 6.36, which is 1.5 units lower than that of photoacid 1. The acidity of 2 after irradiation is lower than 1, which should be due to a less efficient nucleophilic cis-ME-to-SP reaction.

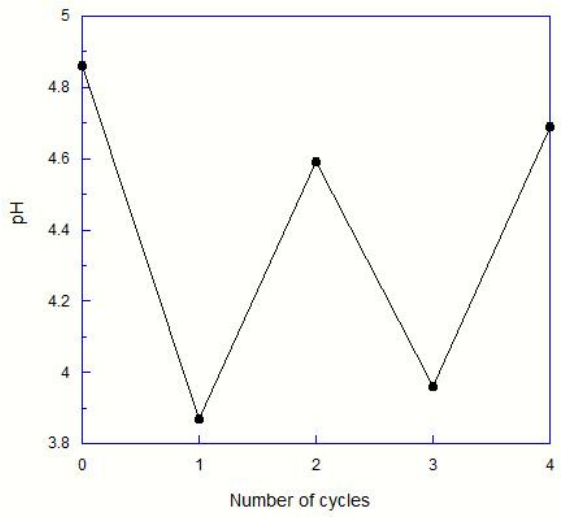

Figure 7. Cycles of pH change of photoacid 2

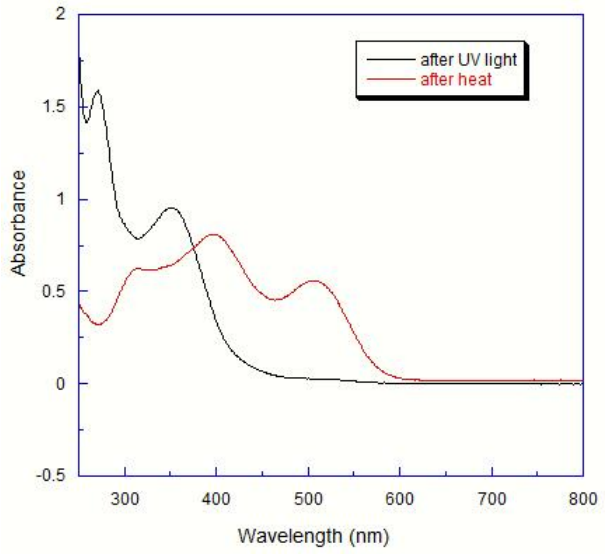

Figure 8. UV-Vis spectra of Photoacid 2 after heating

2.2.3 Study of Photoacid 3

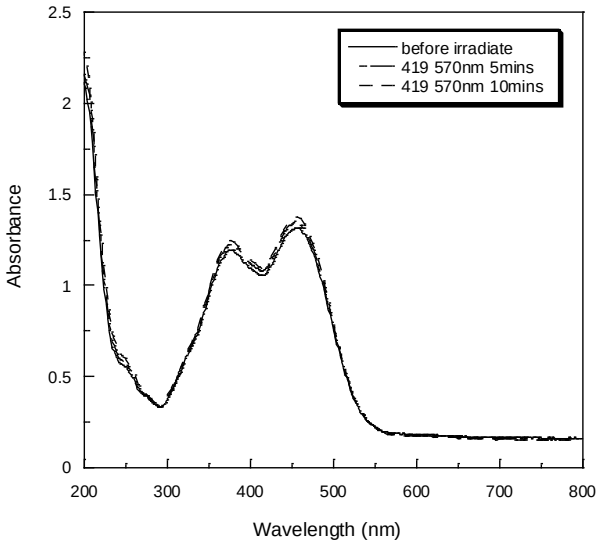

Figure 9. UV-Vis spectra of photoacid 3 in water

Compound 3 has an electron-donating group OH on the phenol moiety compare with photoacid 1. Figure 9 shows the UV-Vis spectra of photoacid 3 dissolved in water. From the spectra, there are two major bands with maxima at λ_{MEH}=390 nm and λ_{ME}=470 nm after the photoacid 3 dissolved in water. However, photo irradiation is not good enough to drive the MEH form change to the SP form in this case even with both 419 nm and 570 nm wavelength light irradiation. The reason may be the cis-MEH form cannot undergo proton dissociation under irradiation, so the cis-ME form is not able to generate.

2.2.4 Study of Photoacid 5

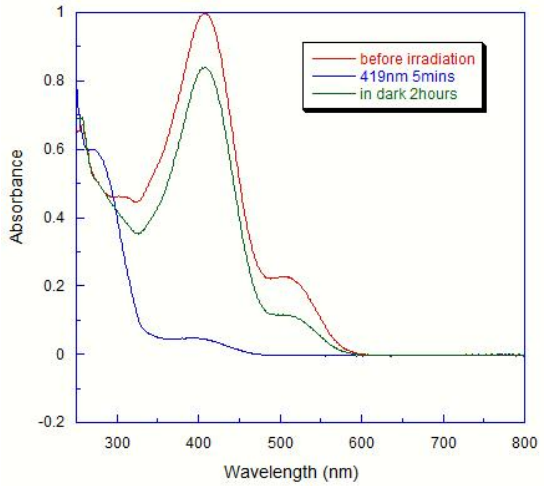

Figure 10. UV-Vis spectra of photoacid 5 in water

The solubility of photoacid 4 is too bad in both water and organic solvent to be tested. Compare photoacid 1 and 4, the only difference is the propyl sulfonate group which increases the solubility of the photoacid 1. However, the solubility of photoacid 5 is much better in water. Figure 10 is the UV-Vis spectra of an aqueous solution of photoacid 5(1.40×10^{-4} M). MEH form (λ=430 nm) is the major compound in water after dissolved in water in the dark with a small amount of ME form (λ=530 nm). After 5minutes 419 nm irradiation, both of MEH and ME peak decrease and the new peak around 300 nm increases which is assigned to SP form. The process is reversible too, but SP form of photoacid 5 took almost 2hours to revert back to MEH in the dark.

pH test provides the same result. Photoacid 5 has a pH value of 5.90 after dissolved in water, from which the pK_a was calculated to be 7.95. After irradiated by 419 nm light, pH drops to 4.53. It takes more than 1 hour to recover back to pH 5.19. Compare with photoacid 1, the reverse process of photoacid 5 is much longer. The main reason is the alkyl sulfonate groups on the nitrogen of the indoline moiety which could stabilize the open ring forms (MEH and ME)[63]. Another reason is the positive charge of N+ on the indoline moiety without the shield from SO3-

will help the nucleophilic ring-closing reaction of the phenoxy anion, and favor the forward reaction.

2.2.5 Applications of the Photoacid

Three kinds of experiments were conducted to demonstrate the application of this type of photoacid. Since this type of photoacid after irradiation will generate proton and become a strong acid, it could be used as a catalyst to catalyze a Fisher esterfication reaction. In the second type of experiment, the volume of a pH sensitive polymer was changed in this photoacid solution under different wavelength irradiation. In the last experiment, this photoacid was doped with other conductive polymer and reversibly changed its conductivity by UV or Vis irradiation. With respect to the conductive polymer, polyaniline(PANI) is one of the most studied conductive polymers due to its low cost of the monomer, tunable properties and good stability[64]. These polyaniline related experiments and results will be extensively discussed in Chapter 4.

According to previews result, the proton concentration in the solution could be directly controlled by switching the light on and off. This feature could be used to directly control the process of those reactions which need acid as a catalyst. In this application, a Fischer esterfication reaction was controlled by adding photoacid 1. Commonly used catalysts are strong acids, for example sulfuric acid or tosic acid. When the light turned on, the photoacid 1 generated protons and was a strong acid. When the light turned off, SP form reverted to MEH form and became a weak acid. Thus photoacid 1 (3.1mM) was added to a mixture of acetic acid (12.5mM) in ethanol. Ethyl acetate was generated by irradiated at 419 nm and 570 nm and the process was monitored by HPLC. Figure 11 shows the yields of the esterfication reaction were 33%, 50% and 66% after 1, 2 and 3 hours irradiation respectively. The reaction didn't happen in

the sample without light irradiation. No ethyl acetate was detected in the control experiment using photoacid 2 instead of photoacid 1 after 3 hours irradiation.

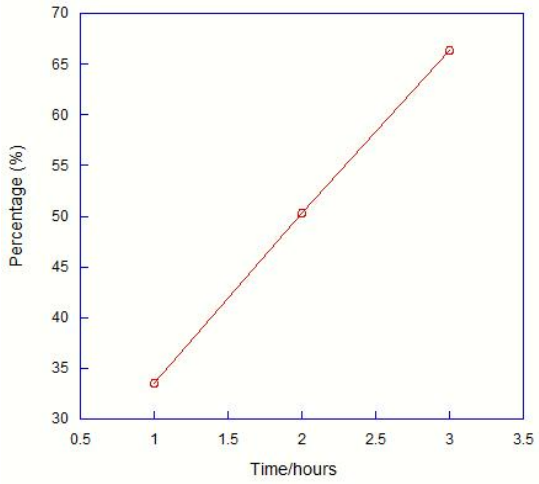

Figure 11. HPLC result of the esterfication reaction progress

With different temperature or solvent composition, various kinds of hydrogels have been observed the volume phase transition, for example discontinuous volume change.[65-71]Till the date, no experimental demonstration have been made to alter the volume of a gel by photo control the pH value of the solvent. Thus the cross-linked polyacrylamide hydrogel was prepared according to Dr. Tanaka's method[67]. Soaked in 1M NaOH solution, a copolymer of poly (acrylic acid) and polyacrylamide was partially hydrolyzed. All of the sample hydrogels were cut into similar size cuboids and then soaked in 1mg/ml photoacid 1 aqueous solution. After irradiate this solution by a 470 nmLED light, the cuboid was taken out of the solution and measured the volume on a ruler. Figure 12 shows the volume of the hydrogel shrank to almost 1/8 of its original volume. The gel didn't increase to original volume after soaking in this aqueous solution in the dark while the pH of the solution already increased. However this property is not due to the photoacid but the hydrogel. In the control experiment, the cuboid of hydrogel shrinked in strong acid solution but kept the same size in weak acid solution.

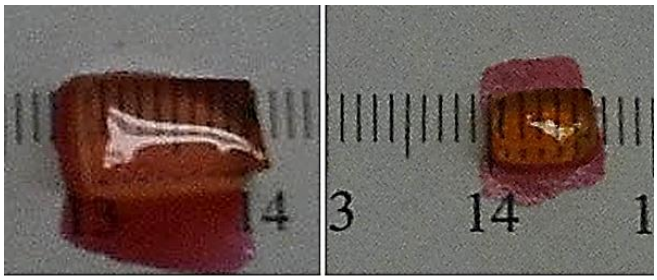

Figure 12. pH sensitive hydrogel

2.2.6 Conclusions

Instead of using UV light, a new visible light activatable photoacid was discovered and a series experiments about the proton dissociation process was investigated. According to the UV-Vis spectroscopy experiments, the half life time of the proton dissociation states was around 70 s. A sequential intramolecular reaction is the main reason to keep the proton dissociation state lifetime so long. Several photoacid have successfully altered the pH value of the whole solution by reading from a pH meter. The photoinduced pH change is around 2 units which are large enough for real applications. Two demonstration experiments were tested with this photoacid: It successfully catalyzed a Fischer esterfication reaction and shrank the volume of a pH sensitive hydrogel. More effort should be put forth to develop more useful applications based on this photoacid, such as using fiber optics or noncontact irradiation to control photoresponsive actuators or artificial muscles.

2.3 Visible Light Activatable and Thermostable Carbon Based Photoacid

2.3.1 Background

Carbanions are one of the most important intermediated in organic chemistry and are the key step in organic synthesis due to their facility in forming C-C bonds. Most of the photoacids or photoacid generators have been reported are based on oxygen acid. Although there are a few literatures reported carbon based photoacids[72-74], none of their lifetime of the proton

dissociation sate is long enough to be used in real application. Another of the potential problems of the applications of oxygen acid (such as spiropyrans) is that UV light has to be used to open the thermostable spiro form, which could cause photodegradation during the photochromic process. In addition, since the visible-light absorbing merocyanine form also absorbs UV-light, a high degree of conversion is difficult to achieve. It is desirable to develop a photochromic compound that has a thermostable form which absorbs visible light, and has a zwitterionic form. Herein we synthesized another novel photochromic compound 6(scheme 2) based on carbon photoacid.

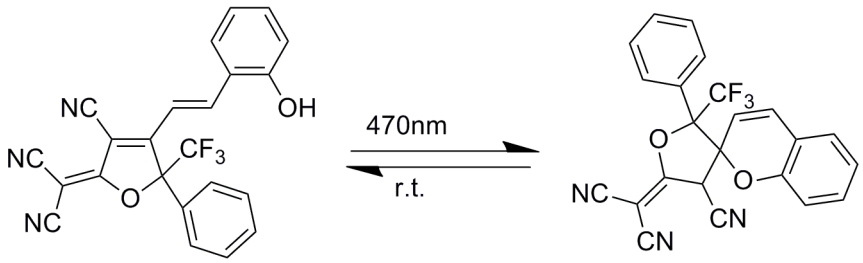

Scheme 2. Photoacid 6

This compound has a neutral and thus thermostable form that absorbs visible light. Upon visible-light irradiation, the neutral form quickly undergoes a ring-closing reaction and transforms to a UV-absorbing zwitterionic form (scheme 2). The structure of photoacid 6 consists of a tricyanofuran (TCF) moiety and a phenyl moiety, bridged by a double bond. This is a negative photochromic compound that does not belong to any category of the previously reported photochromic compounds[75]. Unlike most of the photochromic compounds, negative photochromic compounds have thermally stable forms that absorb at longer wavelengths than the products of the photochromic reactions[76]. TCF is a very strong electron acceptor that has been successfully utilized in the development of nonlinear optical[77] and fluorescent materials[78]. Its strong electron withdrawing ability makes it possible for the phenyl ring to attack the carbon

adjacent to TCF, via a nucleophilic mechanism. Compound 6was synthesized by our lab mate from a Knoevenagel reaction.

2.3.2 Results and Discussion

In EtOH, compound 6has a maximum absorption (λ_{max}) at 470nm (Figure 13). To study the photochromic behavior of this compound, a 4.37×10^{-5}M solution was irradiated with a 470 nm LED array. Prolonged irradiation did not significantly increase the conversion, which is due to the reverse thermal reaction at room temperature. The cyclized zwitterionic form has a λ_{max} at 310 nm. It lowly transformed back to photoacid 6 at room temperature in dark. UV-Vis spectra were recorded every 12 seconds after 5mins irradiation, and the concentrations of 6 in the first 1.6min were fitted in a first order kinetic equation. A rate constant k =0.9511 min^{-1} was obtained, and thus the half-life ($t_{1/2}$) of 6 was calculated to be 0.693/k = 0.73 min. However, the intensity of the absorption peak at 470 nm was lower than that of the solution before irradiation, while the intensity of the small shoulder at 340 nm increased. When the solution that has been kept in the dark overnight was irradiated at 470 nm again, its UV-Vis spectrum was identical to that of the first-time irradiation; thus, the process is truly reversible. Therefore, we concluded that the small change of the UV-Vis spectrum is not due to decomposition. It may be due to the presence of a small amount of the cis-isomer of 6.

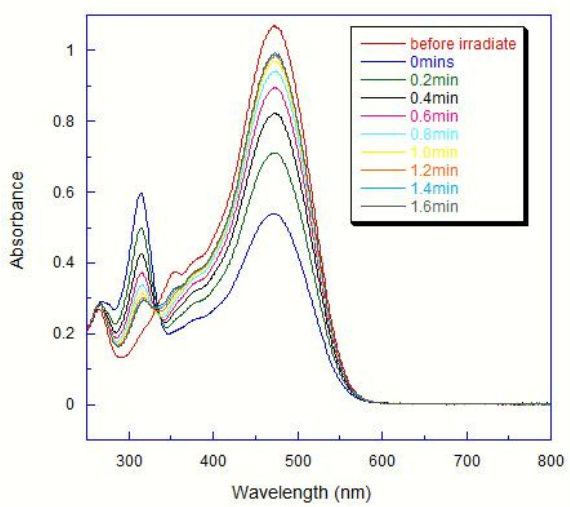

Figure 13. UV Spectra of photoacid 6 in EtOH

Photoacid 6 has very bad solubility in water but dissolves very well in ethanol. So the UV-Vis spectrum and pH test were run in ethanol. After dissolved in ethanol, photoacid 6 is the predominant in the dark, which is indicated by the UV-Vis (Figure 13). A 1.19×10^{-4} M ethanol solution of photoacid 6 has a pH value of 4.70. When the solution was irradiated with 470nm light, pH drops more than 2.5 units to 2.08. When the lights turned off, the pH value increased back to 4.80 in 10 minutes. According to H. Goldschmidt's work[79], ethanol is about 400 times as weak a base as water. The pH number here may not be very precise, but the pH change value is very trustable. More than 2.5 units' difference indicates photoacid 6 generates proton large enough to be used in different applications. This cycle can be repeated many times (Figure 14).

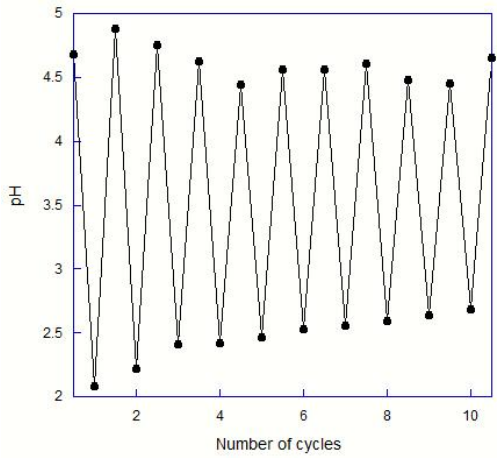

Figure 14. Cycle of pH change under irradiation and in the dark

This kind of photoacid has good solubility in organic solution which could be mixed with other organic pH indicator. The photoacid will donate proton after irradiated by visible light which will change the pH indicator color directly. From the UV-Vis spectrum, the change could be observed clearly (Figure 15). The green line is a 10% pH indicator bromophenol blue sodium salt UV-Vis spectrum in ethanol. There are two major peaks at 600 nm and 430 nm. The peak at 600 nm will not overlap with photoacid 6 UV-Vis spectrum, which could be an indicator to monitor the change of photoacid. The red line is the UV-Vis spectrum of the mixture solution of photoacid (3.97×10^{-5} M) and indicator, which shows a small peak around 600 nm. After irradiated by 470 nm for 5mins, this small peak disappeared and an absorption peak at 300 nm increased, which should be the zwitterionic form based on the UV-Vis spectrum of Figure 13. In the dark, the absorption intensity of 600 nm peak recovered to the level before irradiation in around 10mins. The 300 nm peak decreased to the initial level too. Based on these result, this photoacid could dope with corresponding pH indicator and cast into films which will indicate the pH and change color at the same time. More efforts need to be put into this study to demonstrate the real application.

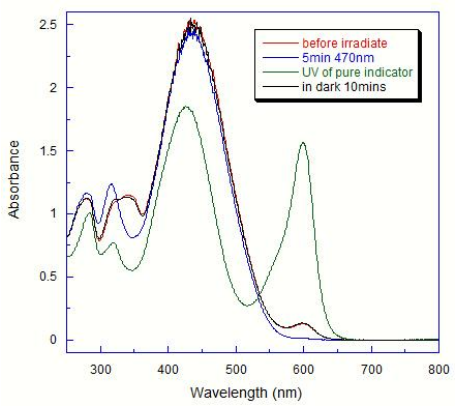

Figure 15. Photoacid 6 with indicator

2.3.3 Conclusions

In conclusion, this novel photoacid compound based on carbon acid transforms to a cyclic zwitterionic form upon visible light irradiation. High degree of conversion and reversibility were demonstrated. Photoacid 6 could be used as a basis for designing desirable photochromic compounds by varying the electron withdrawing moiety and heteroaromatic moiety accordingly. Doped with corresponding pH indicator could vivid monitor the pH change by switching the visible light on and off.

CHAPTER 3. MECHANISTIC STUDY OF PHOTO RETRO-DIELS-ALDER REACTION

3.1 Introduction

The Diels-Alder reaction is a powerful reaction for generate the carbon-carbon bonds in the organic synthesis, which allows facile, stereospecific entry into six-member ring systems. At the early of 20th century[80-84],numerous near-discoveries about the [4+2] cycloaddition reaction was reported by several luminaries in organic chemistry area. Otto Diels and Kurt Alder properly indentified the products from the reaction of cyclopentadiene with quinone and brought the famous reaction that would bear their names[85]. Diels and Alder anticipated the importance of this discovery for the nature product synthesis in this paper: "Thus it appears to us that the possibility of synthesis of complex compounds related to or identical with natural products such as terpenes, sesquiterpenes, perhaps even alkaloids, has been moved to the near prospect." Because of this important discovery, Otto Diels and Kurt Alder received the Nobel Prize in 1950. In 1952, R.B. Woodward *et al.* discover the historic routes to synthesize steroids cortisone and cholesterol[86] which open a truly visionary application for the Diels-Alder reaction. In this paper, Woodward recognized that by using a differentiated quinone nuleus could regioselective control the intermolecular Diels-Alder union. Since then, more than 17000 papers have been published concerning synthetic, mechanistic and theoretical aspects of the reaction[87].

The classical Diels-Alder reaction is a cycloaddition between a conjugated diene and a dienophile (Scheme 3). Hetero-Diels-Alder reaction is a cycloaddition reaction when one or more heteroatoms are present in the diene and/or dienophile.

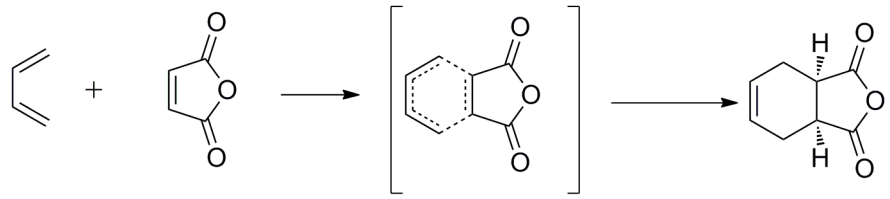

Scheme 3. A Diels-Alder reaction

The Diels-Alder reaction is reversible and the cycloreversion occurs when the diene and/or dienophile are particularly stable molecules or when one of them can be easily removed by consumed in a subsequent reaction. The retro-Diels-Alder (rDA) reaction is almost as old as Diels-Alder reaction when Diels and Alder observed the adduct from furan and maleic anhydride dissociated at its melting point of 125 ℃at 1929[88]. In 1937, Alder and Rickert summarized the retro-Diels-Alder reaction[89].Usually, rDA reaction requires high temperature to surmount the high activation barrier of the cycloreversion. It's still a powerful synthetic tool and has been used for preparing many reactive, strained and metastable chemicals[90-95]. As an unimolecular process, rDA reaction could achieve high yield in solid state since it will not affected by diffusion rate. Also rDA reaction does not require addition of any other reagents such as acids, bases or catalysts which is not possible in processing solid materials or will cause contamination. So rDA reactions have been widely applied to many areas of materials science[96-103].

According to the Woodward-Hoffman rules[104], if a reversible DA process proceeds via a concerted mechanism, it is thermally allowed and photochemically forbidden. However, the Woodward-Hoffman rules cannot be applied to a stepwise or a nonadiabatic mechanism, which are both common to organic photoreactions. In fact, photo-rDA (PrDA) reactions have been sparsely reported in literature[96, 105-107]. For example, Nozaki and Kato reported that the DA adduct of anthracene and styrene yielded anthracene under photoirradiation, while the adduct of anthracene and 2-butene is photostable[106]. Jones *et al.* published PrDA reactions of a chiral

compound that may be used as a chiral auxiliary[105]. Recently, Nakagawa *et al.* demonstrated a photoinducible HNO releasing agent based on a PrDA reaction[96].

The PrDA reaction, which allows spatial and temporal control, may find applications in photoresponsive materials, photolithography, drug delivery and mechanistic research[108]. Although individual cases of PrDA reactions have been reported, no systematic study of PrDA reactions has been done either experimentally or theoretically, and no quantum yield of any PrDA reaction has been reported. Consequently, there was no guide to predict whether a compound could undergo PrDA reaction. All of these factors obstruct the wide application of PrDA reactions in chemistry and materials science. This chapter will focus on the structure-reactivity relationship and the mechanism of the PrDA reaction, which may help researchers design photoresponsive materials. One example application based on these photoresponsive materials will be present at the end.

3.2 Mechanistic Study

A variety of normal-electron-demand DA adducts were prepared by our lab[109-113], and systematic mechanistic studies about these components on the PrDA reaction was performed (Scheme 4). Aromatic DA adducts were used since they can efficiently absorb at 254 nm, which was the wavelength chosen for measuring the quantum yields of these photoreactions. These DA adducts were prepared by mixing the corresponding dienophiles and aromatic dienes at room temperature or elevated temperatures.

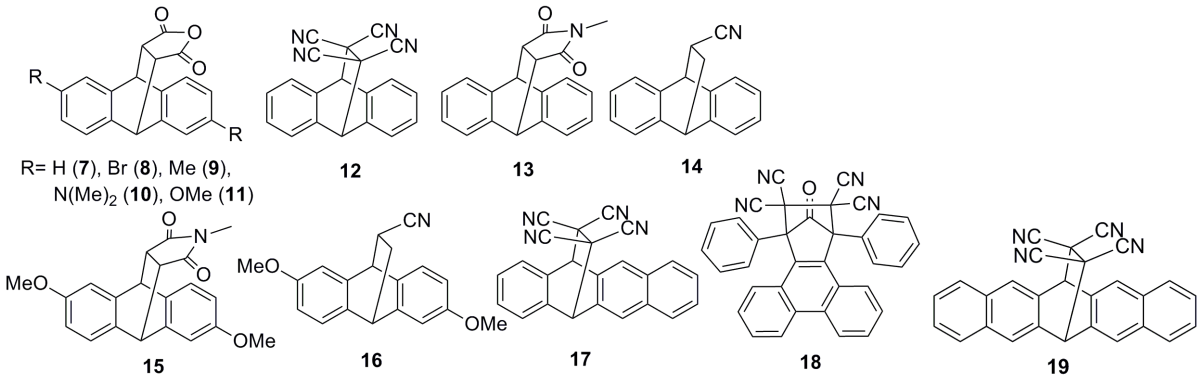

Scheme 4. Structures of the studied DA adducts

3.2.1 Study Based on TCNE and Polyaromatics

All of these compounds' quantum yields in acetonitrile were measured by the chemical actinometry method. The actinometer was uridine, which is hydrated under UV irradiation with a known quantum yield of 0.018 at 254 nm[114, 115].All of the solution was degassed by freeze-thaw method and kept in an inert atmosphere. The 254 nm UV lamp is only 8 W and the reaction was conducted in a ventilation hood. Under these conditions, photo heating effect can be ignored and the "total absorption" required for measuring quantum yield with chemical actinometry can be achieved.

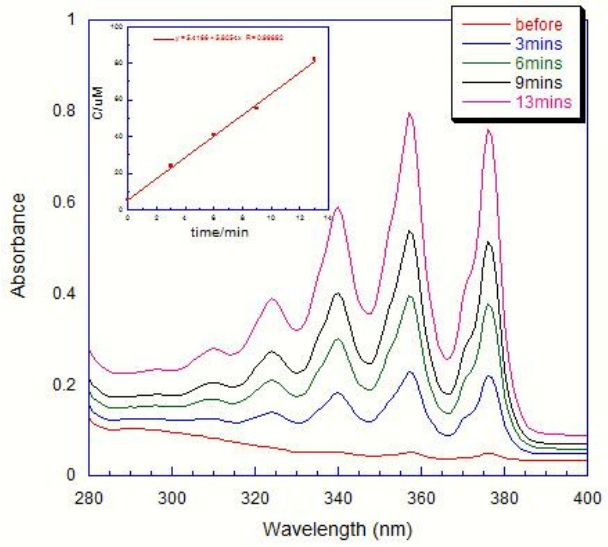

Figure 16. UV-Vis absorption change of TCNE/anthracene adduct (12)

Figure 16 is a UV-Vis absorption change of TCNE/anthracene (3.24×10^{-3} M) solutions after irradiated by 254 nm UV light. The 254nm UV-Vis absorption of all of the DA adduct solutions are more than 2. The transmission of the solution is more than 100 according to the Beer-Lambert law which is account as "total absorption" for quantum yield measurement. These DA adduct solutions do not have specific absorption above 300nm. However, the product anthracene solution has multiple strong peaks between 300nm and 400nm which could be used to monitor the reaction process. One challenge of analyzing PrDA reaction of the TCNE adducts is that TCNE reacts with these dienes so fast that any PrDA products will immediately undergo DA reaction and change back to the DA adduct unless the product is stabilized or reacts with other reagents. Previous work by Brown and Cookson showed that this problem can be solved by adding a small amount of methanol, which prevents the reverse reaction by quickly reacting with TCNE and allows the analysis of the aromatic dienes[116]. Thus the solution was a 1:4 mixture of methanol and acetonitrile. The inserted figure in Figure 16 is a linear relationship indicates a "total absorption" condition in the early stage of the reaction. TCNE/anthracene adduct

underwent PrDA reaction quickly with a quantum yield of 0.021. A control in darkness did not show any reaction during the test time.

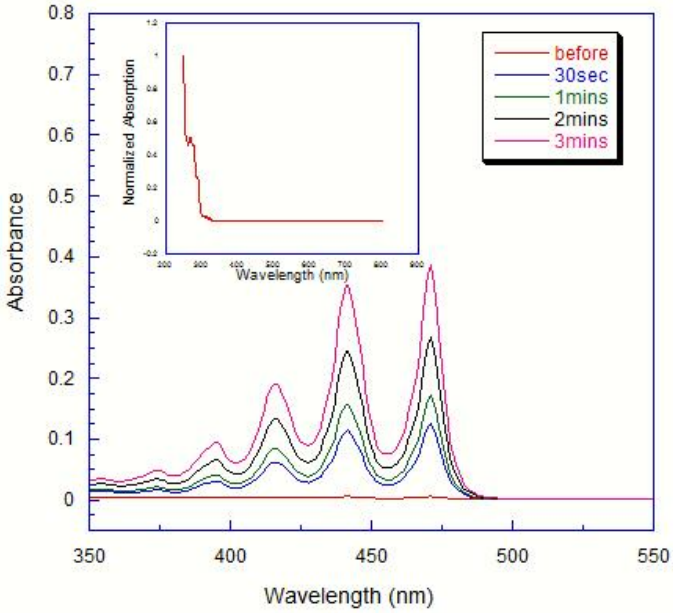

Figure 17. UV-Vis absorption change of TCNE/naphthacene adduct (17)(The insert graph is the UV-Vis spectra of 17)

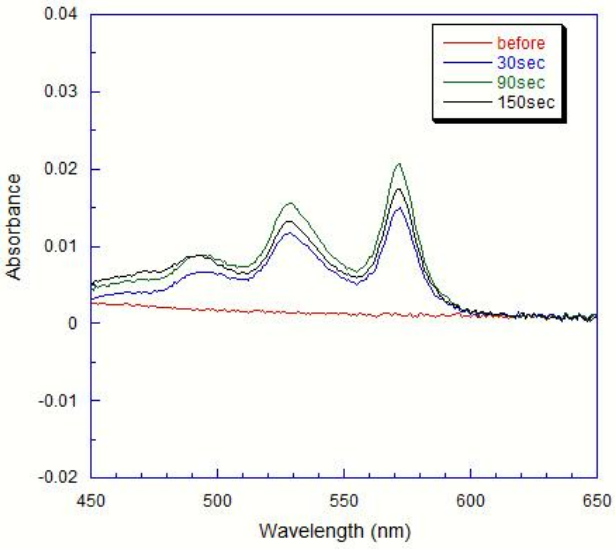

Figure 18. UV-Vis absorption change of TCNE/pentacene adduct (19)

Figure 17 shows the UV-Vis change of TCNE/naphthacene adduct after 254nm UV light irradiation. The insert figure is the UV-Vis absorption of DA adduct before irradiation and the extinction coefficient at 254nm is 1.24×10^4 M^{-1} cm^{-1}. The UV-Vis absorption of naphthacene product red shifts to 400 nm to 500 nm range compare with anthracene. Surprisingly, the PrDA reaction of the thermally more stable TCNE/naphthacene adduct was even faster than TCNE/anthracene adduct. The quantum yield (Φ=0.185) is nearly an order of magnitude higher than the anthracene adduct. Figure 18 is the UV-Vis change of TCNE/pentacene adduct after 254 nm UV light irradiation. Product pentacene has strong absorbance between 450 nm and 650 nm, however the solubility of pentacene is very low which makes the UV-Vis absorbance of pentacene is very low. On the other hand, since the most of the product precipitates out, this PrDA reaction is more straightforward. The quantum yield of TCNE/pentacene (Φ=0.019) is close to that of TCNE/anthracene adduct.

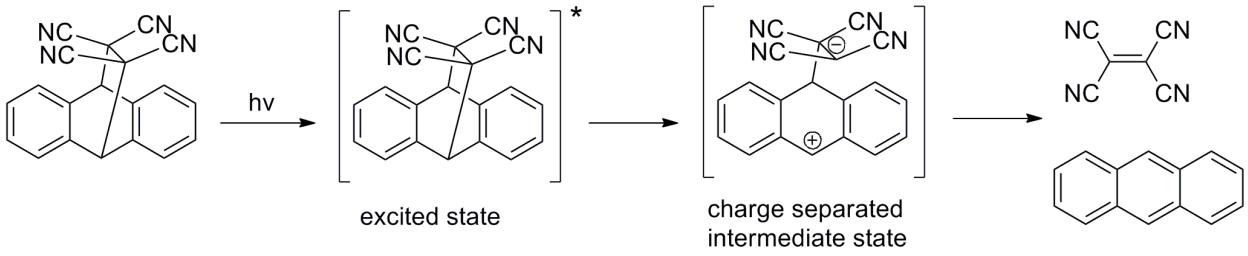

Scheme 5. A step-wise PrDA mechanism of TCNE/anthracene

The trend of the quantum yields (TCNE/naphthacene> TCNE/anthracene ≥ TCNE/pentacene) can be qualitatively explained by a tradeoff between the stability of the charge-separated intermediate states and the stability of the DA adducts (Scheme 5). The more stable the charge-separated intermediate state is, the higher the photo reactivity is; while the more stable the DA adduct is, the lower the photo reactivity is. The stability of the charge-separated intermediate states increases in the order of TCNE/anthracene< TCNE/naphthacene< TCNE/pentacene due to

the increased number of resonance structures. (The numbers of resonance structures for the charge separated intermediate states are 7, 9 and 11 for TCNE/anthracene, TCNE/naphthacene and TCNE/pentacene respectively.) The DA adduct stability may be estimated by the difference between the resonance energy of the DA adduct (starting material) and that of the polyaromatic compound (product). (Since all three compounds produce TCNE, the resonance energy of TCNE can be ignored when we compare the stability among them.) The resonance energy of a DA adduct approximately equals to the sum of its aromatic moieties. For example, the resonance energy of the TCNE/naphthacene adduct is close to the resonance energy of a benzene plus that of a naphthalene. We calculated the resonance energy difference (polyaromatic product - DA adduct) based on the data reported by Herndon and Hosoya[117], and the results are -0.11, -0.37, and -0.66 eV for TCNE/anthracene, TCNE/naphthacene, TCNE/pentacene systems respectively. The loss of resonance energy disfavors the rDA reaction and thus increases the stability of the DA adduct. Therefore the stability of the DA adducts increase in the order of TCNE/anthracene< TCNE/naphthacene< TCNE/pentacene due to increased loss of resonance energy. In fact, TCNE/anthracene adduct undergoes rDA reaction slowly at room temperature and quickly at 40-60 ℃ [116] while the other two adducts are thermally stable. The different trend of the thermal reactivity supports that the observed reactions are indeed photo reactions rather than photothermal ones. One can see that the stability of the charge-separated intermediate states and the stability of the DA adducts have the same trend while opposite effects on PrDA reactivity, which may explain why TCNE/naphthacene adduct that has medium stability of the charge-separated intermediate state and medium stability of the DA adducts showed the highest quantum yield. The more detailed research about this charge separated mechanism will be performed in next study.

3.2.2 Study on Electronic Effects of the Diene and Dienophile

On the other side, electronic effects of the diene and dienophile components on the PrDA reactivity were studied too. The electronic effects of the diene component were examined by varying the 2,6-substituents of the anthracenes. Maleic anhydride was used as the common dienophile in this study because the DA adduct of maleic anhydride and unsubstituted anthracene (7 in Scheme 4) undergo PrDA reaction with a moderate quantum yield of 0.0057 under 254 nm UV irradiation (Figure 19).DA adduct 7 doesn't have any strong absorption above 300 nm and the extinction coefficient at 254 nm is 4.54×10^{2} M^{-1} cm^{-1} (insert figure of Figure 19). When electron donating substituents were introduced, the PrDA reactivity was enhanced. DA adducts of 2,6-dimethyl (9) (Figure 20), tetramethyl-diamino (10) (Figure 21), and dimethoxy (11) anthracenes showed quantum yields of 0.0068, 0.0157, and 0.023, respectively. The extinction coefficient of 9, 10, and 11 at 254 nm is 9.46×10^{2} M^{-1} cm^{-1}, 1.36×10^{4} M^{-1} cm^{-1}, 2.41×10^{3} M^{-1} cm^{-1}, respectively. When the substituent was Br, a weak electron withdrawing group, DA adduct 8 was photostable. The quantum yields of the DA adducts and the Hammett para-substituent constants[118] of the corresponding substituents are listed in Table 1. Hammetpara-substituents constants were measured by Dr.Weng's lab. The trend of the PrDA reactivity is consistent with the trend of the Hammett substituent constants (Table 1).The low reactivity of 2 may also be due to intersystem crossing, which is enhanced by the heavy bromine atoms.

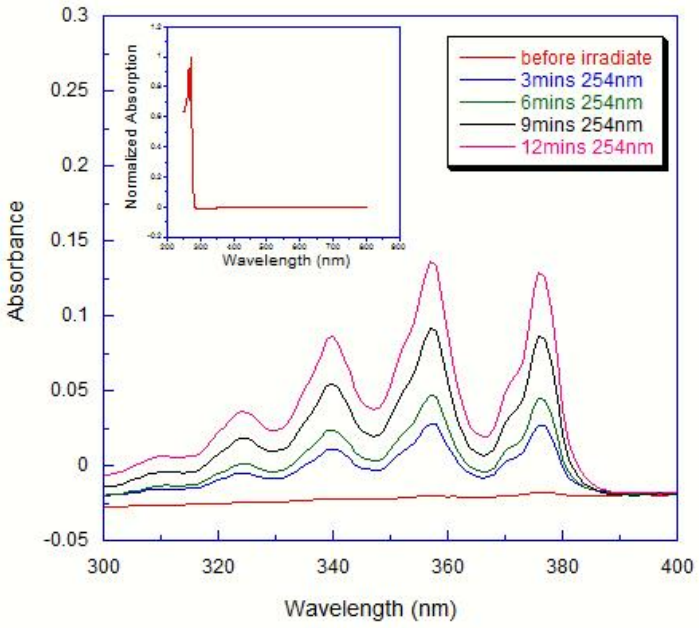

Figure 19. UV-Vis absorption change of DA adduct 7 after 254 nm UV light irradiation (The insert graph is the UV-Vis spectra of 7)

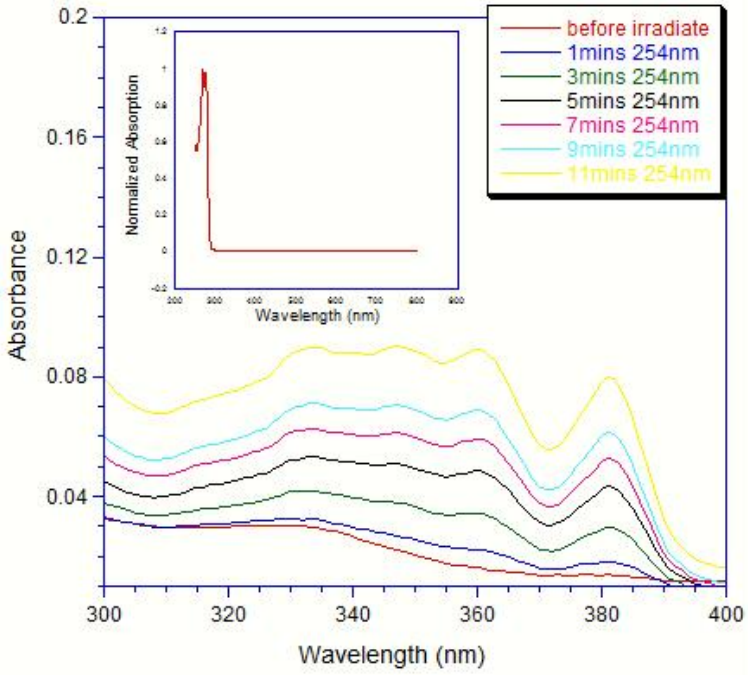

Figure 20. UV-Vis absorption change of DA adduct 9 after 254 nm UV light irradiation (The insert graph is the UV-Vis spectra of 9)

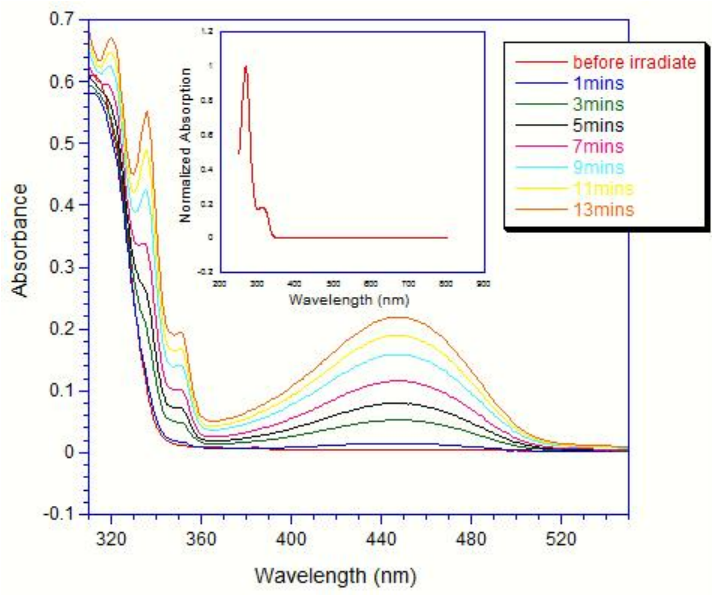

Figure 21. UV-Vis absorption change of DA adduct 10 after 254 nm UV light irradiation (The insert graph is the UV-Vis spectra of 10)

The electronic effects of the dienophile component were also studied. DA adducts of dienophiles including acrylonitrile (14), *N*-methyl maleimide (13), maleic anhydride (7) and tetracyanoethylene (TCNE) (12) were prepared using unsubstituted anthracene as the common diene. Among the dienophiles, TCNE has the strongest electron withdrawing ability and the adduct (12) has a quantum yield of 0.021 (Table 2). Maleic anhydride is less electron deficient than TCNE. As described above, maleic anhydride/anthracene adduct 7 was also photoactive. However, the quantum yield (0.0057) was significantly smaller than that of the TCNE adduct. When the electron-withdrawing ability of the dienophile was further reduced, as in N-methylmaleimide/anthracene adduct 13 and acrylonitrile/anthracene adduct 14, the adducts became photostable.

Table 1. Quantum yields and Hammett para substituent constants of the DA adducts of substituted anthracenes and maleic anhydride

DA adducts	Substituent	Hammett constant σ_p	Φ
8	Br	+0.232	X[a]
7	H	0	0.0057
9	Me	-0.170	0.0068
10	$N(Me)_2$	-0.205	0.016
11	OMe	-0.268	0.023

[a] The quantum yield is too low to be measured because prolonged irradiation caused unidentified side reactions.

Table 2. Quantum yields of the DA adducts studied to understand the electronic effects of the dienophile

DA adducts	Φ
12	0.021
7	0.0057
13	X[a]
14	X[a]
15	0.0094
16	0.0015

[a]The quantum yield is too low to be measured because prolonged irradiation caused unidentified side reactions.

The results indicate that the PrDA reactivity of a DA adduct depends on both the electron-donating ability of the diene and the electron-withdrawing ability of the dienophile. If this structure-reactivity relationship holds, DA adducts of weakly electron-withdrawing dienophiles may become photoactive when a strong electron-donating diene is used, and adducts of weakly electron-donating dienes may become photoactive when a strong electron-withdrawing dienophile is used. To test this, adducts of *N*-methyl-maleimide/2, 6-dimethoxy-anthracene (15) and acrylonitrile/2,6-dimethoxy-anthracene (16) were studied since the adducts of *N*-methyl-maleimide/anthracene (13) and acrylonitrile/anthracene (14) are photostable. When the electron-rich dimethoxyanthracene was used as the diene, the DA adduct of *N*-methyl-maleimide (15) underwent PrDA reaction with a moderate quantum yield of 0.0094(Figure 22) and extinction coefficient at 254 nm is 1.34×10^3 M^{-1} cm^{-1}. Even acrylonitrile adduct 16 became photoactive, although the quantum yield was low (Φ=0.0015).

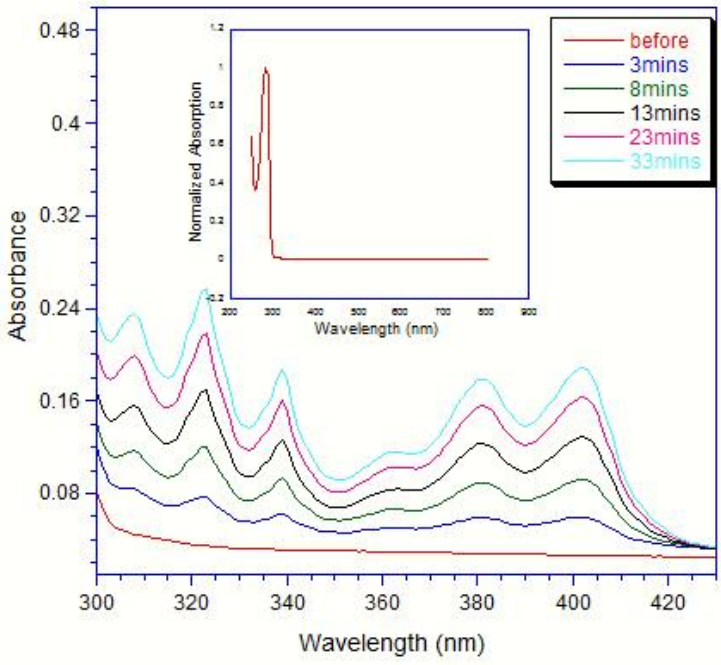

Figure 22. UV-Vis absorption change of DA adduct 15 after 254 nm UV light irradiation (The insert graph is the UV-Vis spectra of 15)

The structure-reactivity relationship also indicates that mechanism may involve a charge separated intermediate, on which a positive charge is localized on the diene and a negative charge on the dienophile. One might think that the structure-reactivity relationship could be a result of the relative thermal stabilities of the DA adduct since the mechanism is a nonadiabatic one. However, we found that the DA adduct of naphthacene and TCNE (17) has a PrDA quantum yield of 0.18, which is much higher than that of 12 (0.021), while 11 is obviously more thermally stable than 6, which slowly decomposes at room temperature. The higher photoreactivity of 11 than 6 can be contributed to the extended aromatic structure that stabilizes the positive charge in the intermediate. To determine the structure of the charge-separated intermediate, the adduct 17 was irradiated in a solution of 20% of methanol in acetonitrile for an extended time. Large amount of methanol was used to trap the intermediate. The product was analyzed by GC-Mass. Besides the expected PrDA products, a product showed a fragment with m/e=259.0, which is the mass of the cation resulting from the fragmentation of the trapped intermediate (a in Scheme 6). More convincing evidence was obtained from the reaction of 18, which is a DA adduct of TCNE and phencyclone. Photo-irradiation of TCNE/phencyclone adduct also yielded the PrDA product, phencyclone. However, phencyclone was only a minor product. The major product was the compound in scheme 6, which is resulted from a nucleophilic reaction of methanol. After 8 hrs irradiation, the product is a mixture of approximately 3:1 compound (b) and phencyclone together with a small amount of unidentified side products.

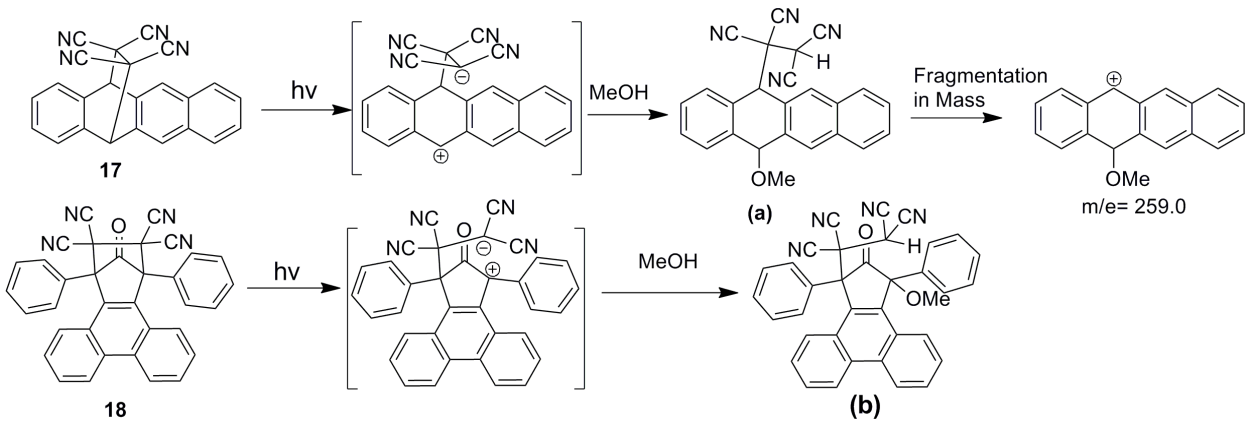

Scheme 6. Trapping the charge-separated intermediate in the PrDA reactions of 17 and 18

Further more oxygen quenching experiments were conducted to understand the excited states involved in the reaction. A solution of 17 saturated with air was irradiated for 5 min and was compared to a carefully degassed solution irradiated under the same conditions. The UV absorption of naphthacene, the product of the PrDA reaction, was only slightly lower than that of the degassed sample, which is due to the oxidation of naphthacene. Since oxygen does not quench the PrDA reaction, the reaction does not involve a triplet state. This result is consistent with the charge-separated intermediate a shown in Scheme 6. The intermediate must be in a singlet state since all the electrons are paired. Therefore it is unlikely that is from a triplet excited state. The excited states of 17 were further studied by femtosecond time-resolved absorption spectroscopy by Dr.Weng's lab and the results also support the charge separated intermediate mechanism. On the basis of all the results, the PrDA reaction mechanism is proposed in Scheme 7.

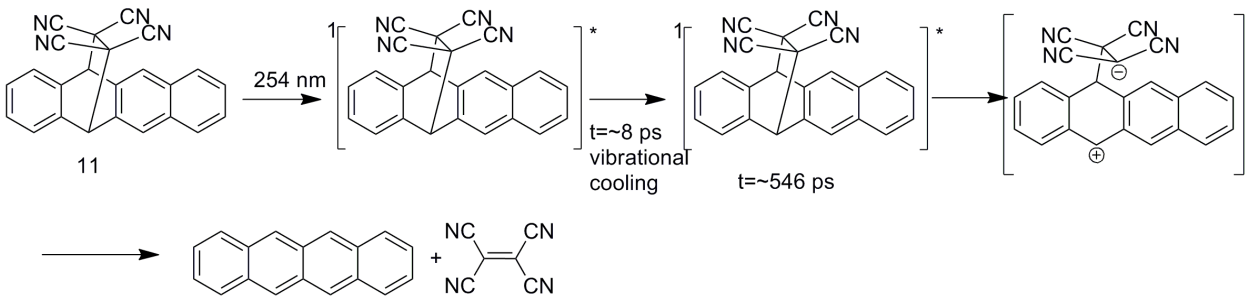

Scheme 7. Proposed mechanism of the PrDA reaction of 11

Based on these studies, the photoactivity depends on the electron-withdrawing ability of the dienophile component and the electron-donating ability of the diene component. The mechanism was studied by trapping the reaction intermediate, O_2 quenching and femtosecond time-resolved absorption spectroscopy. All the results support a mechanism that involves a charge-separated intermediate generated from a singlet excited state. It may be worth mentioning that we used 254 nm light for all of the PrDA adducts so that their photoactivities could be compared. However, if a high reaction yield is desired, 254 nm may not be a suitable wavelength for some of the DA adducts due to the strong absorption of the products at this wavelength. For real applications, a suitable wavelength must be carefully chosen so that only the reactant absorbs strongly at this wavelength, while the products do not or only weakly absorb. In biology environment, a visible light instead of UV light will be more preferred since it will bring less damage to the tissue and less toxic. Based on this PrDA reaction, a novel CO-releasing material was designed and studied.

3.3 CO-releasing Materials Based on PrDA Reaction

3.3.1 Background

The use of gaseous molecules in biological and therapeutic field has attracted great attention in recent years. At the beginning of last century, John Haldane first described the physiological effects of carbon monoxide (CO) on the human body through its binding to hemoglobin[35]. For

decades CO has been viewed as a “silent killer” owing to its strong affinity with hemoglobin. But at the end of last century, it became clear that CO has versatile properties as a signaling mediator and participates in many important biological processes [36, 119].

The mere mention of CO as a potential therapeutic that imparts potent beneficial effects draws even greater attention when it is presented as a clinically viable medicinal agent. However, other gases are already in clinical use or in clinical development, such as nitric oxide (NO) and hydrogen sulphide (H_2S). Around twenty years ago, people found NO works as a messenger in processes essential for almost all living organisms, including humans [120, 121]. NO relaxes blood vessel walls and regulates blood pressure in mammals. In 1998, the Nobel Prize in Medicine was awarded to scientists who discovered NO physiological functions for its important roles in biology and medicine. Organic NO-releasing compounds which have similar life-saving effects to nitroprusside in the treatment of angina pectoris, have been synthesized and studied extensively, as well[122]. Hydrogen sulphide (H_2S), produced from L-cysteine in mammalian cells, have shown anti-apoptotic and anti-inflammatory effects, and novel H_2S releasing molecules have been developed[123, 124].

The advantage of using CO for therapeutic purposes stems from its unique chemistry, because unlike NO and H_2S, which interact indiscriminately with several intracellular targets, CO reacts exclusively with transition metals. Because of its inherent chemical reactivity, CO is a relatively stable molecule compared with NO and H_2S. It primarily targets metals with a specific redox state, (for example iron), offering more flexibility and versatility for the development of CO-based pharmaceuticals. There is a steadily increasing interest in new complexes as solid storage forms for carbon monoxide[119]. The challenge is to develop non-cytotoxic water-soluble compounds that release CO relatively fast, with half lives of less than two hours; slower release

is unlikely to result in a high enough CO concentration from an acceptable CO-releasing molecules (CO-RMs) concentration, due to CO circulation within the body and the reduction in effective CO concentration by complexation with heme.

Until now, there have been two major types of CORMs, one of which is transition metal carbonyl complexes[125, 126]. This class of compounds formed the basis for the design of CORM as therapeutic agent aimed at delivering controlled amounts of CO to tissues and organs. However, most of this type of CORMs are metal carbonyls. Introducing heavy metals to the human body could lead to severe side effects even though these CORMs have shown relatively low cytotoxicity in vitro. In addition, control of the CO release is difficult, since the affinities of the multiple COs bonded to the metal center in any of the CORMs are different, and metal carbonyls often have low stability in biological fluids[127].

The other type is comprised of main group element compounds, which is very rare. Boranocarbonate and its derivatives are so far the only compounds studied that release CO at a reasonable rate under physiological conditions. The formation of the CO adduct of borane H_3B-CO in significant amounts was described in the 1969 by Parry and Malone [128]. This type of CORMs is less studied than the metal compounds perhaps because H_3BCO_3 is difficult to synthesize and handle. It has been proposed that boranocabonate could be transformed into esters or amides to introduce targeting moieties for delivering CO to specific targets [129]. However, no progress has been reported.

In the manipulation of complex biological systems with externally applied chemical agents, it's of great important to control the agent's activity. This may be achieved by the precise control of spatial and temporal aspects, as well as the amount, of each dose delivered. This is why a

precursor which could be activated only by light otherwise stable is very attractive in drug design. Some manganese carbonyl complexes such as $Mn_2(CO)_{10}$ and $[Mn(CO)_3(tpm)]PF_6$ release CO upon photo-irradiation[130].This is a desirable property since it promises precise spatial and temporal control of CO release. However, These CORMs need ultra-violet (UV) light to release CO, which is apparently undesirable for biological applications. Herein a novel unsaturated cyclic *a*-diketones encapsulated in micelles are effective CORMs that can be activated by visible light. Unlike most of previously developed CORMs, the materials reported here are organic compounds, which promises easy modification and relatively low toxicity.

3.3.2 Vitro and Vivo Testing of PrDA Adducts

The unsaturated cyclic *a*-diketones (DKs) were prepared by our lab mates and the structures of these DKs list in Scheme 8. This type of diketone is known to undergo a photoreaction that releases CO (Scheme 8), and the mechanism has been previously studied [131, 132]. Upon irradiation at a wavelength in the absorption band of its n-π* transition (400-550 nm), the diketones release two CO molecules and generate anthracene derivatives. It is worth mentioning that unlike many polycyclic aromatic hydrocarbons, anthracene, is not acutely toxic, carcinogenic, or mutagenic[133]. Although the anthracene derivatives could be more or less toxic than anthracene, it is reasonable to expect that the remaining chemicals after CO release could have low toxicity, at least for some diketones, which is one of the advantages of these CORMs.

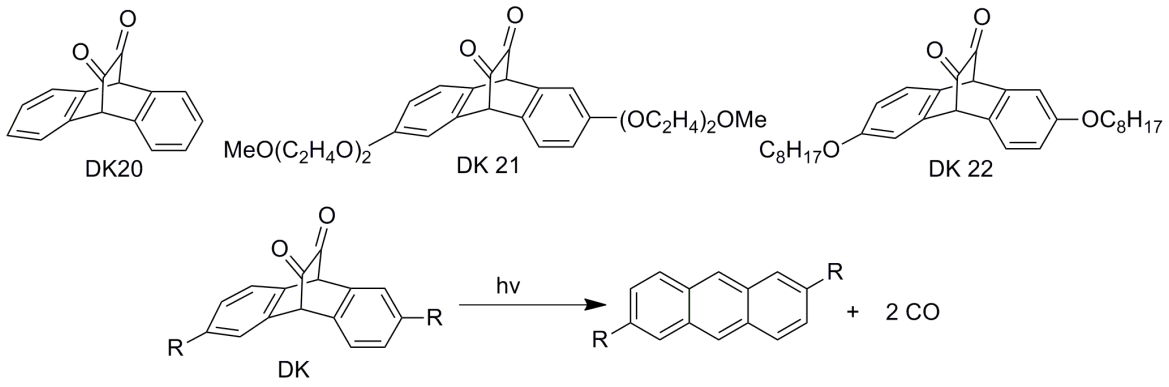

Scheme 8. Structures of the studied DKs and the PrDA reaction of DKs

The photochemical reactions of DKs are examined in DMSO, acetonitrile and dichloromethane (DCM) solutions. UV-Vis spectra showed that the expected photoreactions occurred for all the three compounds. The absorption spectrum of DK22 in DMSO is shown in Figure 23. The absorption of the n-π^* transition is between 400 nm and 550 nm with a maximum (λ_{max}) at 465 nm. After irradiation with a 470 nm LED array (Elixa, Ltd.) for 10 min, the absorption of DK3 disappeared completely and the UV-Vis spectrum matched that of 2,6-bis(octyloxy)anthracene, which means the photoreaction occurred quantitatively in the organic solvents.

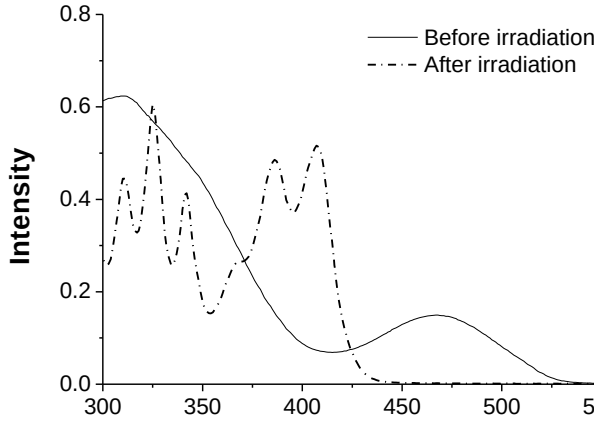

Figure 23. Absorption of DK22 in DMSO solution before and after irradiation at 470 nm

To test the CO releasing capability of DKs in aqueous media, DK21, which has two hydrophilic PEG chains, was dissolved in DMSO (1%)/water mixture. The absorption peak at 465 nm

disappeared in the UV-Vis spectrum of the solution (Figure 24), and photo-irradiation at 470 nm, 419 nm, 365 nm and 254 nm did not generate the corresponding anthracene derivative. Addition of DMSO to the solution regenerated the absorption peak at 465 nm, which indicates that the deactivation of the diketone is most likely due to reversible hydration of the carbonyl groups. All ketones form equilibrium with the corresponding hydrates in water, in which the ketone form is often predominant. However, in the *a*-diketones, one of the carbonyl groups is activated by the other one, which shifts the equilibrium to the hydrates.

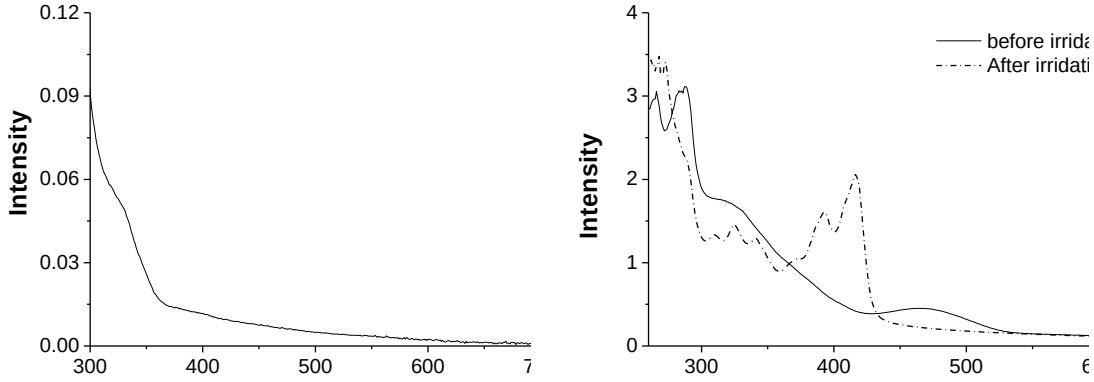

Figure 24. UV-Vis spectrum of DK21 in 1% DMSO/water mixture (left), and UV-Vis spectrum of aqueous solutions of Pluronic encapsulated DK22 before and after irradiation (right)

To solve this problem, DKs were encapsulated in Pluronic F127 micelle following a literature method[134]. Pluronics are biocompatible block copolymers of polyethylene oxide and polypropylene oxide, which have been widely used as carriers for drug delivery[135, 136].The inner environment of Pluronic micelle is hydrophobic and thus can protect the DKs from hydration. In addition, encapsulating DKs in Pluronic micelles allows all the three DKs, including the hydrophobic DK22, to be dissolved in water without addition of DMSO. As shown Figure 24, pluronic encapsulated DKs showed 400-550 nm absorption band in their UV-Vis spectra. After irradiating the aqueous solutions of encapsulated DKs (407μM) for 10 min, the

400-550 absorption peak disappeared, and the absorption peaks for the corresponding anthracene derivatives appeared. To determine the yield of the photoreactions, DMSO was added and the UV-Vis spectra of the resultant solution were compared to that of the DMSO solutions of the corresponding anthracene derivatives at the same concentration. The photoreaction yields for the micelles of DK20, DK21 and DK22 were 78%, 71% and 90% respectively. Unlike the reactions in organic solvents, these reactions did not give quantitative yields, which indicates that encapsulation with Pluronic does not completely stop hydration of the diketons. DK21, which is the most hydrophilic one, showed the lowest yield, and DK22 which is the most hydrophobic one, showed the highest yield.

Release of CO was qualitatively confirmed by using the CO sensitive Rh complex recently reported by Esteban and coworkers[137].CO release is often detected by a solution of myoglobin Fe(II), i.e. MbFe(II), freshly reduced with excess sodium dithionite under nitrogen. However, we found that the diketones react with sodium dithionite, so an *in situ* measurement of CO with MbFe(II) is not possible. Cis-$[Rh_2(C_6H_4PPh_2)_2(O_2CCH_3)_2](HO_2CCH_3)_2$ dispersed on silica gel is highly sensitive to CO. Therefore, we sealed some silica gel powders absorbed with the Rh complex in a side arm of a round bottom flask filled with an aqueous solution of DK22 micelle. After irradiating the micelle solution, the color of the Rh complex changed from violet to orange, which is consistent with the color change reported in the literature (Figure 25).Reflectance UV-vis spectrum of the powder showed that mono-CO complex formed after the reaction.

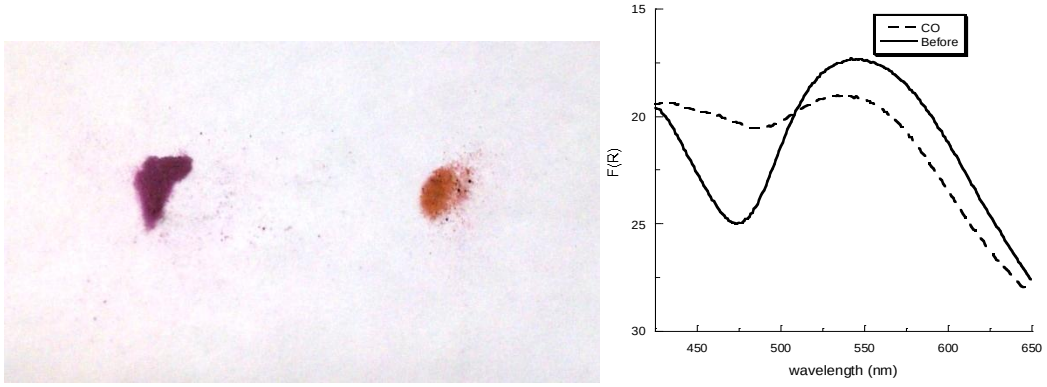

Figure 25. Photograph (left) and reflectance UV-Vis spectra (right) showing silica gel containing adsorbed cis-$[Rh_2(C_6H_4PPh_2)_2(O_2CCH_3)_2](HO_2CCH_3)_2$ before irradiating the micelle solution and after irradiating the micelle solution

Another advantage of this type of CORM is that the anthracene derivatives generated simultaneously with CO are fluorophores, which allows fluorescence imaging of the studied cells. For example, anthracene has a fluorescence quantum yield of 0.36[138]. To demonstrate this advantage, micelles of DK22 were incubated with acute myeloid leukemia cell KG-1. The following day cells were irradiated by a single wavelength of light (λ = 470 nm) for six 30 second pulses. Photo-activation of the CORM was assessed by fluorescence microscopy (Figure 26). The fluorescence image showed bright blue fluorescence in the cell, originating from the emission of the corresponding anthracene derivative. These results confirmed that DK22 were taken by the cells and the photo-induced CO release occurred in the cells.

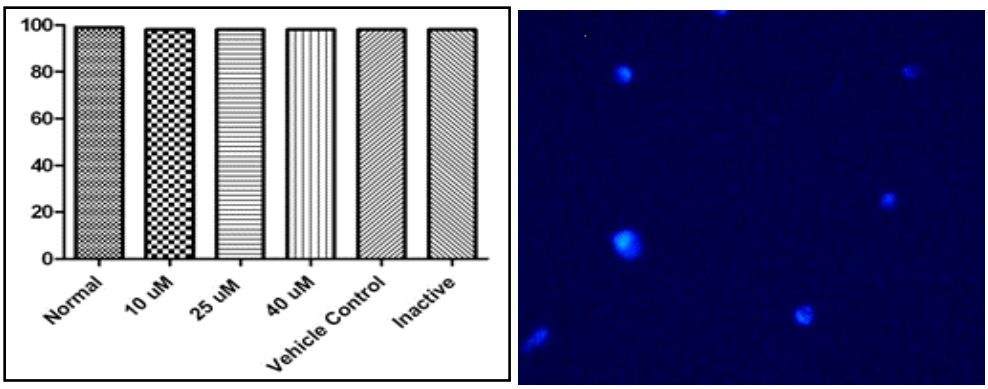

Figure 26. Cell viability for DK micelle (Normal: KG1 cell only, vehicle control: KG1 cell with Pluronic, inactive: KG1 cell with the anthracene derivative), and fluorescence image of the cells incubated with DK3 micelles and irradiated with 470 nm light (right)

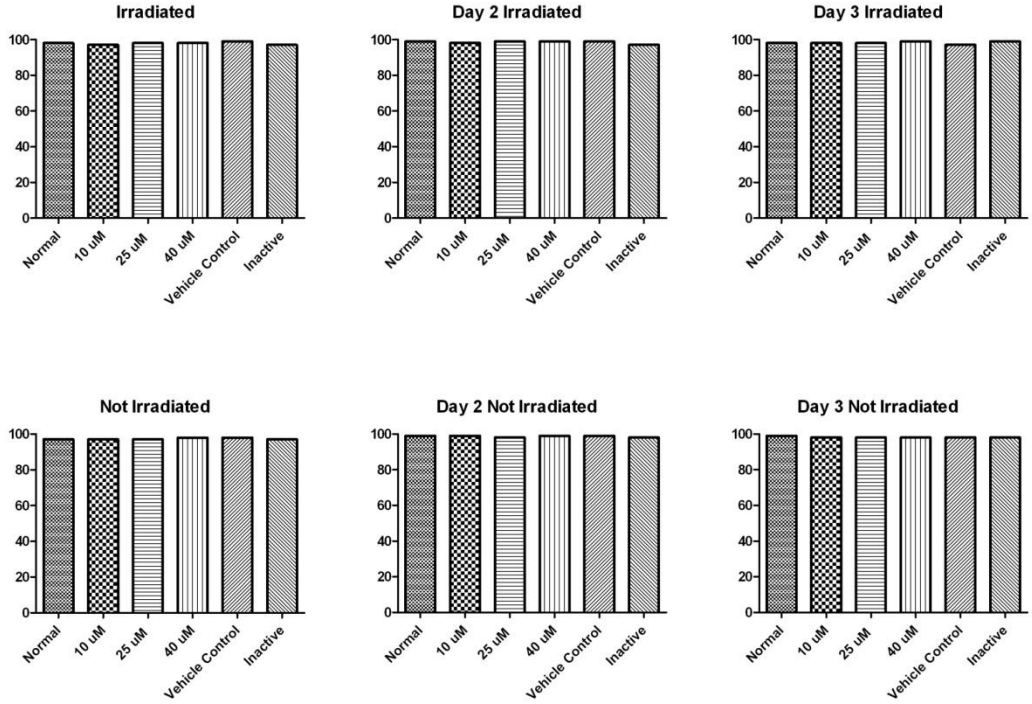

Figure 27. Cell viability tests of the irradiated and not irradiated samples. (Normal: KG1 cell only, vehicle control: KG1 cell with Pluronic, inactive: KG1 cell with the anthracene derivative)

Cell proliferation and viability were monitored over a 3-day period (Figure 26 and Figure 27).

No differences were observed in the viability of the cells exposed to the micelles of DK22 and

light activation as compared to control cells. Neither the photo CORM nor the anthracene based fluorophore (up to 40 μM) had effects on cell viability as assessed by measurement of the number of apoptotic and necrotic cells by flow-cytometry. Furthermore, no photo damage was observed under experimental conditions. Thus, this system is well suited for possible targeted delivery of gasotransmitter carbon monoxide to biological systems to study its function in signaling as well as for potential therapeutic applications. Detailed experiment procedure and data are given in the supporting information.

3.3.3 Conclusions

CORMs based on micelle encapsulated diketons were synthesized and their CO releasing capability was studied. These organic CORMs can be activated by visible light, have potentially low toxicity, allow the delivery of CO to be monitored by fluorescence imaging techniques, and thus could be useful tools for the study of the biological function of CO.

CHAPTER 4. PROTONATED POLYANILINE UNDER PHOTOIRRADIATION BY PHOTOACID GENERATOR

4.1 Introduction

In 1976, Alan J. Heeger, Alan MacDiarmid and Hideki Shirakawa together discovered conductive polymer which is able to be doped over the full range from insulator to metal [139, 140]. This discovery opens a brand new area of research not only for chemistry but also for condensed-matter physics. Before this, most of the polymers were saturated insulator polymers which are not interested as electronic materials. In conjugated polymers, they have one unpaired electron per carbon atom which is the π-electron. This π-bonding helps the electron delocalization along the backbond of the polymer and generates a new way for charge mobility move along the backbond of the polymer chain. So the semiconducting or metallic properties of these polymers are determined by the electronic structure, such as the number of one specific repeat unit. Although there are many conductive polymers, most of them are not able to be processed in metallic form and could not be used in industrial products. Polyaniline (PANI) is a conducting polymer discovered in the late 19th century[19], which is the one to solve this major problem. Because of its ease of synthesis, low cost, tunable properties, and good stability, PANI become one of the most widely investigated polymers during the last decade. This interest allows PANI has many potential applications such as electrical materials [141], novel biosensors[142], and energy storage materials[143]. The electrical conductivity of the PANI depends on its oxidation and protonation state. PANI exists in three different states (Figure 28): leucoemeraldine, emeraldine and pernigraniline. Leucoemeraldine is fully reduced and all of the nitrogen atoms are amine forms. Pernigraniline is fully oxidized and all of the nitrogen atoms are imine forms. In both the leucoemeraldine and pernigraniline states, polyaniline is an insulating material. Emeraldine states is the half oxidized form which the ratio of amine form to imine

forms is 0.5. When the half-oxidized emeraldine base (EB) form is protonated, the polymer becomes conductive and the conductivity can be as high as $10^{2}S/cm^{-1}$[144, 145].

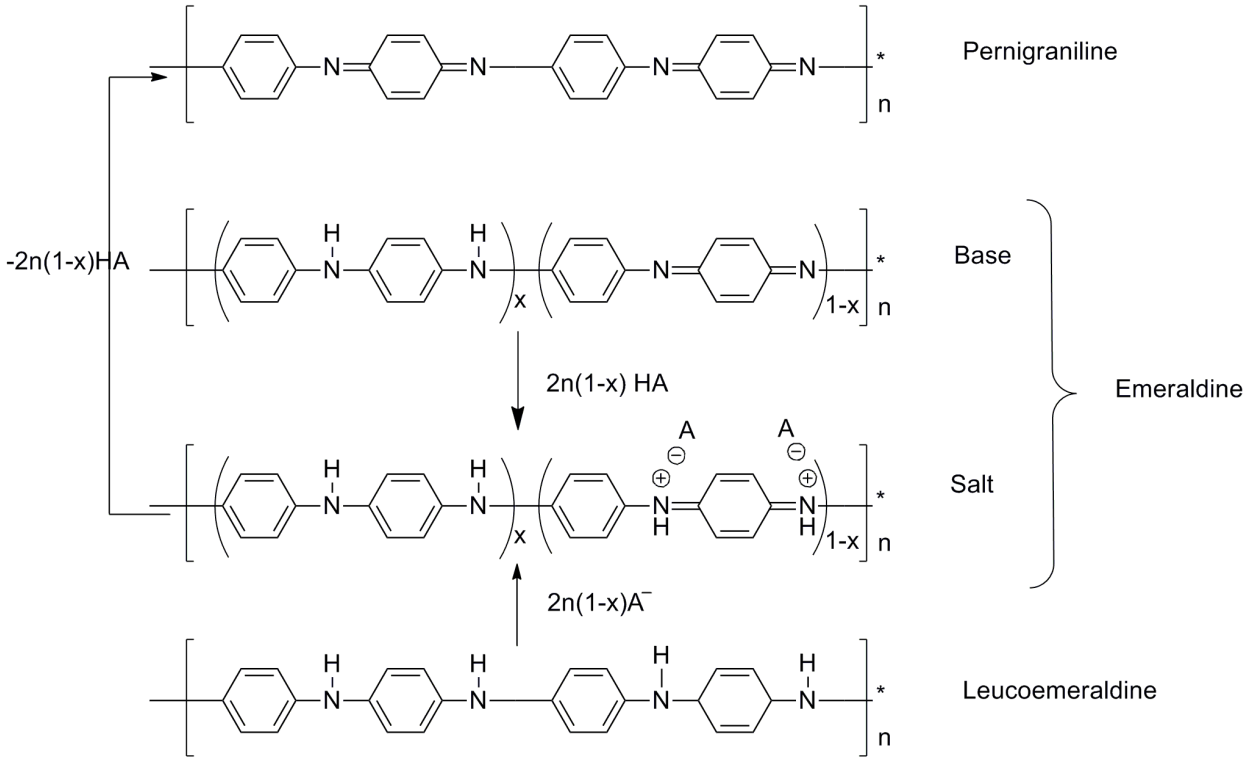

Figure 28. Three different doping states of polyaniline

Therefore it is expected that when a composite of insulating PANI-EB and a photo-acid generator (PAG) is irradiated, the PAG produces a Bronsted acid. This Bronsted acid protonates PANI to form the conductive salt form [146, 147].Photoacid generator (PAG) is a compound which could generate acids under light irradiation. PAG is different from photoacid which is based on excited-state proton-transfer reactions. Many photoacid generators are based on their photolysis mechanism. There are two major types of PAG: ionic and non-ionic compounds[148]. Those onium salts such as aryldiazonium, diaryliodonium, triarylsulfonium and triaryphosphonium salts that contain complex metal halides such as BF_4^-, SbF_6^-, AsF_6^- and PF_6^- belong to ionic photoacid generators. These onium salts have been discovered for nearly a

century and the mechanism of these photoacid has been studied in detail[149]. Under particular wavelength in the range of 200 nm to 300 nm, they will undergo photolysis to generate a protic acid. The advantage of this kind of PAG is their thermal stability. They could be easily structurally modified to change their absorption wavelength without changing their photoacid characteristics. About the non-ionic compounds, many of those will generate carboxylic acid, sulfonic acids, phosphoric acids and hydrogen halides through photoinduced reaction. Non-ionic photoacid generators, such as O-Nitrobenzyl esters of carboxylic acid and 1-oxo-2-diazonaphthoquinone-5-arysulfonate derivatives will produce carboxylic acid under photo irradiation. Most of Non-ionic photoacid generators have much better solubility in most organic solvent and in polymer films than ionic photoacid generators. However, compare with ionic photoacid generators, their thermal stability is not very good.

Many new commercially important technologies have been greatly improved with these photoacid generators. One of the most important applications of photoacid generators is in photoinitiated cationic polymerizations. They have opened an entire new area for this kind of applications, such as in coatings, inks[150]. Another application is in the area of new photoresists in the microelectronics industry. Such a photo-responsive material could be utilized to make conductive patterns [151]. In fact, photo patterning of PANI has been attracted a lot of interest since early nineties [146, 147, 151]. However, the conductivity after irradiation was normally quite low (~10^{-4}-10^{-6}S/cm^{-1}) [152, 153]. Conductivity higher than 10^{-3} S/cm^{-1}could only be achieved after treatment with HCl vapor. Treatment with strong acids not only increases a processing step, but also may be harmful for some parts of the devices. Therefore, it is desirable to achieve high conductivity only by photo-irradiation. Theoretical calculations have suggested that hydrogen bonding could improve the conductivity [154]. Hydrogen bonding may help

proton transfer and lock adjacent PANI chains together [155]. Herein, my work is focused on utilizing hydrogen bonding to improve the photo-induced conductivity of PANI/PAG composites.

Photoacid which has been discussed in chapter 2 is a very strong acid after visible light irradiation and gives very good reversibility. So another part of this chapter is focused on this photoacid mixing with PANI to improve the photo-induced conductive reversibility.

4.2 PANI with Irreversible Photoacid Generator

4.2.1 Background

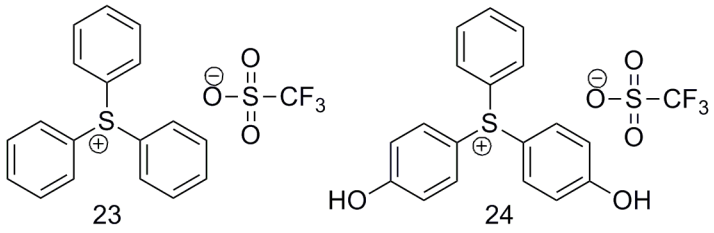

Scheme 9. Structure of Ph3S+ OTf− (PAG 23) and [(PhOH)2PhS^{+}OTf^{-}] (PAG 24)

The photoacid was synthesized by my lab mate by reacting diphenyliodonium triflate with bis-paradihydroxydiphenylsulfide in a pressure vessel. Copper (II) benzoate was added to it as a catalyst. As described above, photo-irradiation of composites of PANIEB/PAG often resulted in low conductivity increase. There could be several reasons for this. These include low quantum yield of the PAG, low proton transfer rate and low film quality, etc. In this work we studied composites of PANI-EB, triphenylsulfoniumtriflate(Ph3S^{+}OTf^{-}) (PAG 23) and PVA. Ph3S+ OTf− is a PAG with a very high quantum yield of∼50% [156]. PVA was added for two reasons. First, the hydroxyl groups of PVA can form a hydrogen bonding network, which may assist proton transfer from PAG 1 to PANI-EB. Second, addition of PVA can also increase film quality by forming hydrogen bonds with PANI. In fact, film quality could be a major reason of low conductivity and low reproducibility. Theoretically, to achieve maximum conductivity, at least

0.5 molar equivalence of the PAG to the monomer of PANI must be added. At this ratio, the weight of the PAG is often more than that of PANI. The PAG and PANI tend to form macrophases, which cause low film quality, and thus low conductivity and reproducibility [157]. The PVA we used was 88% hydrolyzed. It is not hygroscopic and is easy to handle. Therefore, it is unlikely that doping PVA in the films significantly increased their water content, which could affect the conductivity[158].

4.2.2 Results and Discussion

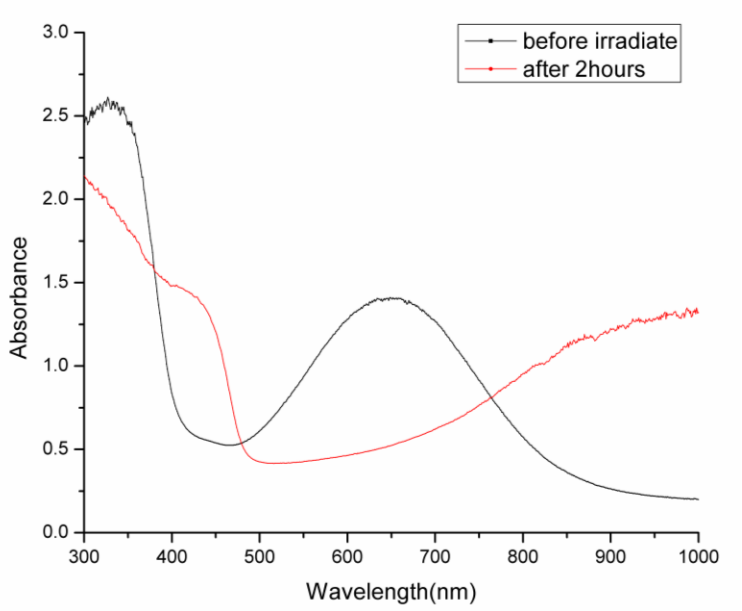

Figure 29. UV–visible spectra of PANI/PAG/PVA film before and after irradiation at 254 nm

To study the effect of PVA, different ratios of PVA were added to a mixture of PANI-EB/PAG 1 with a fixed PANI-EB/PAG molar ratio of 2:1 (molar ratio of the polymers mentioned in this article refers to that of the corresponding monomers). Addition of PVA significantly improved film quality, and thus the reproducibility. After irradiation at 254 nm for 1 h, the conductivity of the thin films with PVA/PANI ratio of 0.5 changed from below 10^{-9} S/cm^{-1} to10^{-3} S/cm^{-1}. As described before, such conductivity is difficult to achieve by photo-irradiation of PANI-EB/PAG

composites without treatment of HCl. The protonation of PANI-EB was proved by UV-Vis spectrometry (Figure 29). The color of the film was blue before UV irradiation and changed to green after irradiation. PANI-EB shows a band at 650 nm attributed to an intermolecular and/or intramolecular charge-transfer process from the benzenoid to the quinoid ring. This leads to the formation of a molecular "exciton"[159]. After exposure to UV light, the peak centered at 650 nm disappeared. The disappearance indicates the absence of the exciton in the polaron lattice formed upon protonation of the imino groups [64]. Two absorption peaks appeared in the spectrum after irradiation. One centered at 445 nm and the other centered around 850 nm. They are ascribed to the polaron-π* and π-polaron transition, respectively[160]. These peaks suggest the formation of mid gap states due to protonation [64].

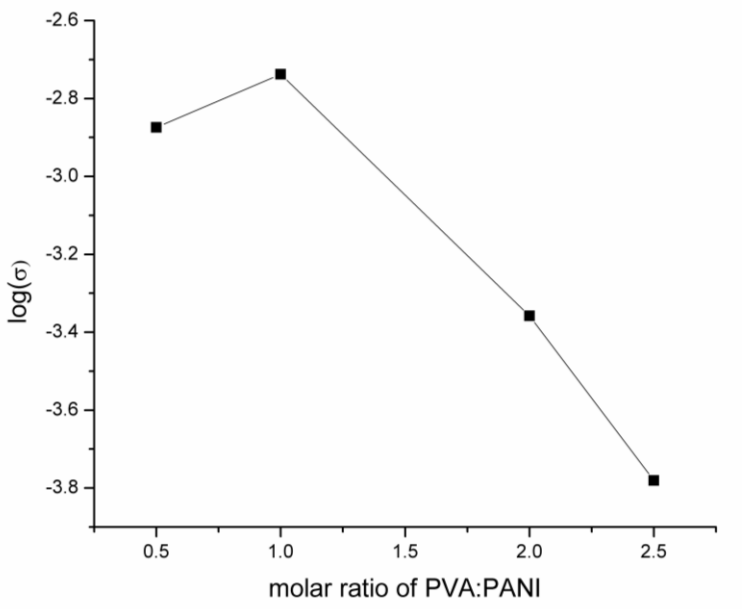

Figure 30. Conductivity (S/cm^{-1}) of various concentrations of PVA (the molar ratio of PANI-EB to PAG is fixed to 1:0.5)

When more than 0.5 molar equivalence of PVA was added to the1:0.5 PANI-EB/PAG mixture, the conductivity slightly increased at first and maximized at~1.0 equivalence (Figure 30). When

too much PVA was added, the conductivity started to decrease. Addition of PVA dilutes PAG and increases the average distance between PAG and PANI. When a high percentage of PVA was added, the dilution effect overcame the assistance of PVA in protonation, and thus decreased the conductivity. To optimize the composite, different ratios of Ph3S+ OTf− were added to a mixture of PANI-EB and PVA with a fixed ratio of 1.1:1. In Figure 31, the conductivity increased with the amount of the PAG 1 until the molar ratio of PAG: PANI was∼0.6. At this ratio, the composite has a conductivity of 10^{-2} S/cm^{-1}. Further increasing PAG does not significantly increase the conductivity after irradiation even though the conductivity is still much lower than that could be achieved by protonation of PANI (10^{-2} S/cm^{-1}). This is most likely due to the aggregation of the PAG when its concentration is high [157].

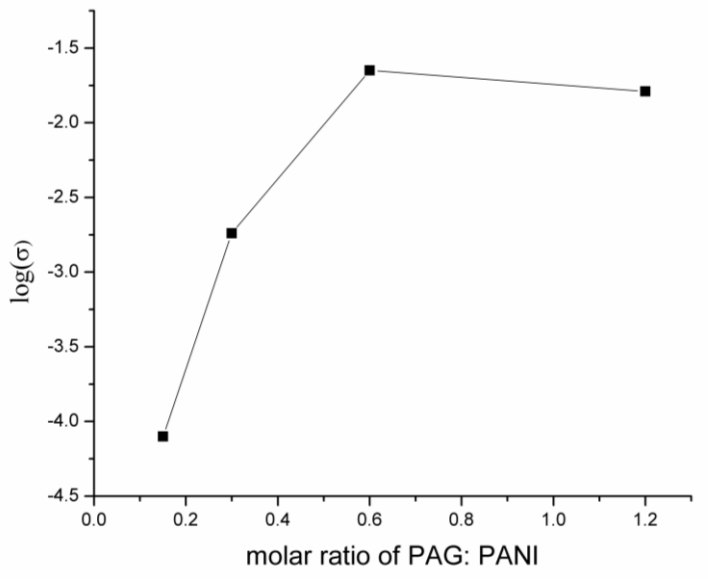

Figure 31. Conductivity (S cm^{-1}) of various concentration of PAG (the molar ratio of PANI-EB to PVA is fixed to 1.1:1)

Hydrogen bonding between PANI and PVA as well as protonation of PANI was studied by ATR-IR spectroscopy. Given that hydrogen bonding and proton transfer occur on the quinoidal nitrogen, C=C and C=N stretches of the quinoidal ring, which are located at∼1590 cm^{-1}[161-

163], shall be the vibration that is affected most. In fact, when PVA was doped in PANI, the quinoidal stretch shifted from 1585 cm^{-1} to 1591 cm^{-1}, which is due to the hydrogenbondingbetween PVA and PANI [164-166]. Even after PAG 1 was added to the composite, the quinoidal stretch did not shift to a lower wavenumber. In fact, the peak shifted to a little higher wavenumber(1594 cm^{-1}), which indicates strong hydrogen bonding between PVA and PANI. After a film of PANI/PVA/PAG 23 was irradiated, the quinoidal stretch shifted to 1575 cm^{-1}, which is typical for PANI salt[164]. In addition, a band at 1134 cm^{-1} can be assigned to a vibration mode of the protonized quinoidal structure [167]. The broadening of the peaks makes it difficult to analyze hydrogen-bonding effects although IR spectroscopy of PANI-salt/PVA has been studied before[166] (Figure 32).

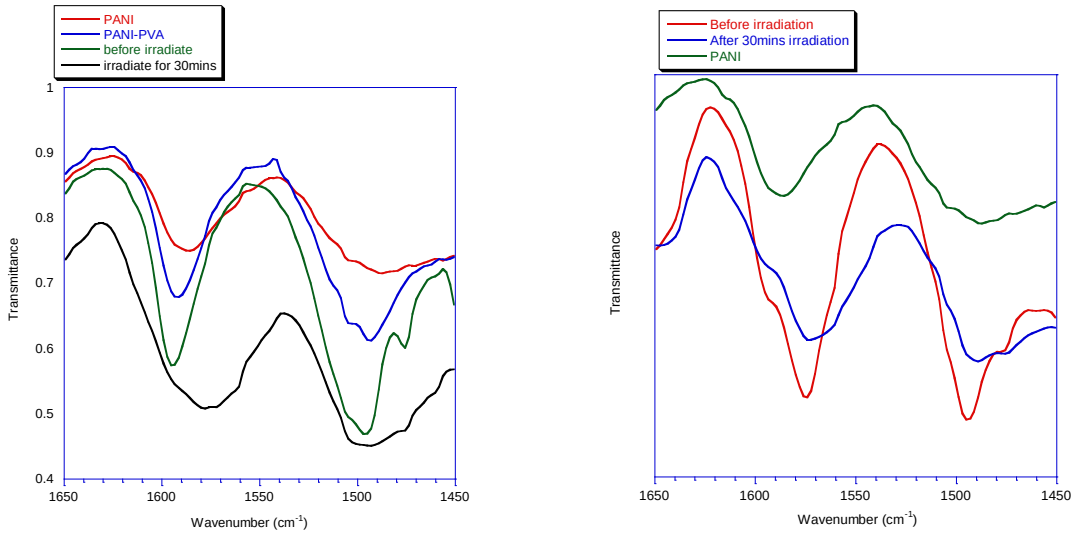

Figure 32. FTIR spectra of PANI films: (a) just PANI film, PANI doped with PVA film, before irradiate the PANI doped with PVA and PAG 23 film, after irradiate at 254 nm for 30mins PANI doped with PVA and PAG 23 film and (b) just PANI film, before irradiate the PANI doped with novel PAG 24, after irradiate at 254 nm for 30mins PANI doped with novel PAG 24 film

To further improve the photo-induced conductivity, (PhOH)2PhS^{+}OTf^{-} was synthesized and used as the PAG 24.This PAG 24 has not previously been used in photo-responsive PANI composites. Compared to PAG 23, PAG 24 has two hydroxyl groups that can form hydrogen bonds with PANI. Since the PAG 24 itself can form hydrogen bonds with one or two PANI polymers, it is not necessary to dope PVA. In addition, the hydrogen bonding between the PANI and PAG 24 may assist the PAG to distribute around the PANI better. Thus, 0.5 equivalence of the PAG 24 was doped in PANI-EB. The conductivity reached 10^{-1}S/cm^{-1}after irradiation, which is an order of magnitude higher than that of PAG 1. However, the initial conductivity of the thin films, before irradiation, was as high as 10^{-5}S/cm^{-1}. The quinoidal stretch in the IR spectrum was located at 1575 cm^{-1}. This was approximately the same as that of the irradiated films, although the conductivity was four orders of magnitudes lower. We suspected that PAG 24 contained some acidic impurity. However, both 1H and 13C NMR spectra were clean and the conductivity results were reproduced with different batches of PAG 24. Therefore, the high initial conductivity shall be due to the relatively high acidity of the phenol groups in PAG 24, which is enhanced by the sulfonium group at the para position.

4.3 PANI with Reversible Photoacid

4.3.1 Background

As mentioned in chapter 2, a long lived reversible photoacid could be used in many applications, such as catalyze an esterification reaction. Here we report another application concerning the reversible control of the electronic properties of a conductive polymer by irradiation with different wavelengths of light. With respect to conductive polymers, polyaniline (PANI) is one of the most studied conductive polymers due to its low cost of the monomer, tunable properties and good stability[64]. The electrical conductivity of PANI depends on the level of oxidation and

the degree of protonation (Figure 28). We could control the extra acid/base (doping/de-doping) to switch PANI between base form and salt form and to further change the conductivity. Some photo-switchable conductive materials based on PANI have been reported[11, 168]. However, all of those photoacids were based on spiropyran structure and took proton from protonated PANI salt. The stable form of this novel photoacid is the protonated merocyanine structure and it will generate a proton to dope PANI base form. PANI conductivity studies showed the reversible and stable changes when blended with this novel photoacid and irradiated with different wavelengths of light.

4.3.2 Photoacid 1 Doped with PANI

Inter conversion among MEH and SP states upon visible light irradiation is showed in Scheme 10. From the result of chapter 2, this photoacid could switch from MEH form to SP form under visible light irradiation and convert back to MEH with or without UV light irradiation. If the proton generated by this photoacid could be taken by PANI base form under visible light and released under UV light, then the electrical conductivity of PANI will be reversible.

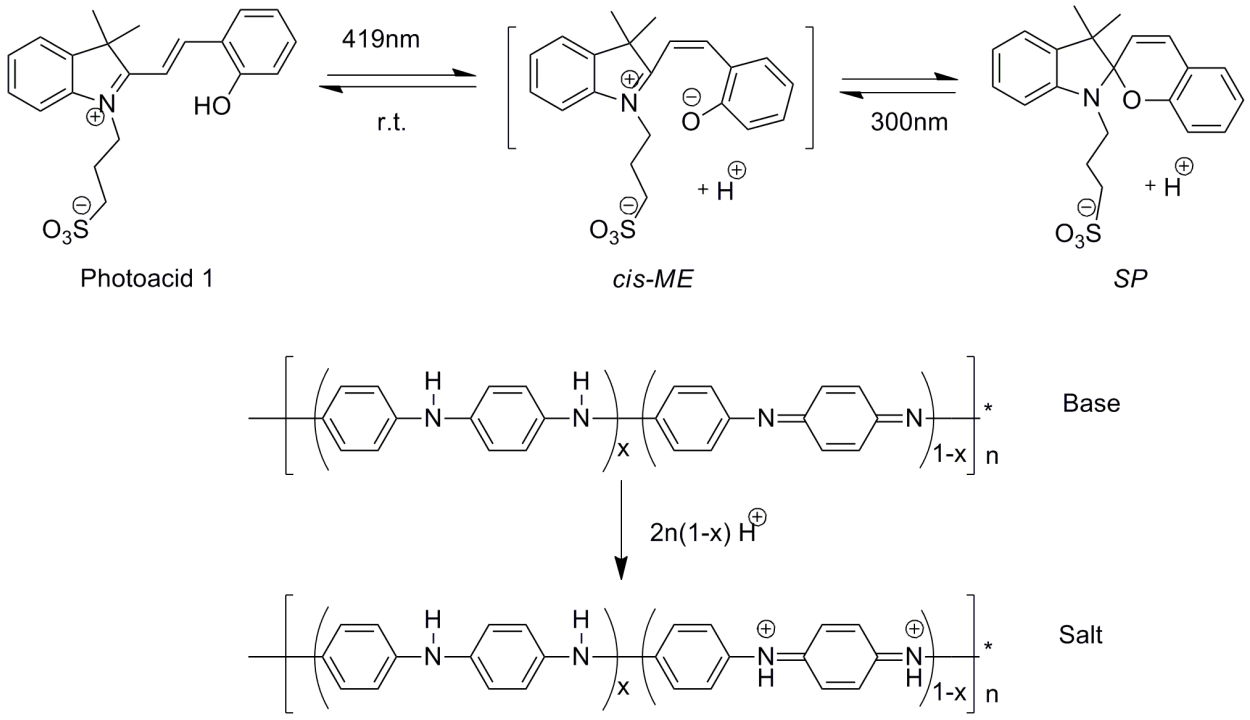

Scheme 10. Illustration of photoinduced proton transfer between PANI and a three-states structure switch photoacid

Since the previous result is generated from solution condition while this study is performed in thin films. First of all is to test whether this photoacid could generate proton in solid state. Figure 33 shows the photoacid/PMMA/PEG film before and after irradiation. In order to make a good quality film, PMMA is the major matrix to dope with photoacid. Polyethylene glycol (PEG) is added to help the proton transfer with the help of hydrogen bond. The original color of this film is orange, which is the MEH form color. Then the film color changes to light yellow after 470 nm irradiation, which is the SP form color. This film indicates even in solid states, MEH form will convert to SP and generate a proton under visible light irradiation. This color change is consistent with UV-Vis spectra result of this thin film (Figure 34). Initially, the photoacid is in MEH form and gives relatively high absorption peak at 450 nm. After irradiating with 470 nm light, this 450 nm peak decrease, which shows the MEH form convert to SP form. Then this

450nm peak increases under 254 nm light irradiation, which shows the SP form convert back to MEH form under UV light. The change between MEH and SP form is reversible by switch between visible light and UV light irradiation. Thus, these results indicate that this photoacid could release and retake proton under different light irradiation in solid state.

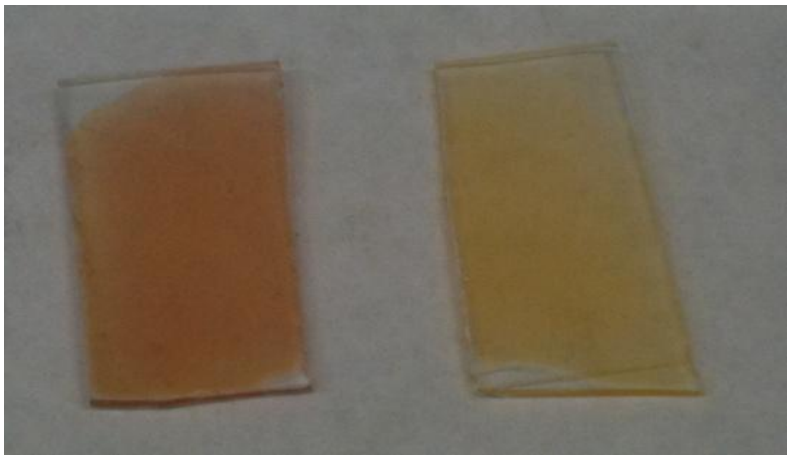

Figure 33. The color change of a photoacid/PMMA/PEG film

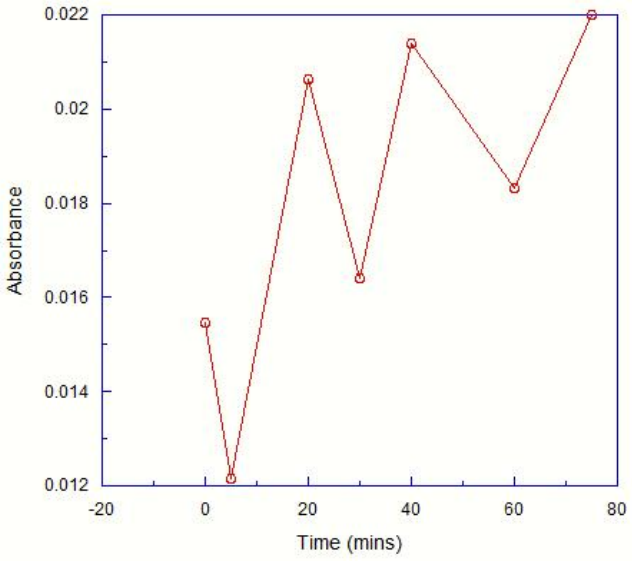

Figure 34. 450 nm UV-Vis absorption change between 470 nm and 254 nm light irradiation

Figure 35 shows not only the photoacid's UV-Vis absorption changes but also the PANI absorption. PANI/PEG/PAA/PAH films containing the SP structure were prepared by spin-

coating onto quartz slides. PANI-EB was dissolved in N-methylpyrrolidinone(NMP), and then mixed with PEG and PAA. Photoacid was dissolved in NMP and irradiated at 470 nm for 5minutes in order to change into SP form. Under 470 nm LED light irradiation, the PANI solution was mixed with the photoacid solution and irradiated another 5minutes. By this method, PANI was doped with SP form and partially protonated during mixing. The 420 nm absorption band of the photoacid decreased after 5mins of 470 nm light irradiation, while the 300 nm peak, which is associated with the SP structure, increasing at the same time. The 800 nm peak, which is characteristic of the "salt form" of PANI, increased a small amount after irradiation and implies some degree of protonation. The absorption band around 600 nm is the typical "base form" band of PANI, which decreased a small amount after irradiation. The other characteristic absorption band of the "salt form" of PANI around 400 nm is overlapped with 420 nm MEH absorption band. So the change is not very clear in this UV-Vis spectrum. Under 300 nm UV-light irradiation for 5mins, the reverse phenomenon was observed on the UV-Visible absorption spectrum. These spectra clearly indicate proton transfer from photoacid to PANI under visible light irradiation followed by proton recapturing by the SP structure from PANI under UV irradiation. However, from the change of 600 nm peak and 800 nm peak, the degree of proton transfer between PANI and photoacid is small. This is probably due to the limited ability of the proton transfer to PANI. Although a large amount of the photoacid could switch between MEH and SP form, most of these generated protons stay around photoacids and could not reach PANI. This result is consistent with electrical conductivity test result.

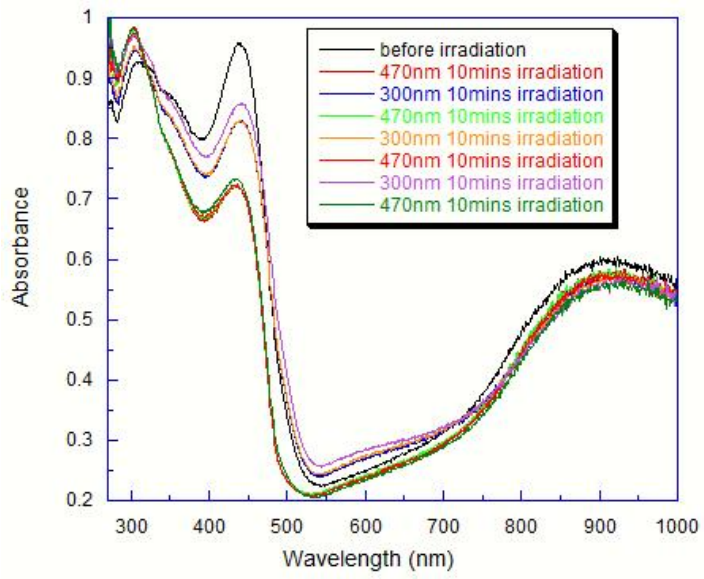

Figure 35. The absorption spectra of PANI with photoacid under different light irradiation

A dark bluish green film was prepared by spin coat the mixture solution of PANI and photoacid (more detail procedure see Experimental Chapter). Figure 36 demonstrates the switchable conductivity variation of the PANI/PEG/PAA/PAH thin film upon UV and visible light irradiation for 5 different cycles. According to Venugopal's results[157], conductivity of PANI increases significantly from 40% acid doping level. So 20% of PAA as a weak acid was added into PANI-EB solution which will increase the initial conductivity of PANI films to observe the largest conductivity increase. On the other hand, less amount of photoacid will be added into this film composition to receive better quality films. The initial conductivity was relative high compared with the conductivity of PANI EB. After the first 5minutes of 470 nm irradiation, conductivity only increased around 5% which also demonstrated that most of the photoacid was in the SP form. Then the electrical conductivity was decreased almost 50% under 300 nm UV light irradiation for 10minutes. With another 5minutes of visible-light irradiation, the electrical conductivity of thin films was restored to the value after the first 470 nm 5mins irradiation. Figure 36 demonstrates this reversible electrical conductivity variation upon visible light and UV

light irradiation for 5 consecutive cycles. From these results, the repeatability and stability of this switchable photoacid with PANI is very good.

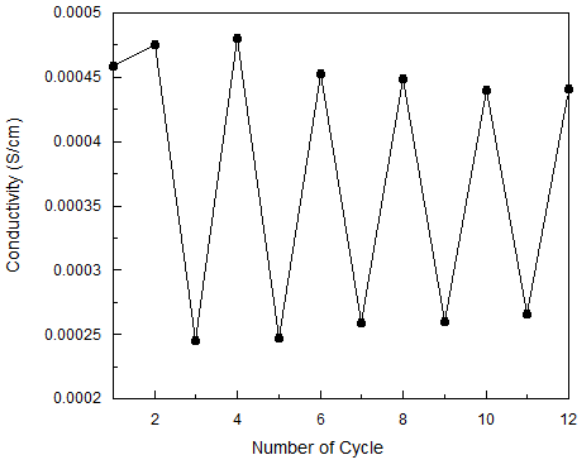

Figure 36. Film conductivity switches by different light irradiation

4.3.3 Photoacid 2 Doped with PANI

Some other photoacid I mentioned in Chapter 2 have been tested with PANI too. Photoacid 2 is one of them which also give good pH change in aqueous solution (from 4.9 to 3.9) and show good reversibility. However there is no report about this photoacid in solid states. So in this part, I dopedphotoacid2 with PANI and observed the conductivity and UV spectra change.

Absorption spectral studies showed that before irradiation, most of the photoacid was in MEH form which gave a strong peak between 400 nm and 500 nm. So there is no obvious observation about proton transfer between PANI and photoacid before irradiation. Then after 10minutes 470 nm light irradiation, MEH peak decreased. At the same time, a 300 nm peak showed up. These changes indicate after 470 nm irradiation, photoacid changes from MEH form to SP form and should generate a proton. At the long wavelength area, PANI peak gave a blue shift from near 900 nm to 800 nm. This observation indicates that PANI receives a proton which is generated

from photoacid during visible light irradiation. Then I used 300 nm light to irradiate this film. The MEH peak increased double and 300 nm peak also decreased a little, which means the photoacid changed from SP back to MEH under UV light irradiation. However, the absorption band at around 800 nm -- the characteristic absorption band of the "salt form" of polyaniline-- decreased only a little bit. This observation indicates that the proton shift from MEH photoacid form to PANI-EB is easier than the proton shift from PANI salt form back to SP photoacid. Then I repeated this whole process one more time and the absorbance indicated the switching between SP and MEH again.

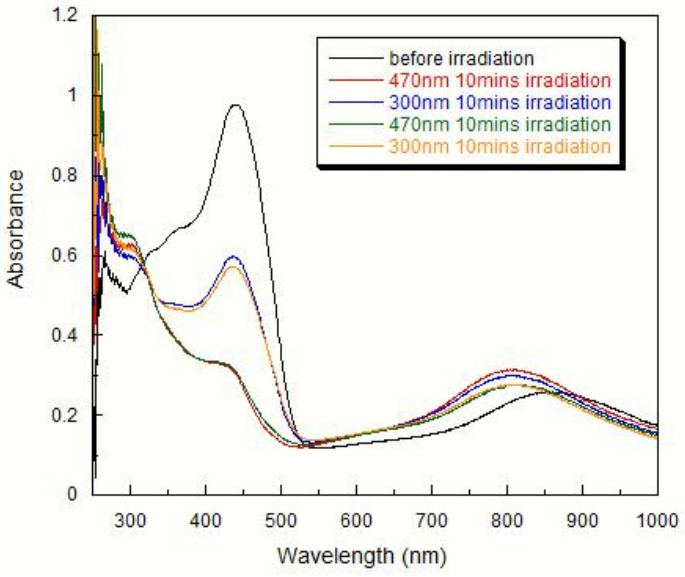

Figure 37. The absorption spectra of photoacid 2 with PANI

The electrical conductivity of the PANI thin film doped with photoacid increased from 0.0017 S/cm to 0.0038 S/cm which is more than double of the original conductivity after irradiation with 470 nm for 10minutes. This increase of conductivity is almost certainly due to the proton generated by photoacid and doped with PANI-EB form. With 10minutes irradiation of 470 nm, PANI-EB doped with a proton and increased conductivity. Figure 38 also demonstrates the conductivity of this change after several cycles and this result is consistent with the UV spectra.

From the UV spectra, the first 10minutes 470 nm irradiation gave a big shift around 800 nm which indicated the proton doped with PANI-EB. After that, UV spectra showed a little change after both UV and visible light irradiation. From the electrical conductivity result, the first 470 nm light irradiation increased the conductivity a lot. However, after that, both the UV and visible light irradiation didn't give much change.

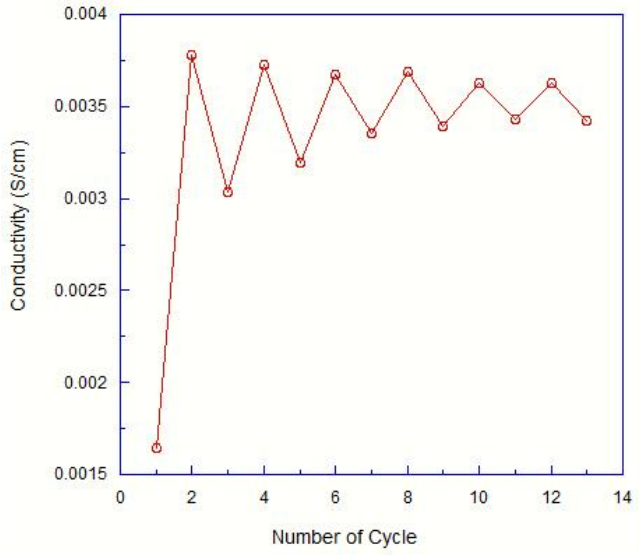

Figure 38. Electrical conductivity of photoacid 2 with PANI

All of these results indicate that this photoacid is easier to change from MEH to SP form and SP form is the relatively stable state. From this photoacid solution result, the initial pH of this photoacid is 4.9, which means in aqueous solution before irradiation, part of the MEH form has already changed to SP form and generates protons. Compared with photoacid 1, the initial pH of photoacid 2 is one unit higher. This indicates the SP form of photoacid 2 is more stable than photoacid 1 SP form in aqueous solution. Another reason is the film's pH. PANI EB is a little basic which will help the MEH form donate a proton and favor the SP form.

4.4 Conclusions

Electrical conductivity change of PANI doped with irreversible and reversible photoacid were investigated and compared with the solution spectroscopy. It was observed that proton transferred from photoacid to PANI both in solid state and solution. With the help of hydrogen bonding from PVA, electrical conductivity of PANI film could reach to 10^{-1} S/cm^{-1}after irradiation when doped with irreversible photoacid generator. For reversible photoacid, the conductivity of the PANI thin film could be controlled by switching UV or visible light. According to these results, the new composition of PANI with different photoacid could be a new electrical material for semiconductor industry.

CHAPTER 5. INSTRUMENTATION AND EXPERIMENT

5.1 Photoacid Solution Experiments

5.1.1 Photoacid Sample Preparation

A photochemical reaction is a process that a molecule absorbs the appropriate energy form light radiation. The excited molecule could change, in one or several steps, into a product or an intermediate compound that will participate into other chemical reaction, such as radical polymerization reactions. Because of its easy precisely controllable character, photochemical reactions draw great attention and many literatures about photochemical reactions has been published. Most of these reactions require one operating condition: excitation of the reactant is only performed by light energy without extra heating energy. So the reaction set up should have very poor heating aptitudes or good cooling systems.

To prepare all of the photoacid solution for the photoreaction, around 1gram of photoacid was weighed and dissolved by 20 ml of DI water under dark. To dissolve the photoacid fully, this solution was ultrasonicated for 30 seconds and then kept in dark for 10 minutes. This solution was transferred into a quartz test tube. This test tube will be inserted into the Rayonet photochemical reactor or clamped under 470 nm LED light bundle.

In the photocatalyzed esterification reaction, a solution of the reactants and the photoacids was divided into two solutions and placed in Pyrex test tubes. One of the test tubes was wrapped with aluminum foil and used as the control. As a blank control, a third Pyrex test tube was filled with only reactants without photoacid. These test tubes were sealed under ambient atmosphere. All three test tubes were placed together in a RPR-100 Rayonet photochemical reactor and were irradiated with a 419 and/or a 570 nm light. The photoreactor was equipped with a ventilation

fan, which kept the temperature close to room temperature. After each hour irradiation, 1ul sample from each test tube was taken and tested by HPLC.

In the experiment that demonstrated the photoinduced volume change, the hydrogel cuboid was placed in an open beaker filled with an aqueous solution of the photoacid. The mixture was irradiated in the photochemical reactor, and the size of the cuboid was measured by placing the wet cuboid on a ruler.

5.1.2 Instruments

5.1.2.1 Photoreactor

Figure 39. Photoreactor used in photoreaction

Table 3. Intensity reading of each wavelength

Wavelength (A °)	Center	2 Inches From Lamps	1.5 Inches From Lamps
2537	12800	16000	21000
2652	388	488	640
2804	14	16	21
2894	18	22	29
2967	66	83	109
3022	32	40	52
3129	250	313	411
3654	213	267	351
4047	250	316	416
4359	768	960	1260
5461	418	523	687
5780	91	113	149

The photoreactions were performed by using a RPR-100 Rayonet photochemical reactor equipped with 16 lamps with different emission wavelength. This photoreactor is 16”high, 12”square and equipped with a ventilation fan, which keeps the temperature close to room temperature. Table 3 lists intensity readings in $\mu W/cm^2$ at each wavelength.

A light-emitting diode (LED) is a semiconductor light source which was first introduced as a practical electronic component in 1962 by Nick Holonyak, Jr.. LEDs are very efficiency which emit more light per watt than incandescent light bulbs and could generate an intended color without using any color filter. LEDs radiate much less heat in the form of IR compare with the most light sources, so LED light are the good source for the photoreaction. A LED contains a chip of semiconducting material doped with impurities to create a p-n junction. The current

flows from p-side (anode) to the n-side (cathode). The electrons and holes flow into the junction from electrodes from two sides. When they meet each other, an electron will fall into a lower energy level and release energy in the form of a photon. So the wavelength of the light emitted is determined by the band gap energy of the materials forming the p-n junction. The LEDs used in this research are the blue lights with wavelength between 450 nm and 500 nm. These bright blue LEDs are based on the wide band gap semiconductors GaN (gallium nitride) and InGaN (indium gallium nitride). To study the photo behavior, some of the compounds were irradiated with a 470 nm LED array with 120 10000 mcd LEDs (Elixa, Ltd.).(Figure 40)

Figure 40. 470 nm LEDs

5.1.2.2 UV-Vis Spectroscopy

For those highly conjugated organic compounds, like chromophores, UV-Vis spectroscopy is the most common technique to use. A typical spectrometer usually has two light sources, a deuterium (D2) lamp to generate ultraviolet light and a tungsten lamp to generate visible light. A diffraction grating will separate a beam of light into its component wavelengths and a half-mirrored device will be used to split each single wavelength beam into two equal intensity beams. One beam will pass through a sample cuvette which contains the sample we want to test and the other beam will pass through an identical cuvette which only contains the pure solvent the sample using. The intensities of both light beams will be collected and compared by electronic detectors. All of the wavelengths we selected will be scanned one by one. The intensity of the reference beam is defined as I_0 and the sample beam is defined as I. Beer-Lambert law will be used as a quantitative method to determine the concentration of the sample compound:

$$A = \log_{10}(I_0/\mathrm{I}) = \varepsilon \cdot c \cdot L \quad (3)$$

The UV absorption spectral studies were collected with a Varian Cary 50 Scan UV-vis spectrophotometer using a quartz cuvette with 1 cm path length. The decay UV spectra were collected with time intervals of 10 or 20 seconds.

5.1.2.3 Fluorescence

Fluorescence emission spectra were taken with a NanologTM HoribaJobin Yvon fluorimeter using the same cuvette used in UV-vis absorption measurements.

5.1.2.4 pH meter

Fisher Scientific accumet Research AB15 pH/mV/℃ Meter and an accumet liquid-filled, glass body combination pH Ag/AgCl Electrode was used to run pH tests.

5.1.2.5 High performance liquid chromatography (HPLC)

All of the HPLC tests were run by PerkinElmer series 200 HPLC with Microsorb-MV C8 5um 100A HPLC column from Rainin Instruments Co. INC.

HPLC is a chromatographic technique used to separate a mixture of compound based on the different retention time caused by the process of different distributions of the individual compound between two phases: the mobile phase and the stationary phase. It's a very common technique in the analytical chemistry and biochemistry to identify, quantify and purify the individual compound.

In liquid chromatography, the mobile phase is a liquid which is a solvent to carry the compounds passing through a separating medium, often within the closed environment of a column. The difference interaction time will led the mixture towards the large separation and redistribution from the time of the start after injection. Then the appearance of individual component zones in time will be recorded during the elution by a detector as the chromatogram. In order to more or

less complete separate the individual compound from the mixture, the subjecting solute molecules should generate different velocity and lead to selective movement based on the stationary- and mobile- phase inside the column.

HPLC typically uses different type of stationary phase inside column, a pump keeping the mobile phase and compounds flowing, and a detector which will tell the retention time and the amount of each analyte passed. Sometimes, the detector will provide more detail information such as UV-Vis spectra of each analyte. By choosing different stationary phase, the composition and flow rate of mobile phase, and the column dimensions, the retention time of each compound will vary. Compare with ordinary liquid chromatography, HPLC usually choose small size columns and higher mobile phase pressure. So it's a very efficient method to provide a good separation of a mixture.

Common mobile phases used include any miscible combination of water with organic solvents, such as acetonitrile or methanol. In order to provide better separation result, acids or buffers or salts may be added into the mobile phase. The composition of the mobile phase could keep constant during the whole analysis as an isocratic elution mode or varied as gradient elution mode. When the compounds are relative similar in the affinity for the stationary phase, isocratic elution will be effective in separation. In gradient elution, the composition of the mobile phase is typically increased from low to high eluting strength. The composition of the mobile phase depends on the intensity of interactions between analytes and the stationary phase. In order to find the best condition which is the shortest time to complete separate the mixture, a series of trial runs will be performed to choose the best mobile phase components, additives and gradient conditions.

Figure 41. PerkinElmer series 200 HPLC

5.1.3 Supporting Data

An aqueous solution of photoacid 6 (5.27×10^{-3} M) gives a UV-Vis spectrum like Figure 44. Basically, 5.6mg of photoacid 6 was weighted and dissolved in 2ml of ultrapure water by ultrasonic in the dark. Filled the quartz cuvette with 2ml of the same ultrapure water and collected the UV-Vis spectrum as background. Filled another cuvette by this photoacid solution and collected the UV-Vis spectrum as before irradiation. Then irradiated this quartz cuvette by 300 nm UV light for 10minutes and collected the UV-Vis spectrum as after irradiation. All the other UV-Vis spectrum of photoacid solution was followed the same procedure.

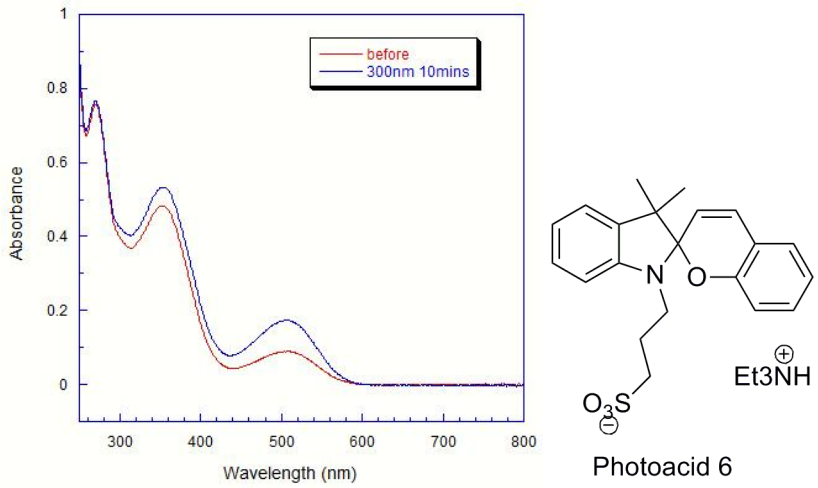

Figure 42. UV-Vis spectra of photoacid 6

Some of the photoacid was dissolve in solution and mixed with polymer to cast into films. 40mg Poly(methyl methacrylate beads) (PMMA) (avg MW 35000, ACROS ORGANICS) was dissolved in 1ml chloroform and then 2mg of carbon based photoacid 6 was added into this solution.

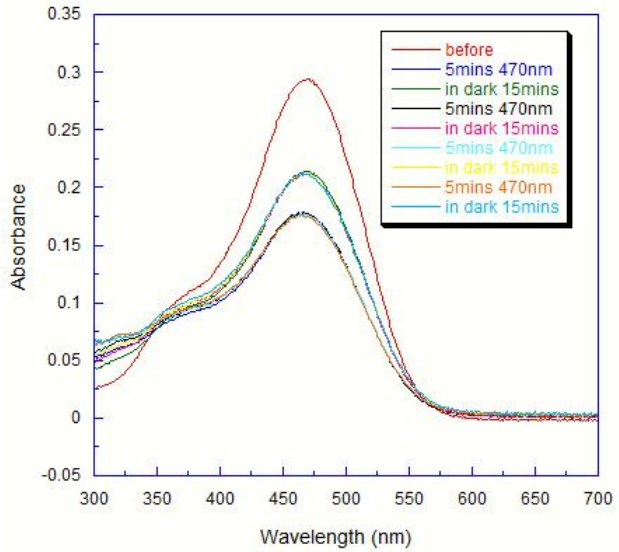

Figure 43. UV-Vis spectrum of photoacid 6 PMMA film

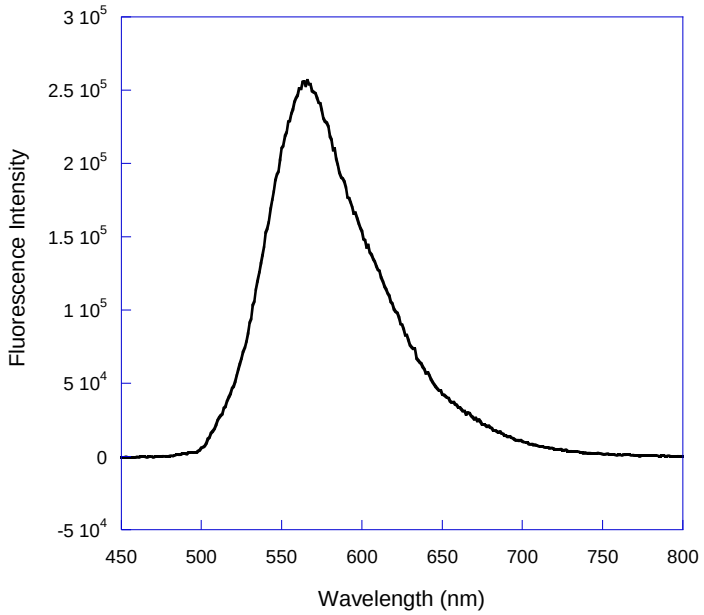

Figure 44. Fluorescence of photoacid

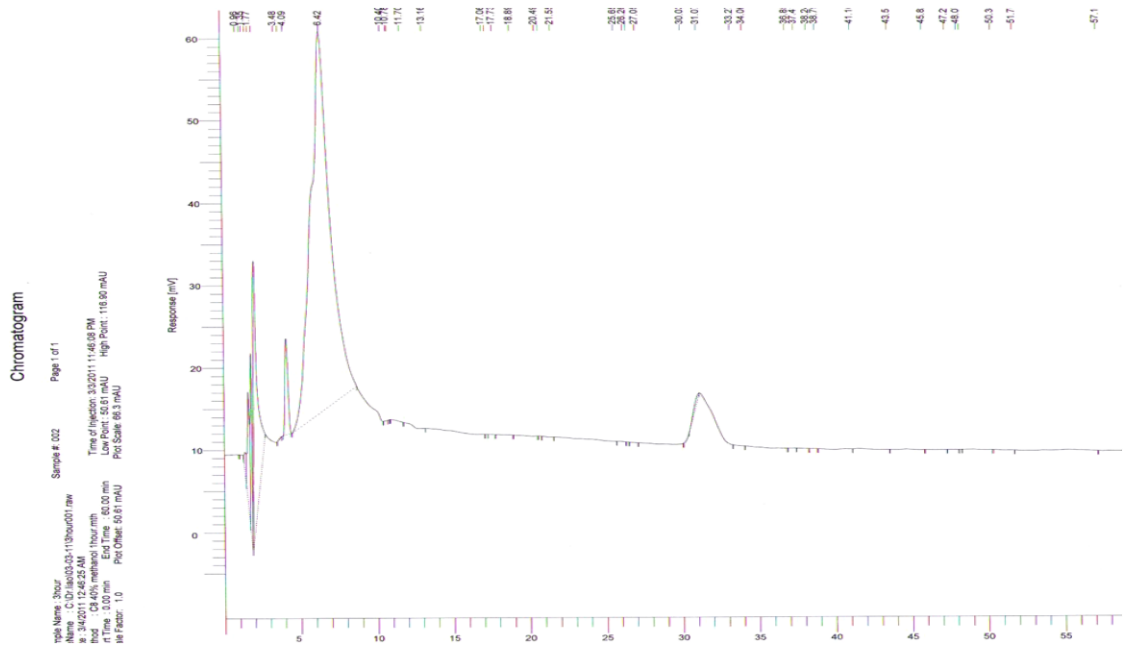

Figure 45. HPLC of esterification reaction catalyzed by photoacid

5.2 PrDA Reaction

5.2.1 PrDA Sample Preparation

5.2.1.1 PrDA Mechanistic Study Sample

All starting materials for preparing the DA adducts were purchased without further purification. HPLC grade solvents were used without further purification except degassing. Acetonitrile was distilled over molecular sieve under nitrogen before being used.

Millimolar solutions of the adducts in acetonitrile or acetontrile/methanolmixture were irradiated under 254 nm UV light in an inert atmosphere at room temperature. The power of the UV lamp is only 8 W, and the reaction was conducted in a ventilation hood. Under these conditions, the photo heating effect can be ignored and the "total absorption" required for measuring quantum yield with chemical actinometry can be achieved. Quantum yields were measured by chemical actinometry using uridine as the chemical actionmeter[169, 170].

For each solution, before irradiation under 254 nm, the concentration was carefully calculated to make the absorption at 254 nm well above 2. Except the solution for the oxygen quenching experiment, all solutions were carefully degassed before irradiation. Transferred the sample solution into a large quartz test tube and sealed with a rubber stopcock. Stopcock was double tapped with 3M Scotch Super electrical tape. Hooked the test tube up to a Schlenk line (leave the attached hose on vacuum) and froze the liquid in dry ice acetone solution. When the solution was frozen, opened the hose to vacuum and pump off the atmosphere for 15minutes. Sealed the test tube again and thawed the solution until it just melted using a tepid water bath. Filled the test tube with ultrapure nitrogen gas and sealed the test tube again. Changed to cooling bath and refroze the solution again. Repeated the above steps for three cycles, the solution was filled with ultrapure nitrogen and ready to use.

The reaction time was controlled so that less than 5% of starting material reacted, which lowers the error caused by the absorption of the product. The concentrations of the products were analyzed by the long-wavelength absorption of the anthracene products. Before irradiation, 0.5ml of solution was taken and tested by UV-Vis spectroscopy. During each reaction time intervals, 0.5ml of the solution was taken and tested by UV-Vis spectroscopy again till the end of the reaction.

Multiple measurements were conducted to obtain are liable value. For each sample, if an approximate linear relationship is obtained from the data at different time intervals, the first data was used to calculate the quantum yield using the following equation[170]. The quantum yield is defined as the number of the photo events divided by the number of the photons absorbed. Unlike the reaction rate, it is independent of the absorption at the irradiation wavelength. Therefore, although the DA adducts have different molar absorption coefficients at 254 nm, their quantum yields are comparable.

$$\emptyset = (\varepsilon^{\circ} t^{\circ} \emptyset^{\circ} / \Delta A^{\circ})(\Delta A / \varepsilon t) \quad (4)$$

ε°, t°, Φ°, and ΔA° are the molar absorption coefficient, irradiation time, quantum yield, and absorption change of the standard, and ε, t, Φ, and $\Delta A$are the molar absorption coefficient, irradiation time, quantum yield, and absorption change of the PrDA product. The quantum yield of uridine at 254 nm is 0.019 and the absorption coefficient is 10338 M^{-1} cm^{-1}. The absorption and absorption coefficient of each PrDA product was carefully measured (see chapter 3).

For the TCNE adduct, the backward DA reaction also occurs at room temperature unless one of the products is stabilized or reacts with other reagents. According to previous results[116], methanol was added to the acetonitrile solution of the TCNE adducts immediately before the photoreaction. Except in the reaction of 18, such amount of methanol did not produce detectable amount of trapped inter mediate in the experimental condition for quantum yield measurement, and thus did not significantly alter the results.

In the trapping experiment of 18, a 1mM solution of 18 in 1:3 methanol/MeCN was irradiated at either 254 nm or 365 nm under nitrogen using an 8W UV lamp. After 6 hours reaction, two major products were isolated by filtration and column chromatography. One is phencyclone,

which is the product of the corresponding PrDA reaction. The other is the methanol trapped product.

5.2.1.2 CORM Sample Preparation

All chemicals are obtained from commercial sources and used without further purification. 100mg Pluronic 127 was dissolved in 5ml DI water and ultrasonicated for 5minutes. 1mg of DKs was dissolved in 5ml of CH_2Cl_2 and mixed with Pluronic solution. The resulting mixture was stirred at room temperature for 48 h to slowly evaporate the CH_2Cl_2. The DK concentration was approximately 0.5 mM in water, as estimated by absorption spectra. The whole process was produced in dark.

In order to detect CO generated by CORM, two-compartment myoglobin test was used. The setup of the two-compartment test is illustrated in Figure 42. Specifically, myoglobin solution was degassed and mixed with excess amount of $Na_2S_2O_4$ in a sealed Erlenmeyer flask. Reduction of the MbFe(III) to MbFe(II) was confirmed by UV-Vis absorption spectroscopy. DK22 micelle solution in PBS buffer was degassed and stocked in an air-tight syringe. The long needle tip of the syringe was positioned at the very bottom of the MbFe(II) solution. The syringe was chilled in ice-water bath to increase the solubility of CO in water and irradiated by 470 nm LED light. The plunger of the syringe was pulled very slowly in order to draw the Mb solution from the flask into the syringe without making gap between the solution and the plunger. The amount of Mb is ~4 times that of the theoretical yield of CO. The absorbance of the mixture solution was recorded again in a quartz cuvette. The concentration of MbCO was calculated by using the following equations[171].

$$\frac{A_{542}}{A_{iso}} = \frac{\varepsilon_{d542}[Mb] + \varepsilon_{CO542}[MbCO]}{\varepsilon_{iso}([Mb] + [MbCO])} = \frac{\varepsilon_{d542}}{\varepsilon_{iso}} - \frac{\varepsilon_{d542} - \varepsilon_{CO542}}{\varepsilon_{iso}} \cdot \frac{[MbCO]}{[Mb] + [MbCO]}$$

$$\therefore \frac{[MbCO]}{[Mb]+[MbCO]} = \left(\frac{\varepsilon_{d542}}{\varepsilon_{iso}} - \frac{A_{542}}{A_{iso}}\right) \cdot \frac{\varepsilon_{iso}}{\varepsilon_{d542}-\varepsilon_{CO542}} \quad (5)$$

Where A542 and Aiso are the absorbance at 542 and 552 nm, and [Mb] and [MbCO] are the concentration of Mb and MbCO.

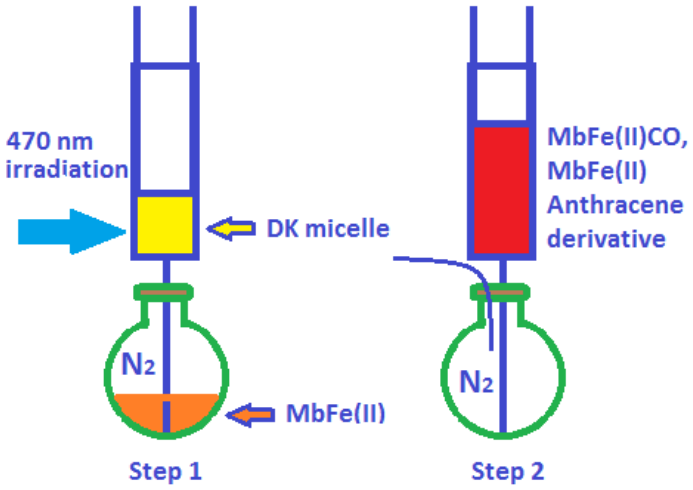

Figure 46. Setup for the two-compartment myoglobin test of CO released from the photoCORM

5.2.2 Instruments

5.2.2.1 UV-Vis Absorption and Fluorescence

The UV-Vis absorption and fluorescence spectra were collected using the same instruments as for the photoacid solutions.

5.2.2.2 NMR

The 1H spectroscopic measurements were performed using a Varian 500 NMR spectrometer ant 500 MHz with tetramethysilane (TMS) as internal reference.

5.2.2.3 High Resolution Mass Spectrometer (HRMS)

High resolution mass spectrometers are measured in Agilent 6210 TOF-MS.

5.2.3 Supporting Data

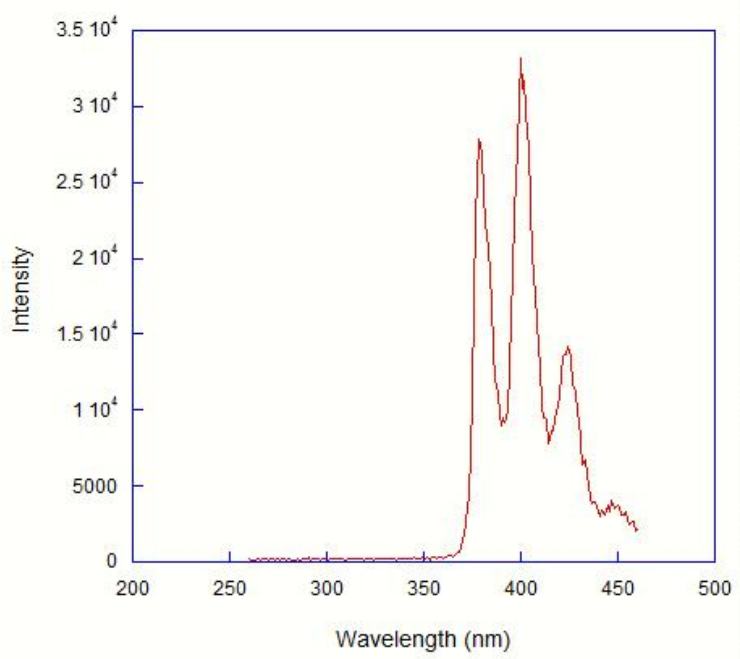

Figure 47. Fluorescence of anthracene

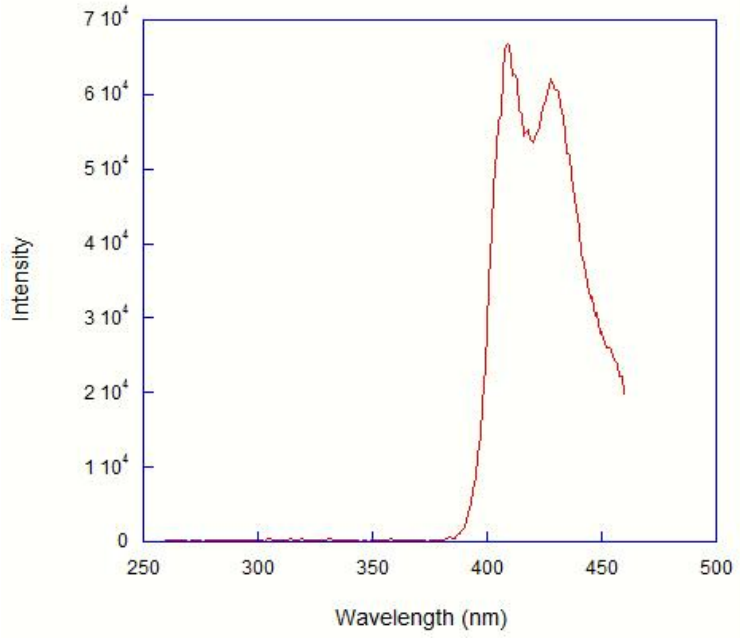

Figure 48. Fluorescence of diphenylanthracene

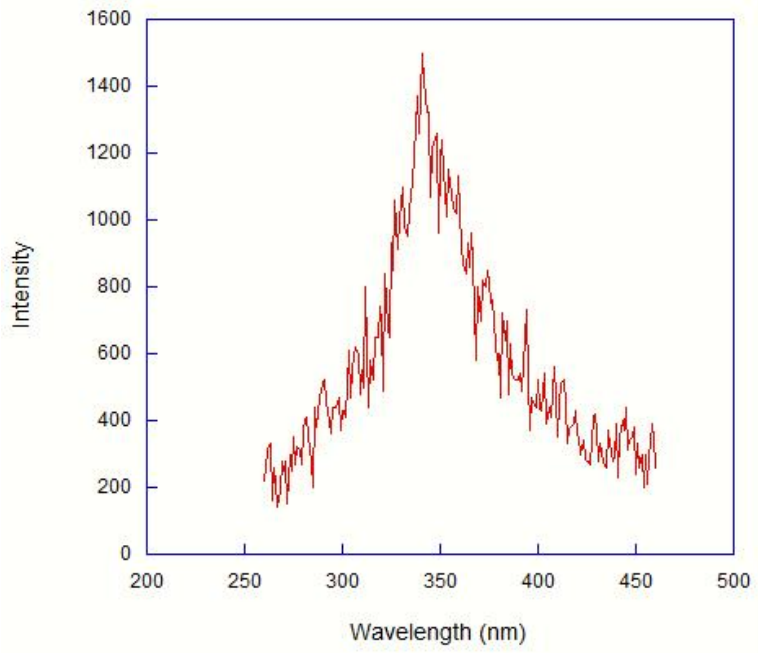

Figure 49. Fluorescence of naphthacene TCNE

5.3 PANI Thin Films

5.3.1 Thin Film Sample Preparation

To have an ultra clean slide is a prerequisite in PANI thin films experiments. Every slide was ultrasonically cleaned by soap water, DI H_2O, acetone, and DI H_2O again for 20 minutes each. At the end, each slide was blow-dried with N_2 gas before using for PANI sample preparation. For all of the films with gold electrodes, they were covered with a 1mm strip mask and then put into the electron beam evaporation system (Thermionics). First, a 2-nm chromium layer was deposited on the film by this system. Then a 50-nm thick gold layer was deposited on top of chromium in the thermal evaporator under high vacuum ($< 10^{-6}$Torr).

Polyaniline emeraldine base (MW=20,000), Poly(ethylene glycol) (MW=8000), Poly(acrylic acid), triphenylsulfoniumtriflate were purchased from Aldrich. Polyvinyl alcohol (PVA)

(MW=88,000, 88% hydrolyzed) was purchased from Acros Organics. All of the solvents were used without further purification.

For all of the films tested in PANI with irreversible photoacid generator, PANI-EB and PVA (ratios described in Chapter 4 section 1) were dissolved in N-methylpyrrolidinone (NMP) at room temperature. The solid to solvent ratio (weight) was around 1:10. The PAG was added to the solution, and allowed to stir for 30 min. The resulting blue solution was subsequently filtered through a 0.45 m micropore filter. Thin films of the composites were prepared by spin casting on glass substrates with gold electrodes. Each thin film was placed in a vacuum oven at room temperature for 36 h to remove the solvent and then kept in the desiccators. The PANI layer thickness is around 1μm which is measured by profilometer. These samples were sealed in quartz tubes filled with argon, then placed in the center of a Rayonet photochemical reactor equipped with 254 nm UV lamps. The conductivity before and after irradiation was measured by *I-V*scan using a Keithley 2400 source meter. Some irradiated samples were also tested with four-point probe method. The conductivities of these samples were in the same order of magnitude as the values obtained by *I-V* scan.

For PANI with reversible photoacid experiments, I used two different methods to test the films. The first one is the mono layer method which is spun coating PANI/PAH/PEG/PAA solution directly on surface of a gold film. PANI-EB was dissolved in N-methylpyrrolidinone(NMP), and then mixed with PEG and PAA. Photoacid was dissolved in another test tube by NMP and irradiated at 470 nm for 5mins. Under LED light irradiation, the PANI solution was mixed with the photoacid solution and irradiated another 5mins. The resulting solution was subsequently filtered through a 0.45 μm micropore filter. Thin films of the composites were prepared by spin casting on glass substrates with gold electrodes. All thin films were vacuum-dried for 24h at

room temperature to remove the solvent and then kept in the desiccators. These samples were sealed in quartz tubes filled with argon, then placed under the 470 nm LED light bundle. The conductivity before and after irradiation was measured by *I-V* scan.

The second way is two layers methods which is represented in Figure 43.The conductivity of each film was measured by I-V scanning or the four-point probe method.

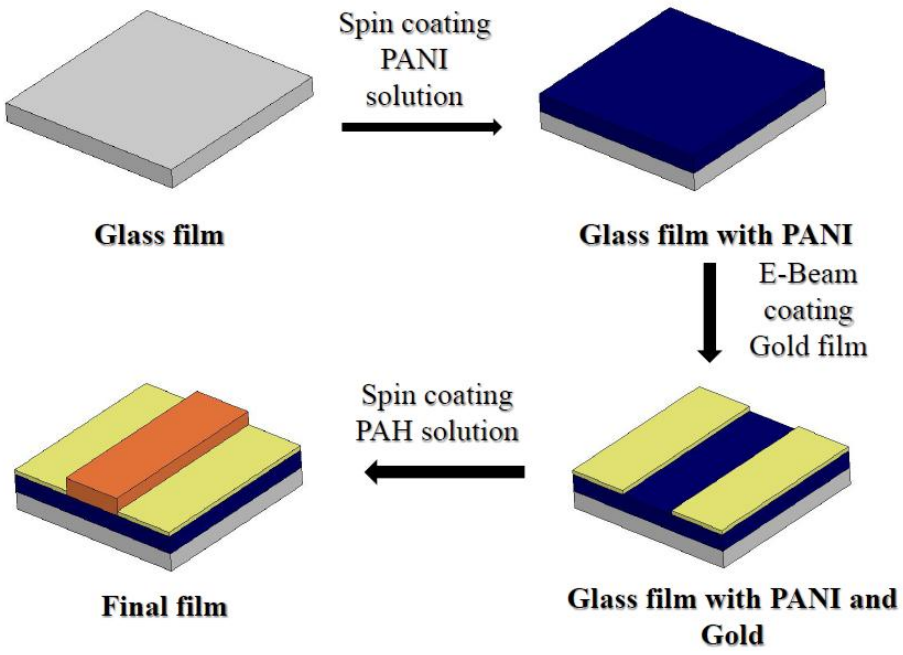

Figure 50. Two layers preparation method of PANI/PEG/PAA/PAH films

5.3.2 Instruments

5.3.2.1 Profilometer

All of the thickness of films was measured by Alpha Step Profilometer from UCF Advanced Materials Processing and Analysis Center.

5.3.2.2 Fourier Transmission Infrared Spectroscopy (FTIR)

In order to study the solid state of DA adducts, Attenuated Total Reflectance (ATR) IR is a suitable technique. An ATR accessory operates by measuring the changes before and after the infrared beam contact with a sample. An infrared beam is directed onto an optically dense crystal

with a high refractive index at a certain angle, and then this internal reflectance generates an evanescent wave to go through the surface of the crystal into the sample, which only a few microns (0.5μm – 5μm). This evanescent wave will change to attenuated energy or altered energy. Only attenuated energy will pass back to the IR beam and be detected by the opposite side detector in the IR spectrometer. The system will generate a resulting spectrum, which represents the molecular absorption and transmission. These absorption or transmission match with different bond or group vibrate frequency. ATR-IR spectroscopy was collected on a Perkin Elmer Spectrum One spectrometer equipped with a Universal ATR Sampling Accessory (single reflection, Diamond/ZnSe). IR spectra were collected in a range of 600-4000 cm^{-1} with a resolution of 1 datum every 2 cm^{-1}.

5.3.2.3 Scanning Electron Microscopy (SEM)

Scanning Electron Microscopy (SEM) image was first obtained in the early 1930's [172]and the first real instrument was developed by DuPont. A SEM is an electron microscope which scans a sample with a beam of electrons in a raster scan pattern and takes its image. Because of its large depth of field and high resolution, SEM becomes one of the most useful methods for physical properties characterization. A SEM generates six different types of signals: secondary electrons, back-scattered electrons (BSE), characteristic X-rays, light (cathode luminescence), specimen current and transmitted electrons. Detectors for secondary electron, BES and characteristic X-rays will provide very high-resolution image of the sample surface and composition of the sample.

In order to generate good SEM images, all of the samples, at least on the surface, must be electrically conductive, and also electrically grounded to prevent the accumulation of electrostatic charge on the surface. Those nonconductive samples will be coated by an ultrathin

layer of electrically conducting material by low-vacuum sputter coating or high-vacuum evaporation to prevent charge when scanned by electron beam, and especially in secondary electron imaging mode. All of SEM image was characterized by a Zeiss (Ultra 55) SEM operated at 10 ke V. The sample for SEM observation was prepared by coating a 20 nm thin layer of gold or platinum.

5.3.3 Supporting Data

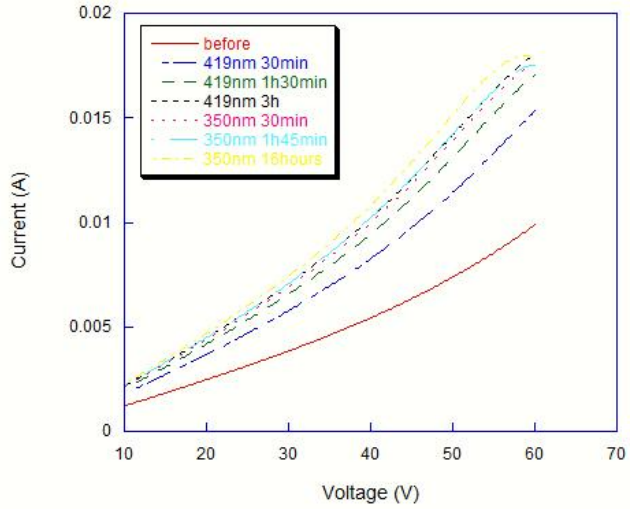

Figure 51. PANI (5.4mg) doped with SP (12mg) in 1:1 ratio NMP: m-cresol

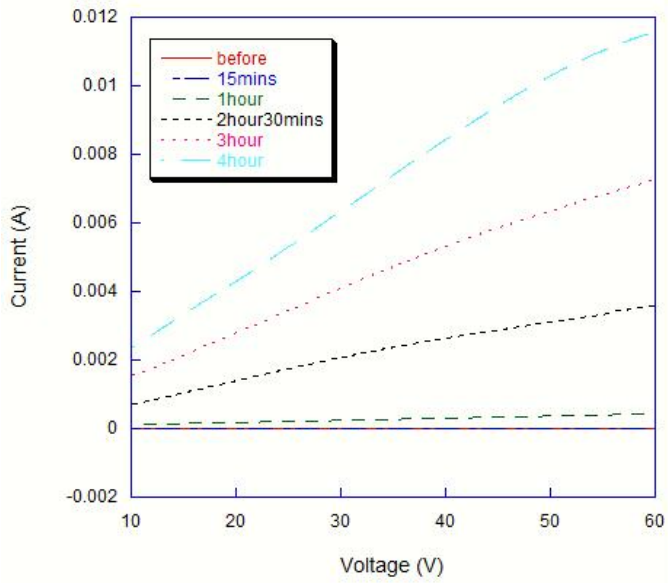

Figure 52. PANI doped with photoacid generator (molar ratio 1:0.4) and PVA

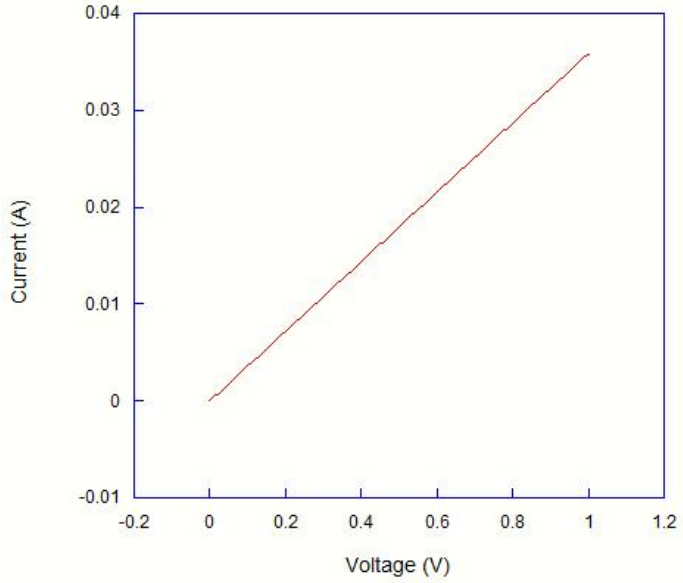

Figure 53. PANI doped with Camphorsulfonic acid (molar ratio 1:1)

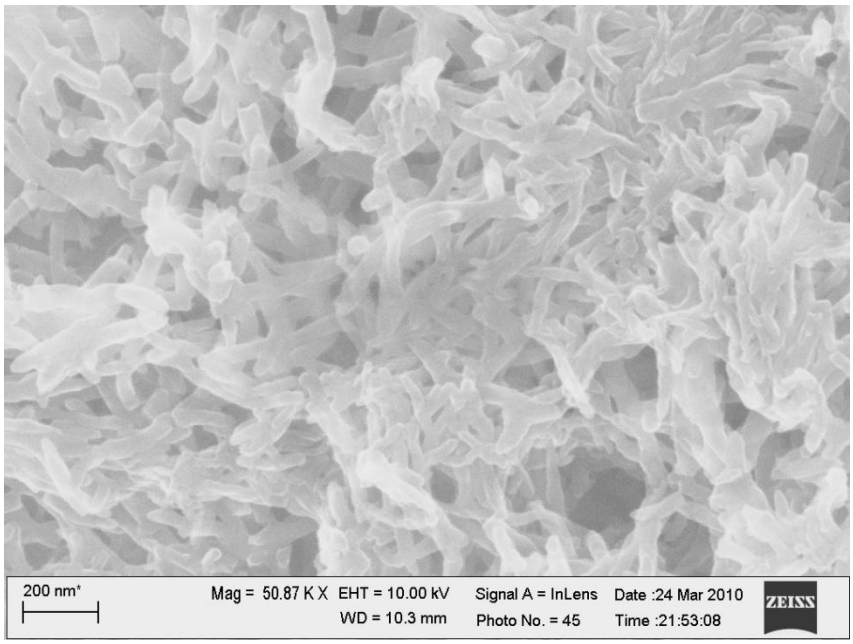

Figure 54. SEM of PANI thin film

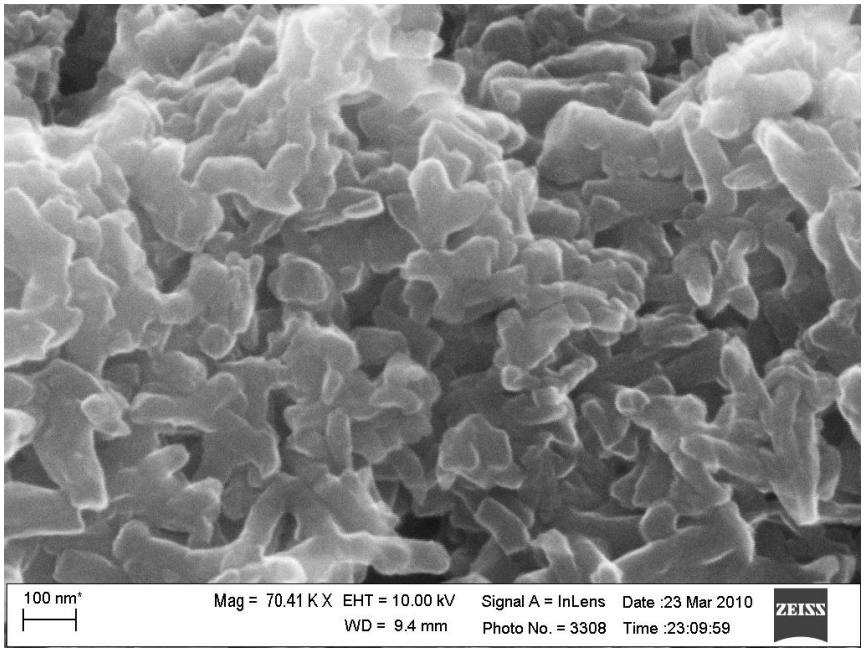

Figure 55. SEM of PANI wrapped with PVA

APPENDIX: LIST OF PUBLICATION

Shi, Z.; Peng, P.; Strohecker, D.; Liao,Y. *A long-lived photoacid based upon a photochromic reaction* Journal of the American Chemical Society, 2011, 133(37).

Shi, Z.; Johns, V.; Liao,Y. *Photoinduced Protonation of Polyaniline Assisted by Hydrogen-Bonding Material*, Synthetic Metals, 2011, 161(13-14)

Johns, V.; Shi, Z.; Hu, W.; Johns, J.; Zou, S.; Liao, Y. *Photo-and Thermal-Induced Isomerization of Diels-Alder Adducts of Pentacene and TCNE,* European Journal of Organic Chemistry, 2012, 14(2707-2710)

Johns, V.; Shi, Z.; Dang, W.; Liao, Y. *Photo Retro-Diels-Alder Reactions*, Journal of Physical Chemistry A, 2011, 115(28)

Tian, R.; Shi, Z.; Liao, Y. *Novel organic materials that permanently increase conductivity upon thermal or photo treatment*, Organic Electronics, 2009, 10(2)

Shah, S.; Tian, R.; Shi, Z.; Liao, Y. *Side-chain free aromatic polyimides containing anthracene units via Diels-Alder precursors*, Journal of Applied Polymer Science, 2009, 112(5)

Shi, Z.; Peng, P.; Johns, V.; Liao, Y. *Novel photoreversible materials based on photoacid and polyaniline*, Polymer Preprints (American Chemical Society, Division of Polymer Chemistry,) 2012, 53(2), 125-126.

Shi, Z.; Johns, V.; Alber, C.; Liao, Y. *Photoinduced protonation of polyaniline assisted by hydrogen-bonding materials*, PMSE Preprints,241st ACS National Meeting & Exposition, (2011)

Johns, V.; Shi, Z.; Liao, Y. *Structure-reactivity relationship of photo-retro-Diel's-Alder reaction*, Abstracts of Papers, 241st ACS National Meeting & Exposition, 2011, ORGN-573.

REFERENCES

1. Ciamician, G. *THE PHOTOCHEMISTRY OF THE FUTURE.* Science 1912, 36, (926), 385-394.
2. Smith, K. C., *Basic Photochemistry*. 2011, Stanford University School of Medicine: Los Gatos.
3. Kopecky, J., *Organic Photochemistry: A Visual Approach*. 1992: VCH Publishers, Inc.
4. Li, J.; Liu, Z.; Tan, C.; Guo, X.; Wang, L.; Sancar, A.; Zhong, D. *Dynamics and mechanism of repair of ultraviolet-induced (6-4) photoproduct by photolyase.* Nature 466, (7308), 887-890.
5. Tobita, H. S. A. S., *Proton Transfer Reactions in the Excited States*. Organic Photochemistry and Photophysics, ed. V.R.a.K. Schanze. 2006: CRC Press.
6. Wan, P.; Shukla, D. *Utility of acid-base behavior of excited states of organic molecules.* Chemical Reviews 1993, 93, (1), 571-584.
7. Arnaut, L. G.; Formosinho, S. J. *Excited-state proton transfer reactions I. Fundamentals and intermolecular reactions.* Journal of Photochemistry and Photobiology A: Chemistry 1993, 75, (1), 1-20.
8. Dempsey, J. L.; Winkler, J. R.; Gray, H. B. *Mechanism of H2 Evolution from a Photogenerated Hydridocobaloxime.* Journal of the American Chemical Society 132, (47), 16774-16776.
9. Morimoto, M.; Irie, M. *Photochemical control of dielectric properties based on intermolecular proton transfer in a hydrogen-bonded diarylethene crystal.* Chemical Communications 47, (14), 4186-4188.

10. Silvi, S.; Arduini, A.; Pochini, A.; Secchi, A.; Tomasulo, M.; Raymo, F. M.; Baroncini, M.; Credi, A. *A Simple Molecular Machine Operated by Photoinduced Proton Transfer.* Journal of the American Chemical Society 2007, 129, (44), 13378-13379.

11. Guo, X.; Zhang, D.; Yu, G.; Wan, M.; Li, J.; Liu, Y.; Zhu, D. *Reversible Photoregulation of the Electrical Conductivity of Spiropyran-Doped Polyaniline for Information Recording and Nondestructive Processing.* Advanced Materials 2004, 16, (7), 636-640.

12. Jiang, G.; Song, Y.; Guo, X.; Zhang, D.; Zhu, D. *Organic Functional Molecules towards Information Processing and High-Density Information Storage.* Advanced Materials 2008, 20, (15), 2888-2898.

13. Stein, M.; Keck, J.; Waiblinger, F.; Fluegge, A. P.; Kramer, H. E. A.; Hartschuh, A.; Port, H.; Leppard, D.; Rytz, G. *Influence of Polymer Matrixes on the Photophysical Properties of UV Absorbers.* The Journal of Physical Chemistry A 2001, 106, (10), 2055-2066.

14. Waiblinger, F.; Keck, J.; Stein, M.; Fluegge, A. P.; Kramer, H. E. A.; Leppard, D. *Light-Induced Opening of the Intramolecular Hydrogen Bond of UV Absorbers of the 2-(2-Hydroxyphenyl)-1,3,5-triazine and the 2-(2-Hydroxyphenyl)benzotriazole Type.* The Journal of Physical Chemistry A 2000, 104, (6), 1100-1106.

15. Keck, J.; Kramer, H. E. A.; Port, H.; Hirsch, T.; Fischer, P.; Rytz, G. *Investigations on Polymeric and Monomeric Intramolecularly Hydrogen-Bridged UV Absorbers of the Benzotriazole and Triazine Class.* The Journal of Physical Chemistry 1996, 100, (34), 14468-14475.

16. Das, K.; Ashby, K. D.; Wen, J.; Petrich, J. W. *Temperature Dependence of the Excited-State Intramolecular Proton Transfer Reaction in Hypericin and Hypocrellin A.* The Journal of Physical Chemistry B 1999, 103, (9), 1581-1585.

17. Smirnov, A. V.; Das, K.; English, D. S.; Wan, Z.; Kraus, G. A.; Petrich, J. W. *Excited-State Intramolecular H Atom Transfer of Hypericin and Hypocrellin A Investigated by Fluorescence Upconversion.* The Journal of Physical Chemistry A 1999, 103, (40), 7949-7957.

18. Krishnan, R.; Fillingim, T. G.; Lee, J.; Robinson, G. W. *Solvent structural effects on proton dissociation.* Journal of the American Chemical Society 1990, 112, (4), 1353-1357.

19. Letheby, H. *XXIX.?On the production of a blue substance by the electrolysis of sulphate of aniline.*1862, 15, 161-163.

20. Green, A. G.; Woodhead, A. E. *CCXLIII.-Aniline-black and allied compounds. Part I.* Journal of the Chemical Society, Transactions 1910, 97, 2388-2403.

21. Green, A. G.; Woodhead, A. E. *CXVII.-Aniline-black and allied compounds. Part II.* Journal of the Chemical Society, Transactions 1912, 101, 1117-1123.

22. Diaz, A. F.; Logan, J. A. *Electroactive polyaniline films.* Journal of Electroanalytical Chemistry and Interfacial Electrochemistry 1980, 111, (1), 111-114.

23. Houk, K. N.; Gonzalez, J.; Li, Y. *Pericyclic Reaction Transition States: Passions and Punctilios, 1935-1995.* Accounts of Chemical Research 1995, 28, (2), 81-90.

24. Branchadell, V.; Font, J.; Moglioni, A. G.; Ochoa De Echagiien, C.; Oliva, A.; Ortuno, R. M.; Veciana, J.; Vidal-Gancedo, J. *A Biradical Mechanism in the Diels-Alder Reactions of 5-Methylene-2(5H)-furanones:Experimental Evidence and Theoretical Rationalization.* Journal of the American Chemical Society 1997, 119, (42), 9992-10003.

25. Montgomery, L. K.; Schueller, K.; Bartlett, P. D. *Cycloaddition. II. Evidence of a Biradical Intermediate in the Thermal Addition of 1,1-Dichloro-2,2-difluoroethylene to*

the Geometrical Isomers of 2,4-Hexadiene. Journal of the American Chemical Society 1964, 86, (4), 622-628.

26. Bartlett, P. D.; Wallbillich, G.; Wingrove, A. S.; Swenton, J. S.; Montgomery, L. K.; Kramer, B. D. *Cycloaddition. V. 2-Alkylbutadienes and 1,1-dichloro-2,2-difluoroethylene. Effect of diene conformation on mode of cycloaddition.* Journal of the American Chemical Society 1968, 90, (8), 2049-2056.

27. Bartlett, P. D.; Wallbillich, G. E. H. *Cycloaddition. XI. Evidence for reversible biradical formation in the addition of 1,1-dichloro-2,2-difluoroethylene to the stereoisomers of 1,4-dichloro-1,3-butadiene.* Journal of the American Chemical Society 1969, 91, (2), 409-414.

28. Bartlett, P. D.; Mallet, J. J. B. *Cycloaddition. XIX. Competing concerted and stepwise [2 + 4]cycloaddition of the dichlorodifluoroethylenes to butadiene and 2,4-hexadiene.* Journal of the American Chemical Society 1976, 98, (1), 143-151.

29. Bunnage, M. E.; Nicolaou, K. C. *The Oxide Anion Accelerated Retro-Diels-Alder Reaction.* Chemistry – A European Journal 1997, 3, (2), 187-192.

30. Bunnelle, W. H.; Randall Shangraw, W. *Acid catalysis of the retro-diels alder reaction. Formation and electrophilic reactivity of 2-methylene-1,3-cyclopentanedione.* Tetrahedron 1987, 43, (9), 2005-2011.

31. Bahr, N.; Guller, R.; Reymond, J.-L.; Lerner, R. A. *A Nitroxyl Synthase Catalytic Antibody.* Journal of the American Chemical Society 1996, 118, (15), 3550-3555.

32. Chantarasiri, N.; Dinprasert, P.; Thebtaranonth, C.; Thebtaranonth, Y.; Yenjai, C. *Synthesis of 2-methylene-1,3-dioxygenated cyclopentanes and cyclopentenes.* Journal of the Chemical Society, Chemical Communications 1990,(4), 286-288.

33. Pagni, R. M.; Kabalka, G. W.; Hondrogiannis, G.; Bains, S.; Anosike, P.; Kurt, R. *The cycloaddition reactions of unsaturated esters with cyclopentadiene on y-alumina.* Tetrahedron 1993, 49, (31), 6743-6756.

34. Atherton, J. C. C.; Jones, S. *Establishing cleavage conditions for an anthracene chiral auxiliary using a photochemical retro Diels-Alder reaction.* Tetrahedron Letters 2002, 43, (50), 9097-9100.

35. Haldane, J. B. *Carbon Monoxide as a Tissue Poison.* Biochem. J. 1927, 21, (5), 1068-1060.

36. Motterlini, R.; Mann, B. E.; Johnson, T. R.; Clark, J. E.; Foresti, R.; Green, C. J. *Bioactivity and Pharmacological Actions of Carbon Monoxide-Releasing Molecules.* Current Pharmaceutical Design 2003, 9, (30), 2525-2539.

37. Nunes, R. M. D.; Pineiro, M.; Arnaut, L. G. *Photoacid for Extremely Long-Lived and Reversible pH-Jumps.* Journal of the American Chemical Society 2009, 131, (26), 9456-9462.

38. Zhou, D.; Khatmullin, R.; Walpita, J.; Miller, N. A.; Luk, H. L.; Vyas, S.; Hadad, C. M.; Glusac, K. D. *Mechanistic Study of the Photochemical Hydroxide Ion Release from 9-Hydroxy-10-methyl-9-phenyl-9,10-dihydroacridine.* Journal of the American Chemical Society 134, (28), 11301-11303.

39. Huppert, D.; Kolodney, E. *Picosecond proton transfer studies in water-alcohols solutions.* Chemical Physics 1981, 63, (3), 401-410.

40. Robinson, G. W.; Thistlethwaite, P. J.; Lee, J. *Molecular aspects of ionic hydration reactions.* The Journal of Physical Chemistry 1986, 90, (18), 4224-4233.

41. Mansueto, E. S.; Wight, C. A. *Excited-state proton-transfer polymerization of amorphous formaldehyde.* Journal of the American Chemical Society 1989, 111, (5), 1900-1901.

42. Leiderman, P.; Genosar, L.; Huppert, D.; Shu, X.; Remington, S. J.; Solntsev, K. M.; Tolbert, L. M. *Ultrafast Excited-State Dynamics in the Green Fluorescent Protein Variant S65T/H148D. 3. Short- and Long-Time Dynamics of the Excited-State Proton Transfer.* Biochemistry 2007, 46, (43), 12026-12036.

43. Mandal, D.; Pal, S. K.; Bhattacharyya, K. *Excited-State Proton Transfer of 1-Naphthol in Micelles.* The Journal of Physical Chemistry A 1998, 102, (48), 9710-9714.

44. Spry, D. B.; Goun, A.; Glusac, K.; Moilanen, D. E.; Fayer, M. D. *Proton Transport and the Water Environment in Nafion Fuel Cell Membranes and AOT Reverse Micelles.* Journal of the American Chemical Society 2007, 129, (26), 8122-8130.

45. Il'ichev, Y. V.; Solntsev, K. M.; Demyashkevich, A. B.; Kuzmin, M. G.; Lemmetyinen, H.; Vuorimaa, E. *Excited-state proton transfer reactions of long-chain derivatives of naphthols in solutions and Langmuir-Blodgett films.* Chemical Physics Letters 1992, 193, (1-3), 128-133.

46. Chou, P.; Mcmorrow, D.; Aartsma, T. J.; Kasha, M. *The proton-transfer laser. Gain spectrum and amplification of spontaneous emission of 3-hydroxyflavone.* The Journal of Physical Chemistry 1984, 88, (20), 4596-4599.

47. Nishiya, T.; Yamauchi, S.; Hirota, N.; Baba, M.; Hanazaki, I. *Fluorescence studies of intramolecularly hydrogen-bonded o-hydroxyacetophenone, salicylamide, and related molecules.* The Journal of Physical Chemistry 1986, 90, (22), 5730-5735.

48. Smith, T. P.; Zaklika, K. A.; Thakur, K.; Walker, G. C.; Tominaga, K.; Barbara, P. F. *Ultrafast studies on proton transfer in photostabilizers.* Journal of Photochemistry and Photobiology A: Chemistry 1992, 65, (1-2), 165-175.

49. Catalan, J.; Fabero, F.; Soledad Guijarro, M.; Claramunt, R. M.; Santa Maria, M. D.; Foces-Foces, M. D. L. C.; Hernandez Cano, F.; Elguero, J.; Sastre, R. *Photoinduced intramolecular proton transfer as the mechanism of ultraviolet stabilizers: a reappraisal [Erratum to document cited in CA112(5):35179y]*. Journal of the American Chemical Society 1991, 113, (10), 4046-4046.

50. Weber, K. Z. Phys. Chem. 1931, B15, 18.

51. Forster, T. Naturwiss. 1949, 36, 186.

52. Forster, T. Z. Elektrochem. 1950, 54, 43.

53. Weller, A. Naturwiss. 1955, 42, 175.

54. Weller, A. Progr. Reaction Kinet. 1961, 1, 187.

55. Donckt, E. V. Progr. Reaction Kinet. 1970, 5, 273.

56. Ireland, J. F.; Wyatt, P. A. H.; Gold, V., *Acid-Base Properties of Electronically Excited States of Organic Molecules*, in *Advances in Physical Organic Chemistry*. 1976, Academic Press. p. 131-221.

57. Adamczyk, K.; Premont-Schwarz, M.; Pines, D.; Pines, E.; Nibbering, E. T. J. *Real-Time Observation of Carbonic Acid Formation in Aqueous Solution.* Science 2009, 326, (5960), 1690-1694.

58. Fritsche, M. Comptes rendus de l'Academie des sciences 1867, 64, 1035.

59. Guglielmetti, J. C. C. A. R. J., *Organic photochromic and thermochromic compounds* Topics in applied chemistry. 1999: Plenum Press.

60. Mason, S. J.; Hake, J. L.; Nairne, J.; Cummins, W. J.; Balasubramanian, S. *Solid-Phase Methods for the Synthesis of Cyanine Dyes.* The Journal of Organic chemistry 2005, 70, (8), 2939-2949.

61. Shi, Z.; Peng, P.; Strohecker, D.; Liao, Y. *Long-Lived Photoacid Based upon a Photochromic Reaction.* Journal of the American Chemical Society 133, (37), 14699-14703.

62. Natali, M.; Soldi, L.; Giordani, S. *A photoswitchable Zn (II) selective spiropyran-based sensor.* Tetrahedron 66, (38), 7612-7617.

63. Tagaya, H.; Kuwahara, T.; Sato, S.; Kadokawa, J.-I.; Karasu, M.; Chiba, K. *Photoisomerization of indolinespirobenzopyran in layered double hydroxides.* Journal of Materials Chemistry 1993, 3, (3), 317-318.

64. Stafstrom, S.; Bredas, J. L.; Epstein, A. J.; Woo, H. S.; Tanner, D. B.; Huang, W. S.; Macdiarmid, A. G. *Polaron lattice in highly conducting polyaniline: Theoretical and optical studies.* Physical Review Letters 1987, 59, (13), 1464.

65. Katayama, S.; Hirokawa, Y.; Tanaka, T. *Reentrant phase transition in acrylamide-derivative copolymer gels.* Macromolecules 1984, 17, (12), 2641-2643.

66. Tanaka, T. *Collapse of Gels and the Critical Endpoint.* Physical Review Letters 1978, 40, (12), 820-823.

67. Tanaka, T.; Fillmore, D.; Sun, S.-T.; Nishio, I.; Swislow, G.; Shah, A. *Phase Transitions in Ionic Gels.* Physical Review Letters 1980, 45, (20), 1636-1639.

68. Hirokawa, Y.; Tanaka, T. *Volume phase transition in a nonionic gel.* The Journal of Chemical Physics 1984, 81, (12), 6379-6380.

69. Ohmine, I.; Tanaka, T. *Salt effects on the phase transition of ionic gels.* The Journal of Chemical Physics 1982, 77, (11), 5725-5729.

70. Ricka, J.; Tanaka, T. *Swelling of ionic gels: quantitative performance of the Donnan theory.* Macromolecules 1984, 17, (12), 2916-2921.

71. Park, T. G.; Hoffman, A. S. *Sodium chloride-induced phase transition in nonionic poly(N-isopropylacrylamide) gel.* Macromolecules 1993, 26, (19), 5045-5048.

72. Brauman, J. I.; Schwartz, J.; Van Tamelen, E. E. *Acid-base behavior of excited states. The photochemistry of cyclooctatetraene dianion.* Journal of the American Chemical Society 1968, 90, (19), 5328-5329.

73. Schwartz, J. *The photochemistry of cyclononatetraenide and bicyclo[4,3,0]nonatriene.* Journal of the Chemical Society D: Chemical Communications 1969,(14), 833-834.

74. Wan, P.; Krogh, E.; Chak, B. *Enhanced formation of 8.pi.(4n) conjugated cyclic carbanions in the excited state: first example of photochemical C-H bond heterolysis in photoexcited suberene.* Journal of the American Chemical Society 1988, 110, (12), 4073-4074.

75. Henri Bouas-Laurent, H. D. *Organic Photochromism.* Pure and Applied Chemistry 2001, 73, (4), 639-665.

76. Henri Bouas-Laurent, H. D., *Photochromism: Molecules and Systems*. Revised Edition ed. 2003: Elsevier Science B.V.

77. Dalton, L. R.; Sullivan, P. A.; Bale, D. H. *Electric Field Poled Organic Electro-optic Materials: State of the Art and Future Prospects.* Chemical Reviews 2009, 110, (1), 25-55.

78. Willets, K. A.; Ostroverkhova, O.; He, M.; Twieg, R. J.; Moerner, W. E. *Novel Fluorophores for Single-Molecule Imaging.* Journal of the American Chemical Society 2003, 125, (5), 1174-1175.

79. Goldschmidt, H. Z. physik. Chem 1914, 89, 129.

80. Staudinger, H. *Über Ketene. 16. Mitteilung: Über Bildung und Spaltung von Vierringen.* Berichte der deutschen chemischen Gesellschaft 1911, 44, (1), 521-533.

81. V. Euler, H.; Josephson, K. O. *Über Kondensationen an Doppelbindungen. I.: Über die Kondensation von Isopren mit Benzochinon.* Berichte der deutschen chemischen Gesellschaft (A and B Series) 1920, 53, (5), 822-826.

82. Wieland, H. *Untersuchungen über Dicyclopentadiën. I.* Berichte der deutschen chemischen Gesellschaft 1906, 39, (2), 1492-1499.

83. Zincke, T.; Günther, H. *Ueberführung von Pentenderivaten in Indenderivate.* Justus Liebigs Annalen der Chemie 1893, 272, (3), 243-270.

84. Zincke, T. *Ueber die Einwirkung von Chlor auf o-Amidophenole und o-Diamine.* Justus Liebigs Annalen der Chemie 1897, 296, (2), 135-158.

85. Diels, O.; Alder, K. *Synthesen in der hydroaromatischen Reihe.* Justus Liebigs Annalen der Chemie 1928, 460, (1), 98-122.

86. Woodward, R. B.; Sondheimer, F.; Taub, D.; Heusler, K.; Mclamore, W. M. *The Total Synthesis of Steroids1.* Journal of the American Chemical Society 1952, 74, (17), 4223-4251.

87. Fringuelli, F. T., Aldo, *The Diels Alder Reaction: Selected Practical Methods*. 2002: Wiley.

88. Diels, O.; Alder, K. *Synthesen in der hydro-aromatischen Reihe, II. Mitteilung: Über Cantharidin.* Berichte der deutschen chemischen Gesellschaft (A and B Series) 1929, 62, (3), 554-562.

89. Alder, K.; Rickert, H. F. *Zur Kenntnis der Dien - Synthese, II. Mitteil.: Über den thermischen Zerfall der Additionsprodukte des Acetylen-dicarbonsäure-esters.* Berichte der deutschen chemischen Gesellschaft (A and B Series) 1937, 70, (6), 1354-1363.

90. Chung, Y.; Duerr, B. F.; Mckelvey, T. A.; Nanjappan, P.; Czarnik, A. W. *Structural effects controlling the rate of the retro - Diels - Alder reaction in anthracene cycloadducts.* J. Org. Chem. 1989, 54, 1018-1032.

91. Chung, Y. S. D., Brook F.; Nanjappan, P.; Czarnik, Anthony W. *Diene -substituent effects on the rate of the retro - Diels - Alder reaction. Cycloreversion reactivity varying over a range of 10^5.* J. Org. Chem. 1988, 53, 1334-1336.

92. Kwart, H.; King, K. *The reverse Diels - Alder or retrodiene reactions.* Chem. Rev. 1968, 68, 415-417.

93. Nanjappan, P.; Czarnik, A. W. *Reversal of electronic substituent effects in the retro - Diels - Alder reaction. A charge neutral analog of oxyanion-accelerated cycloreversion.* J. Org. Chem. 1986, 51, 2851-2853.

94. Rickborn, B. *The retro - Diels - Alder reaction. Part I. C-C dienophiles.* Organic Reactions 1998, 52, 1-393.

95. Rickborn, B. *The retro - Diels - Alder reaction. Part II. Dienophiles with one or more heteroatom.* Organic Reactions 1998, 53, 223-629.

96. Adachi, Y.; Nakagawa, H.; Matsuo, K.; Suzuki, T.; Miyata, N. *Photoactivatable HNO-releasing compounds using the retro - Diels - Alder reaction.* Chem. Comm. 2008, 41, 5149-5151.

97. Afzali, A.; Dimitrakopoulos, C. D.; Breen, T. L. *High-Performance, Solution-Processed Organic Thin Film Transistors from a Novel Pentacene Precursor.* J. Am. Chem. Soc. 2002, 124, 8812.

98. Afzali, A.; Dimitrakopoulos, C. D.; Graham, T. O. *Photosensitive pentacene precursor: synthesis, photothermal patterning, and application in thin-film transistors.* Adv. Mater. 2003, 15, 2066.

99. Chen, X.; Dam, M. A.; Ono, K.; Mal, A.; Shen, H.; Nut, S. R.; Sheran, K.; Wudl, F. *A Thermally Re-mendable Cross-linked Polymeric Material.* Science 2002, 295, 1698-1702.

100. Edwards, J. H.; Feast, W. J.; Bott, D. C. *New routes to conjugated polymers. 1. A two-step route to polyacetylene.* Polymer 1984, 25, 395-398.

101. Gorman, C. B.; Ginsburg, E. J.; Grubbs, R. H. *Soluble, highly conjugated derivatives of polyacetylene from the ring-opening metathesis polymerization of monosubstituted cyclooctatetraenes: synthesis and the relationship between polymer structure and physical properties.* J. Am. Chem. Soc. 1993, 115, 1397-1409.

102. Shah, S.; Tian, R.; Shi, Z.; Liao, Y. *Side-chain free aromatic polyimides containing anthracene units via Diels-Alder precursors.* J. Appl. Polym. Sci. 2009, 112, (5), 2953-2958.

103. Tian, R.; Shi, Z.; Liao, Y. *Novel organic materials that permanently increase conductivity upon thermal or photo treatment.* Org. Electron. 2009, 10, (2), 368-371.

104. Woodward, R. B.; Hoffmann, R. *Stereochemistry of Electrocyclic Reactions.* J. Am. Chem. Soc. 1965, 87, 395-397.

105. Atherton, J. C. C.; Jones, S. *Establishing cleavage conditions for an anthracene chiral auxiliary using a photochemical retro Diels - Alder reaction.* Tetrahedron Lett. 2002, 43, 9097.

106. Nozaki, H.; Kato, H.; Noyori, R. *Retro - Diels - Alder reaction induced by π,π^* excitation and by electron impact.* Tetrahedron 1969, 25, (1661-5).

107. Yamada, H.; Yamashita, Y.; Kikuchi, M.; Watanabe, H.; Okujima, T.; Uno, H.; Ogawa, T.; Ohara, K.; Ono, N. *Photochemical Synthesis of Pentacene and its Derivatives.* . Chem. Eur. J. 2005, 11, 6212-6220.

108. Barachevsky, V. A. *Applied Aspects of Organic Photochemistry.* High Energy Chemistry 2003, 37, (1), 6-16.

109. Kellett, J. C. J. *Diels-Alder student preparation.* J. Chem. Edu. 1963, 40, 543.

110. Brown, P.; Cookson, R. C. *Relative rates of addition of cyanoethylenes to anthracene and its 9-deuterio- and 9,10-dideuterio derivatives.* Tetrahedron 1965, 21, 1993-1998.

111. Noland, W. E.; Baker, M. S.; Freeman, H. I. *The Nef reaction on 9,10-dihydro(11-nitroethano)-anthracenes. A new route to 9,10-dihydro-(11-oxoethano)-anthracenes.* . J. Am. Chem. Soc. 1956, 78, 2233.

112. Keller, F.; Ruechardt, C. *Bimolecular formation of radicals by hydrogen transfer. Part 14. The uncatalyzed transfer hydrogenation of .alpha.-methylstyrene by 2,6-disubstituted 9,10-dihydroanthracenes.* J.Prakt.Chem 1998, 340, 642.

113. Cabellero, A. G.; Croft, A. K.; Nalli, S. M. *Remote aromatic stabilization in radical reactions.* Tetrahedron Lett. 2008, 49, 3613-3615.

114. Gurzadyan, G. G.; Gorner, H. *Depopulation of highly excited singlet states of DNA model compounds: quantum yields of 193 and 245 nm photoproducts of pyrimidine monomers and dinucleoside monophosphates.* Photochem. Photobio. 1996, 63, 143-153.

115. Kuhn, H. J.; Braslavsky, S. E.; Schmidt, R. *Chemical actinometry (IUPAC technical report).* Pure Appl. Chem. 2004, 76, 2105-2146.

116. Brown, P.; Cookson, R. C. *Kinetics of addition of tetracyanoethylene to anthracene and bicyclo[2,2,1]heptadiene.* Tetrahedron 1965, 21, (8), 1977-1991.

117. C. Herndon, W.; Hosoya, H. *Parameterized valence bond calculations for benzenoid hydrocarbons using clar structure.* Tetrahedron 1984, 40, (20), 3987-3995.

118. Hammett, L. P. *The Effect of Structure upon the Reactions of Organic Compounds. Benzene Derivatives* J. Am. Chem. Soc. 1937, 59, 96-103.

119. Johnson, T. R.; Mann, B. E.; Clark, J. E.; Foresti, R.; Green, C. J.; Motterlini, R. *Metal Carbonyls: A New Class of Pharmaceuticals?* Angewandte Chemie International Edition 2003, 42, (32), 3722-3729.

120. Gillman, M. A.; Lichtigfeld, F. J. *NO comments.* Nature 1994, 367, (6458), 28-28.

121. Butler, A. R.; Williams, D. L. H. *The physiological role of nitric oxide.* Chemical Society Reviews 1993, 22, (4), 233-241.

122. Feelisch, M. A. S., J.S, *Donors of nitrogen oxides*. 1996, John Wiley &Sons: New York. p. 71-115.

123. Blackstone, E.; Morrison, M.; Roth, M. B. *H2S Induces a Suspended Animation-Like State in Mice.* Science 2005, 308, (5721), 518.

124. Zhao, Y.; Wang, H.; Xian, M. *Cysteine-Activated Hydrogen Sulfide (H2S) Donors.* Journal of the American Chemical Society 133, (1), 15-17.

125. Foresti, R.; Bani-Hani, M.; Motterlini, R. *Use of carbon monoxide as a therapeutic agent: promises and challenges.* Intensive Care Medicine 2008, 34, (4), 649-658.

126. Motterlini, R.; Clark, J. E.; Foresti, R.; Sarathchandra, P.; Mann, B. E.; Green, C. J. *Carbon Monoxide-Releasing Molecules.* Circulation Research 2002, 90, (2), e17-e24.

127. Clark, J. E.; Naughton, P.; Shurey, S.; Green, C. J.; Johnson, T. R.; Mann, B. E.; Foresti, R.; Motterlini, R. *Cardioprotective Actions by a Water-Soluble Carbon Monoxide-Releasing Molecule.* Circulation Research 2003, 93, (2), e2-e8.

128. Malone, L. J.; Parry, R. W. *The preparation and properties of the boranocarbonates.* Inorganic Chemistry 1967, 6, (4), 817-822.

129. Mann, B. E.; Motterlini, R. *CO and NO in medicine.* Chemical Communications 2007,(41), 4197-4208.

130. Niesel, J.; Pinto, A.; N'dongo, H. W. P.; Merz, K.; Ott, I.; Gust, R.; Schatzschneider, U. *Photoinduced CO release, cellular uptake and cytotoxicity of a tris(pyrazolyl)methane (tpm) manganese tricarbonyl complex.* Chemical Communications 2008,(15), 1798-1800.

131. Uno, H.; Yamashita, Y.; Kikuchi, M.; Watanabe, H.; Yamada, H.; Okujima, T.; Ogawa, T.; Ono, N. *Photo precursor for pentacene.* Tetrahedron Letters 2005, 46, (12), 1981-1983.

132. Yamada, H.; Kuzuhara, D.; Ohkubo, K.; Takahashi, T.; Okujima, T.; Uno, H.; Ono, N.; Fukuzumi, S. *Synthesis and photochemical properties of [small alpha]-diketoporphyrins as precursors for [small pi]-expanded porphyrins.* Journal of Materials Chemistry 20, (15), 3011-3024.

133. Bu-Abbas, A.; Ionnides, C.; Walker, R. *Evaluation of the antimutagenic potential of anthracene: in vitro and ex vivo studies.* Mutation Research/Fundamental and Molecular Mechanisms of Mutagenesis 1994, 309, (1), 101-107.

134. Yao, S.; Ahn, H.-Y.; Wang, X.; Fu, J.; Van Stryland, E. W.; Hagan, D. J.; Belfield, K. D. *Donor-Acceptor-Donor Fluorene Derivatives for Two-Photon Fluorescence Lysosomal Imaging.* The Journal of Organic chemistry 75, (12), 3965-3974.

135. Kabanov, A. V.; Batrakova, E. V.; Alakhov, V. Y. *Pluronic block copolymers as novel polymer therapeutics for drug and gene delivery.* Journal of Controlled Release 2002, 82, (2-3), 189-212.

136. Marin, A.; Sun, H.; Husseini, G. A.; Pitt, W. G.; Christensen, D. A.; Rapoport, N. Y. *Drug delivery in pluronic micelles: effect of high-frequency ultrasound on drug release from micelles and intracellular uptake.* Journal of Controlled Release 2002, 84, (1-2), 39-47.

137. Esteban, J.; Ros-Lis, J. V.; Martínez-Máñez, R.; Marcos, M. D.; Moragues, M.; Soto, J.; Sancenón, F. *Sensitive and Selective Chromogenic Sensing of Carbon Monoxide by Using Binuclear Rhodium Complexes.* Angewandte Chemie International Edition 49, (29), 4934-4937.

138. Du, H.; Fuh, R.-C. A.; Li, J.; Corkan, L. A.; Lindsey, J. S. *PhotochemCAD‡: A Computer-Aided Design and Research Tool in Photochemistry.* Photochemistry and Photobiology 1998, 68, (2), 141-142.

139. Shirakawa, H.; Louis, E. J.; Macdiarmid, A. G.; Chiang, C. K.; Heeger, A. J. *Synthesis of electrically conducting organic polymers: halogen derivatives of polyacetylene, (CH).* Journal of the Chemical Society, Chemical Communications 1977,(16), 578-580.

140. Chiang, C. K.; Fincher, C. R., Jr.; Park, Y. W.; Heeger, A. J.; Shirakawa, H.; Louis, E. J.; Gau, S. C.; Macdiarmid, A. G. *Electrical Conductivity in Doped Polyacetylene.* Physical Review Letters 1977, 39, (17), 1098-1101.

141. Zhang, J.; Kong, L.-B.; Wang, B.; Luo, Y.-C.; Kang, L. *In-situ electrochemical polymerization of multi-walled carbon nanotube/polyaniline composite films for electrochemical supercapacitors.* Synthetic Metals 2009, 159, (3-4), 260-266.

142. Nemzer, L. R.; Schwartz, A.; Epstein, A. J. *Enzyme Entrapment in Reprecipitated Polyaniline Nano- and Microparticles.* Macromolecules 43, (9), 4324-4330.

143. Murugan, A. V.; Muraliganth, T.; Manthiram, A. *Correction to Rapid, Facile Microwave-Solvothermal Synthesis of Graphene Nanosheets and Their Polyaniline Nanocomposites for Energy Storage.* Chemistry of Materials 22, (8), 2692-2692.

144. Lee, K.; Cho, S.; Heum Park, S.; Heeger, A. J.; Lee, C.-W.; Lee, S.-H. *Metallic transport in polyaniline.* Nature 2006, 441, (7089), 65-68.

145. Chiang, J.-C.; Macdiarmid, A. G. *'Polyaniline': Protonic acid doping of the emeraldine form to the metallic regime.* Synthetic Metals 1986, 13, (1-3), 193-205.

146. Lee, C.-W.; Seo, Y.-H.; Lee, S.-H. *A Soluble Polyaniline Substituted with t-BOC: Conducting Patterns and Doping.* Macromolecules 2004, 37, (11), 4070-4074.

147. Angelopoulos, M.; Shaw, J. M.; Lee, K.-L.; Huang, W.-S.; Lecorre, M.-A.; Tissier, M. *Conducting polymers as lithographic materials.* Polymer Engineering & Science 1992, 32, (20), 1535-1540.

148. Shirai, M.; Tsunooka, M. *Photoacid and photobase generators: Chemistry and applications to polymeric materials.* Progress in Polymer Science 1996, 21, (1), 1-45.

149. Papps, S. P. *Photogeneration of acid: Part 6 - A review of basic principles for resist imaging applications* Journal of Imaging Technology 1985, 11, (4), 146-157.

150. Fouassier, J. P. A. R., J.F., *Radiation Curing in Polymer Science and Technology, Vol. 2-Photoinitiating Systems*. 1993, London: Elsevier Applied Science.

151. Salavagione, H. J.; Miras, M. C.; Barbero, C. *Photolithographic Patterning of a Conductive Polymer Using a Polymeric Photoacid Generator and a Traceless Removable Group.* Macromolecular Rapid Communications 2006, 27, (1), 26-30.

152. Venugopal, G.; Quan, X.; Johnson, G. E.; Houlihan, F. M.; Chin, E.; Nalamasu, O. *Photoinduced Doping and Photolithography of Methyl-Substituted Polyaniline.* Chemistry of Materials 1995, 7, (2), 271-276.

153. Potje-Kamloth, K.; Polk, B. J.; Josowicz, M.; Janata, J. *Doping of Polyaniline in the Solid State with Photogenerated Triflic Acid.* Chemistry of Materials 2002, 14, (6), 2782-2787.

154. Foreman, J. P.; Monkman, A. P. *Theoretical Investigations into the Structural and Electronic Influences on the Hydrogen Bonding in Doped Polyaniline.* The Journal of Physical Chemistry A 2003, 107, (38), 7604-7610.

155. Foreman, J. P.; Monkman, A. P. *Theoretical Investigations into the Structural and Electronic Influences on the Hydrogen Bonding in Doped Polyaniline.* Synthetic Metals 2003, 135-136, 375-376.

156. Dektar, J. L.; Hacker, N. P. *Photochemistry of triarylsulfonium salts.* Journal of the American Chemical Society 1990, 112, (16), 6004-6015.

157. G.Venugopal, X. Q., G.E.Johnson, F.M.Houlihan, E.Chin, and O.Nalamasu *Photoinduced Doping and Photolithography of Methyl-Substituted Polyaniline.* Chemistry of Materials 1995, 7, 271-276.

158. Travers, J. P.; Nechtschein, M. *Water effects in polyaniline: A new conduction process.* Synthetic Metals 1987, 21, (1-3), 135-141.

159. Osaheni, J. A.; Jenekhe, S. A.; Vanherzeele, H.; Meth, J. S.; Sun, Y.; Macdiarmid, A. G. *Nonlinear optical properties of polyanilines and derivatives.* The Journal of Physical Chemistry 1992, 96, (7), 2830-2836.

160. Quillard, S. B., K.; Louarn, G.; Lefrant,S.; Lapkowski, M.; Pron,A.; *In situ Raman spectroscopic studies of the electrochemical behavior of polyaniline.* . New Journal of Chemistry 1995, 19, (4), 365-374.

161. Ping, Z. *In situ FTIR-attenuated total reflection spectroscopic investigations on the base-acid transitions of polyaniline. Base-acid transition in the emeraldine form of polyaniline.* Journal of the Chemical Society, Faraday Transactions 1996, 92, (17), 3063-3067.

162. Laska, J.; Widlarz, J. *Spectroscopic and structural characterization of low molecular weight fractions of polyaniline.* Polymer 2005, 46, (5), 1485-1495.

163. Epstein, A. J.; Ginder, J. M.; Zuo, F.; Bigelow, R. W.; Woo, H. S.; Tanner, D. B.; Richter, A. F.; Huang, W. S.; Macdiarmid, A. G. *Insulator-to-metal transition in polyaniline.* Synthetic Metals 1987, 18, (1-3), 303-309.

164. Patil, R.; Roy, A. S.; Anilkumar, K. R.; Ekhelikar, S. *Studies on Fourier transform infrared spectroscopy, scanning electron microscope, and direct current conductivity of polyaniline doped zinc ferrite.* Journal of Applied Polymer Science 121, (1), 262-266.

165. Shacklette, L. W. *Dipole and hydrogen-bonding interactions in polyaniline: a mechanism for conductivity enhancement.* Synthetic Metals 1994, 65, (2-3), 123-130.

166. Chen, S. A.; Fang, W. G. *Electrically conductive polyaniline-poly(vinyl alcohol) composite films: physical properties and morphological structures.* Macromolecules 1991, 24, (6), 1242-1248.

167. Sedenkova, I.; Prokes, J.; Trchova, M.; Stejskal, J. *Conformational transition in polyaniline films-Spectroscopic and conductivity studies of ageing.* Polymer Degradation and Stability 2008, 93, (2), 428-435.

168. Bardavid, Y.; Goykhman, I.; Nozaki, D.; Cuniberti, G.; Yitzchaik, S. *Dipole Assisted Photogated Switch in Spiropyran Grafted Polyaniline Nanowires.* The Journal of Physical Chemistry C 115, (7), 3123-3128.

169. Gagik G. Gurzadyan, H. G. *Depopulation of Highly Excited Singlet States of DNA Model Compounds: Quantum Yields of 193 and 245 nm Photoproducts of Pyrimidine Monomers and Dinucleoside Monophosphates.* Photochemistry and Photobiology 1996, 63, (2), 143-153.

170. H.J.Kuhn, S. E. B. A. R. S. *CHEMICAL ACTINOMETRY.* Pure and Applied Chemistry 2004, 76, (12), 2105-2146.

171. Hasegawa, U.; Van Der Vlies, A. J.; Simeoni, E.; Wandrey, C.; Hubbell, J. A. *Carbon Monoxide-Releasing Micelles for Immunotherapy.* Journal of the American Chemical Society 2010, 132, (51), 18273-18280.

172. Knoll, M. *Aufladepotentiel und Sekundäremission elektronenbestrahlter Körper.* Zeitschrift für technische Physik 1935, 16, 467-475.